Uploaded to VFC Website
~ October 2012 ~

This Document has been provided to you courtesy of Veterans-For-Change!

Feel free to pass to any veteran who might be able to use this information!

For thousands more files like this and hundreds of links to useful information, and hundreds of "Frequently Asked Questions, please go to:

Veterans-For-Change

Veterans-For-Change is a 501(c)(3) Non-Profit Corporation
Tax ID #27-3820181

If Veteran's don't help Veteran's, who will?

We appreciate all donations to continue to provide information and services to Veterans and their families.

https://www.paypal.com/cgi-bin/webscr?cmd=_s-xclick&hosted_button_id=WGT2M5UTB9A78

Note: VFC is not liable for source information in this document, it is merely provided as a courtesy to our members.

Item ID Number:	00057
Author	Jones, E.G.
Corporate Author	Systems Research Laboratories, Inc., Dayton, Ohio
Report/Article Title	Mass Spectrometric Studies: Final Report
Journal/Book Title	
Year	1975
Month/Day	July
Color	☑
Number of Images	228
Description Notes	Contract No. F33615-73-C-4099; Report No. AFOSR-TR-73-1310

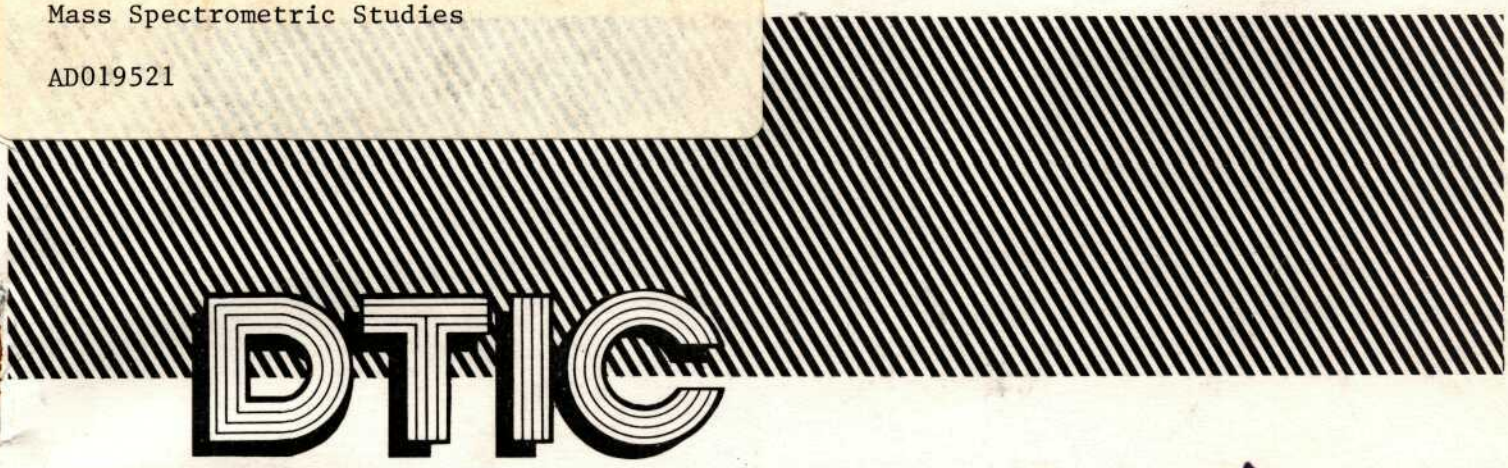

Technical Report

distributed by

Defense Technical Information Center
DEFENSE LOGISTICS AGENCY
Cameron Station • Alexandria, Virginia 22314

AD-A019 521

MASS SPECTROMETRIC STUDIES

E. G. Jones

Systems Research Laboratories, Incorporated

Prepared for:

Air Force Office of Scientific Research

July 1975

Approved for public release;
distribution unlimited.

SRL

SYSTEMS
RESEARCH
LABORATORIES
INC.

UNCLASSIFIED
SECURITY CLASSIFICATION OF THIS PAGE (When Data Entered)

REPORT DOCUMENTATION PAGE		READ INSTRUCTIONS BEFORE COMPLETING FORM
1. REPORT NUMBER AFOSR - TR - 75 - 1570	2. GOVT ACCESSION NO.	3. RECIPIENT'S CATALOG NUMBER
4. TITLE (and Subtitle) MASS SPECTROMETRIC STUDIES		5. TYPE OF REPORT & PERIOD COVERED Final
		6. PERFORMING ORG. REPORT NUMBER
7. AUTHOR(s) Dr. E. G. Jones		8. CONTRACT OR GRANT NUMBER(s) F33615-73-C-4099
9. PERFORMING ORGANIZATION NAME AND ADDRESS Systems Research Laboratories, Inc. 2800 Indian Ripple Road Dayton, Ohio 45440		10. PROGRAM ELEMENT, PROJECT, TASK AREA & WORK UNIT NUMBERS 7023, 61102F, 681303
11. CONTROLLING OFFICE NAME AND ADDRESS AF Office of Scientific Research/NC Bolling AFB, Bldg. 410 Washington, D.C. 20332		12. REPORT DATE July 1975
		13. NUMBER OF PAGES 223
14. MONITORING AGENCY NAME & ADDRESS (if different from Controlling Office)		15. SECURITY CLASS. (of this report) Unclassified
		15a. DECLASSIFICATION/DOWNGRADING SCHEDULE

16. DISTRIBUTION STATEMENT (of this Report)

Approved for public release; distribution unlimited.

17. DISTRIBUTION STATEMENT (of the abstract entered in Block 20, if different from Report)

18. SUPPLEMENTARY NOTES

19. KEY WORDS (Continue on reverse side if necessary and identify by block number)

20. ABSTRACT (Continue on reverse side if necessary and identify by block number)

Mass-spectrometric investigations of diverse areas ranging from the basic understanding of elementary physical-chemical processes to analyses of trace elements in the environment are outlined. Basic thermodynamics and chemical kinetics of ion-neutral phenomena relevant to the solution of problems of immediate importance to the U.S. Air Force are emphasized. Particular emphasis is placed on electron-affinity determinations of small gaseous species of importance as electron-affinity determinations of small gaseous species of importance as electron

DD FORM 1 JAN 73 1473 EDITION OF 1 NOV 65 IS OBSOLETE

SECURITY CLASSIFICATION OF THIS PAGE (When Data Entered)

20. Abstract

scavengers in the atmosphere and electronic excitation in ion-neutral collision processes of direct application to the understanding and prediction of new laser systems.

Sophisticated analytical techniques to quantify trace contaminants such as dioxin in Herbicide Orange and other impurities in solid, liquid, and gaseous environmental samples are outlined. These include sample work-up, column preparation, and gas-chromatographic mass-spectrometric analysis.

Techniques for quantitative adsorption and desorption of noxious gases on selectively prepared columns are described.

Methods of computer interfacing with mass spectrometers for data acquisition are outlined. These include techniques for treating data from both chemical-physical and analytical investigations.

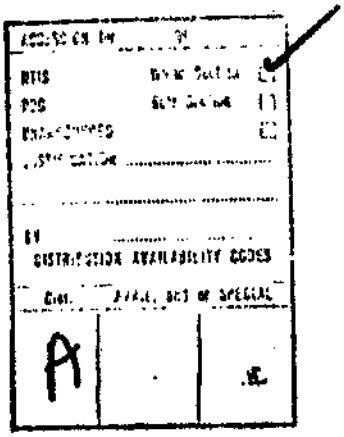

MASS SPECTROMETRIC STUDIES

Final Report

Contract No. F33615-73-C-4099

Prepared for

Air Force Office of Scientific Research (OSR)
Director of Chemistry
1400 Wilson Boulevard
Arlington, Virginia 22209

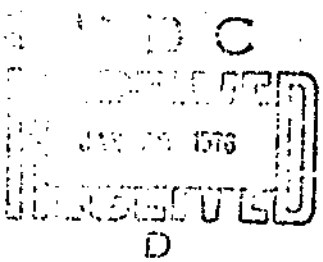

Prepared by

Systems Research Laboratories, Inc.
2800 Indian Ripple Road
Dayton, Ohio 45440
(513) 426-6000

31 July 1975

TABLE OF CONTENTS

4<

LIST OF ILLUSTRATIONS

LIST OF TABLES

ABSTRACT

Mass-spectrometric investigations of diverse areas ranging from the basic understanding of elementary physical-chemical processes to analyses of trace elements in the environment are outlined. Basic thermodynamics and chemical kinetics of ion-neutral phenomena relevant to the solution of problems of immediate importance to the U. S. Air Force are emphasized. Particular emphasis is placed on electron-affinity determinations of small gaseous species of importance as electron scavengers in the atmosphere and electronic excitation in ion-neutral collision processes of direct application to the understanding and prediction of new laser systems.

Sophisticated analytical techniques to quantify trace contaminants such as dioxin in Herbicide Orange and other impurities in solid, liquid, and gaseous environmental samples are outlined. These include sample work-up, column preparation, and gas-chromatographic mass-spectrometric analysis.

Techniques for quantitative adsorption and desorption of noxious gases on selectively prepared columns are described.

Methods of computer interfacing with mass spectrometers for data acquisition are outlined. These include techniques for treating data from both chemical-physical and analytical investigations.

INTRODUCTION

The objective of this program was the development and utilization of advanced mass-spectrometric techniques for the study of fundamental analytical and physical-chemical problems of interest to the U.S. Air Force. The fundamental areas investigated in the course of this contract include: (1) ion-neutral collision studies involved in the determination of basic thermochemical quantities such as electron affinities of refractory metal oxides; (2) development of chemical and mass-spectrometric procedures for determining 2,3,7,8-tetrachlorodibenzo-p-dioxin in Air Force Herbicide Orange and environmental matrices; (3) spark-source mass spectrometric analysis of solid samples of interest to the Air Force; (4) development of mass-spectrometric techniques for studying sorption of noxious gases by selected solids; (5) high-resolution mass-spectrometric analysis of liquid and gaseous samples, and (6) development of an operating interface between laboratory instruments and computer.

The scientific investigations were performed in the Gaseous Excitation and Ionization Processes Group, Chemistry Research Laboratory, Aerospace Research Laboratories, Wright Patterson Air Force Base, Ohio, utilizing the unique instrumentation fabricated during the initial phase of this contract and other sophisticated equipment located in this laboratory.

The authors would like to acknowledge the cooperation of Dr. Thomas O. Tiernan and co-workers at the Aerospace Research Laboratories and the efforts of R. P. Clow, C. A. Davis, C. E. Hill, Jr., J. C. Haartz Smith, and M. L. Taylor during the early phases of the program.

This report describes in detail the work perfor.ed during the past four months and summarizes the results obtained over the entire course of the contract.

SECTION I

GAS-PHASE KINETICS

During the course of this program a number of thermodynamic and kinetic studies have been completed. In these studies, both tandem and time-of-flight mass spectrometers have been used as well as instruments for monitoring the luminescence produced in ion-molecular interactions. Much of this work has been documented in Systems Research Laboratories, Inc., annual and semiannual progress reports.[1-4] Extensive work completed since publication of these reports has resulted in several manuscripts which have been prepared for publication in various scientific journals. This section is comprised of these manuscripts; each manuscript is a self-contained unit having its own page, reference, table, figure, and equation numbers.

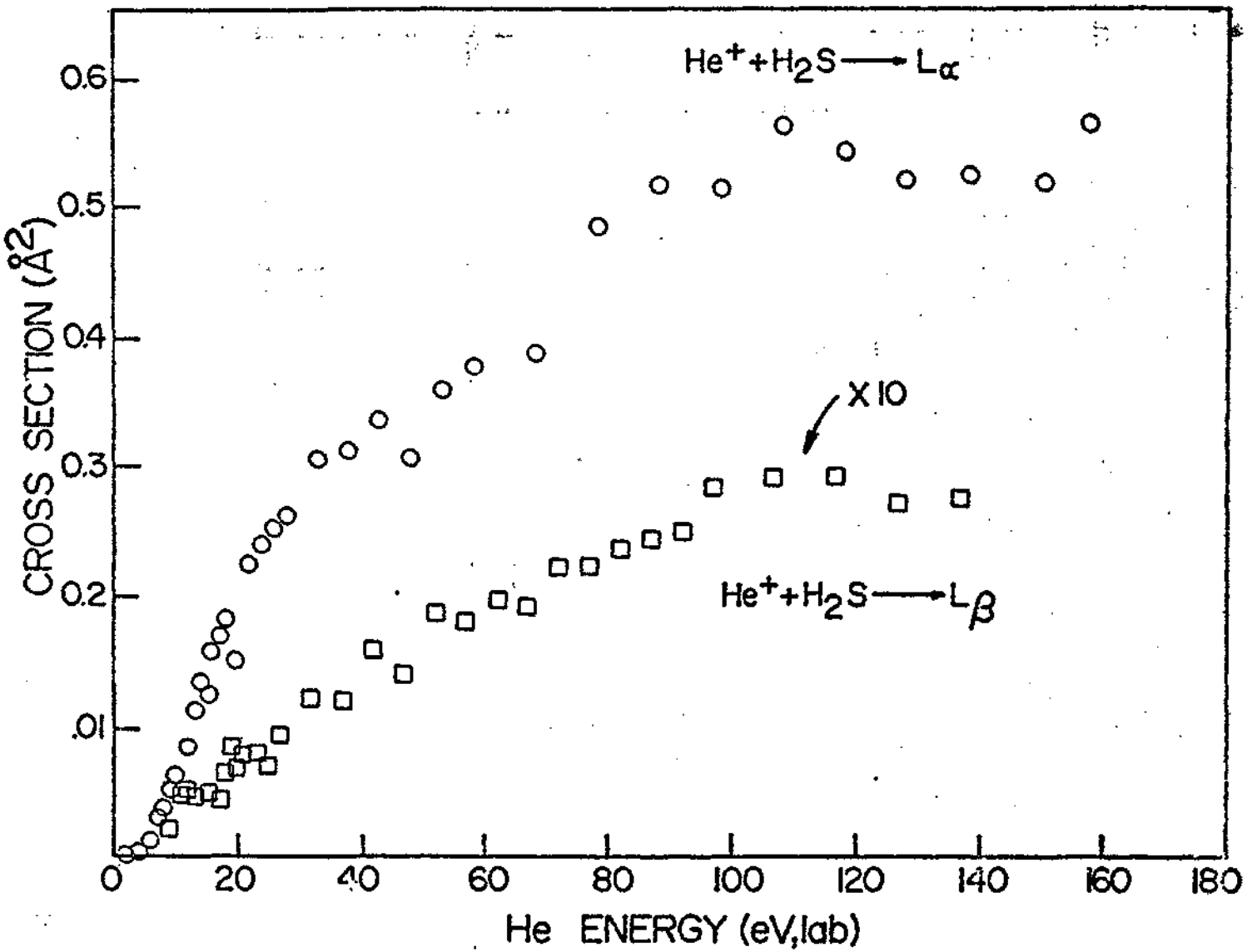
$He^+ + H_2S \longrightarrow L\alpha$
X 10
$He^+ + H_2S \longrightarrow L\beta$
CROSS SECTION (Å²)
0.6
0.5
0.4
0.3
0.2
.01
0
20
40
60
80
100
120
140
160
180
He ENERGY (eV,lab)

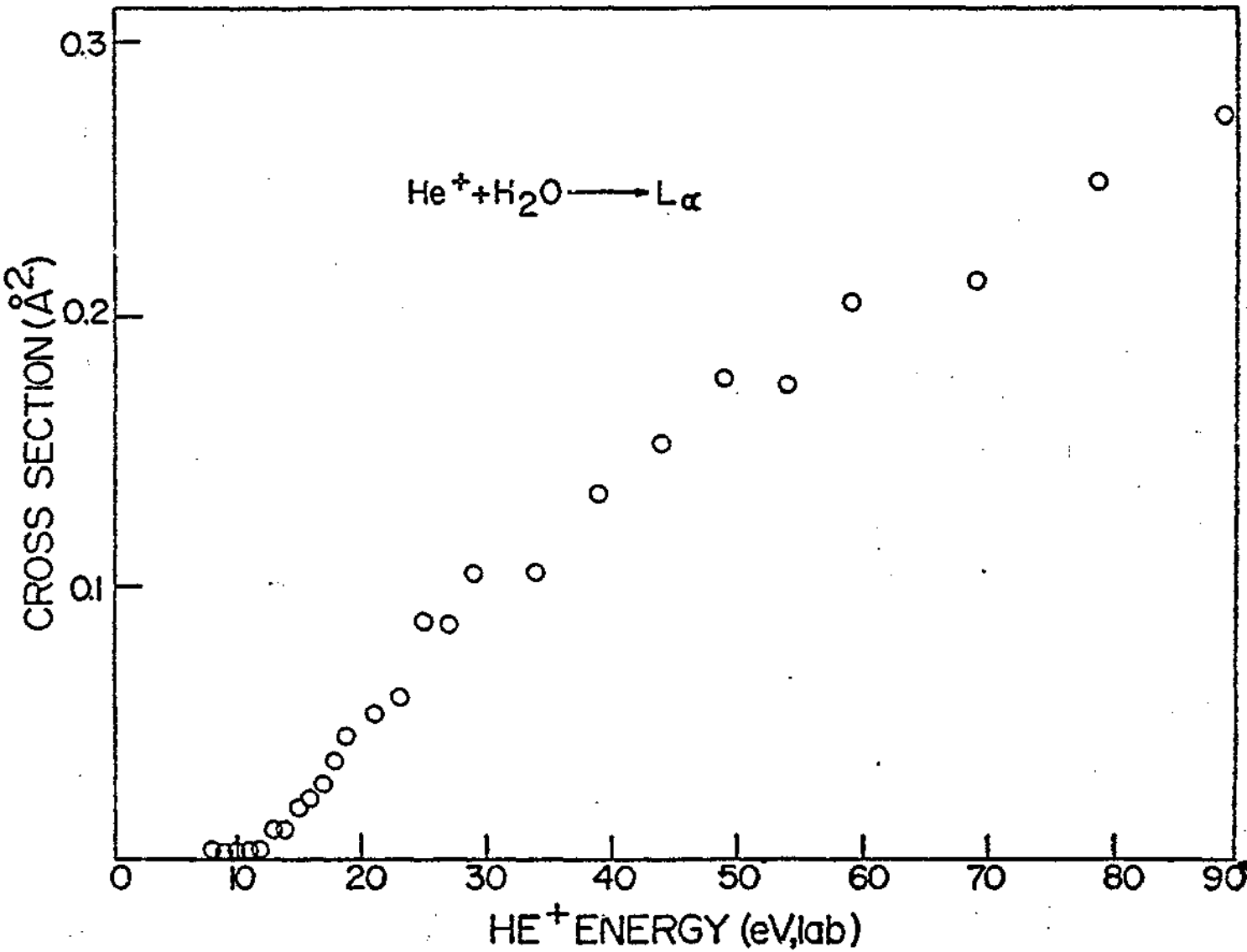
0.3
0.2
0.1
CROSS SECTION (Å²)
He⁺+H₂O ⟶ Lα
0
10
20
30
40
50
60
70
80
90
HE⁺ ENERGY (eV,lab)

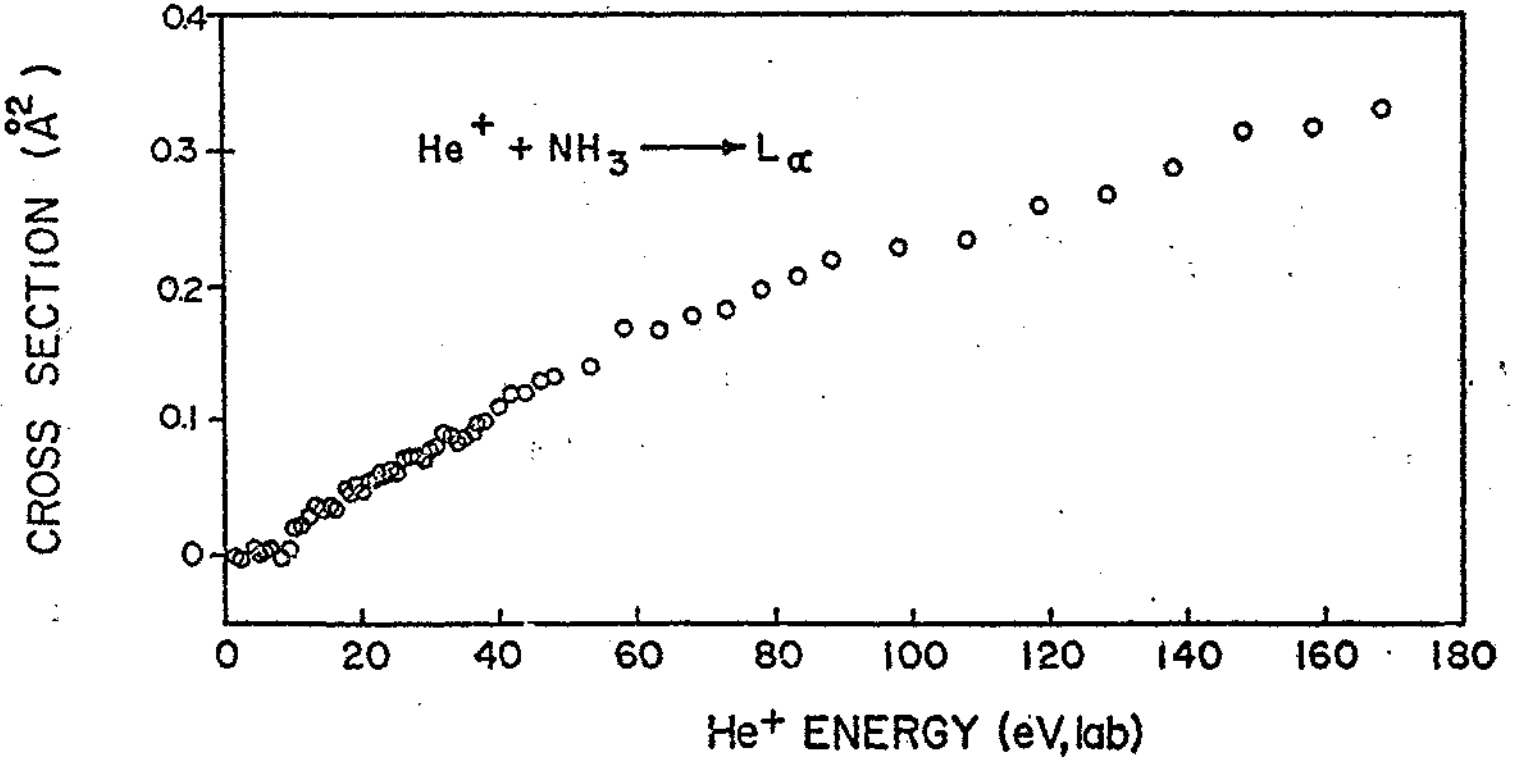
CROSS SECTION (Å²)
0.4
0.3
0.2
0.1
0
He⁺ + NH₃ ⟶ Lα
0
20
40
60
80
100
120
140
160
180
He⁺ ENERGY (eV, lab)

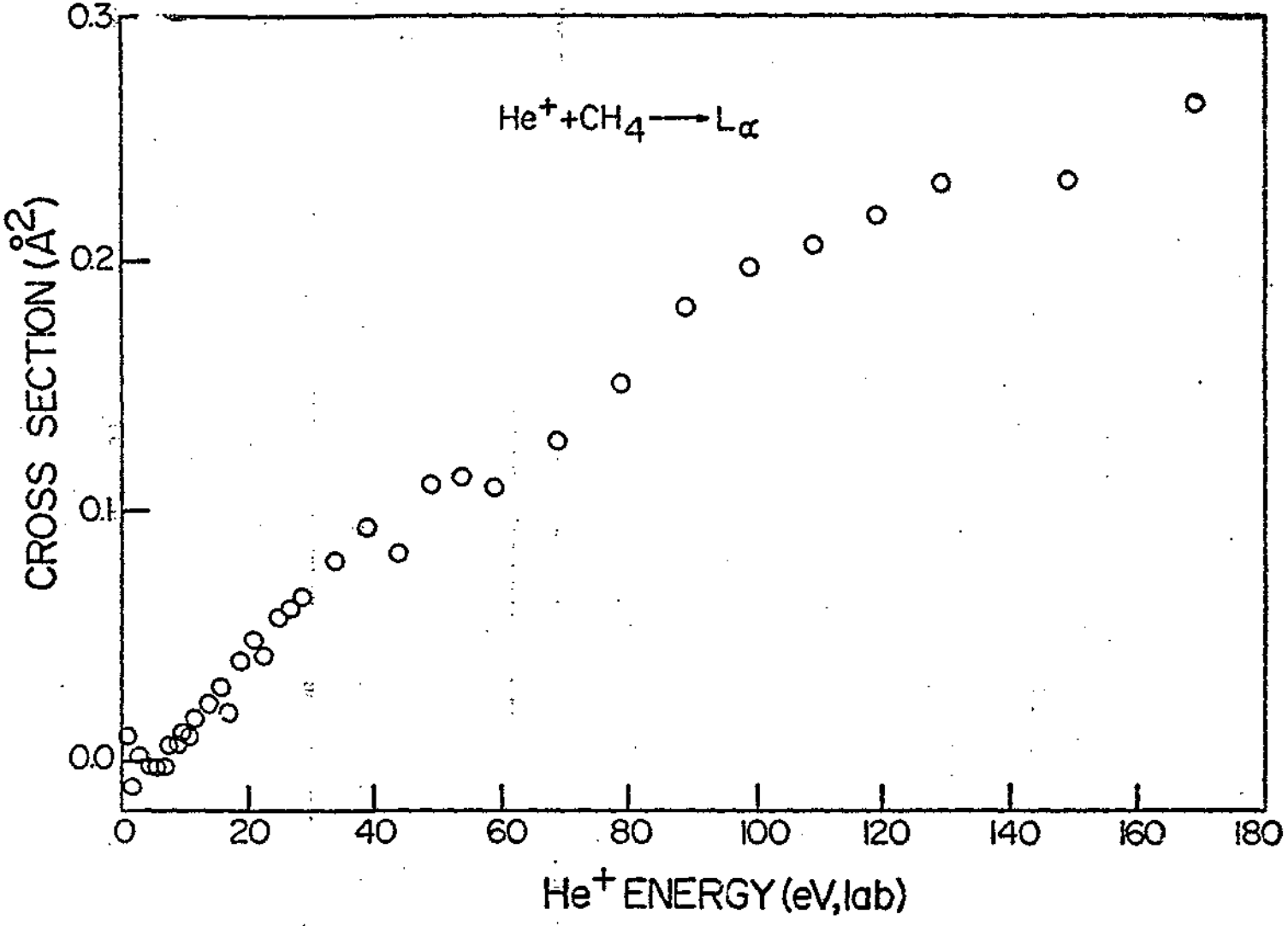
$He^+ + CH_4 \longrightarrow L\alpha$
CROSS SECTION (Å²)
0.3
0.2
0.1
0.0
0
20
40
60
80
100
120
140
160
180
He^+ ENERGY (eV, lab)

Lyman Radiation From He^+/Molecule Interactions

B. M. Hughes and T. O. Tiernan

Aerospace Research Laboratories, LJ
Wright Patterson Air Force Base, Ohio 45433

E. C. Jones

Systems Research Laboratories, Inc.
2800 Indian Ripple Road
Dayton, Ohio 45440

Introduction

In this laboratory extensive investigations of the luminescence produced in ion-neutral collisions have been undertaken. The studies have emphasized the low kinetic energy region (1-200 eV) in which a significant number of electronically excited product species are formed. Certain of these states can radiate. By monitoring the luminescence, information concerning the interaction of an ion and a neutral can be ascertained. In particular, information concerning the energy distribution of reaction products can aid in the design of potential laser systems. Ion-neutral reactions in certain cases have been found to be an efficient laser-pumping mechanism.[1]

Low-energy collisions of He^+ ions with hydrogen-containing molecules frequently produce H atoms in a series of excited levels. For example, reaction of 100 eV, lab He^+ ions with a hydrogen molecule has been shown to produce H(n) for n = 2,3,4,5,6 as determined by monitoring the subsequent Lyman or Balmer radiation from these states.[2] In this kinetic energy region, the intensity of the luminescence is strongly dependent upon the kinetic energy of the colliding partners.[2,3] Production of all of these excited states of the hydrogen atom is endoergic for thermal energy collisions. In a companion study[2] conducted in this laboratory, the individual kinetic energy onsets for H(n); n = 2,3,4 were determined.

In the present study the investigation has been extended to include reactions of He^+ ions with a series of H-containing polyatomic molecules. Results of an analogous investigation of L_α emission following bombardment by electrons have been published by McGowan and co-workers[4,5] and Vroom and de Heer.[6]

Cross sections for the production of L_α and L_β radiation for impact of 100 eV He^+ ions are reported. The kinetic energy dependence of the L_α radiation and the threshold behavior are discussed.

Experimental

The apparatus has been described previously.[2,7] It consists of a single focusing mass spectrometer which prepares He^+ ions (~ 1 nA) with kinetic energy in the range 1-170 eV and focusses and transmits them into a collision chamber containing a target gas at a pressure of 2-10 mTorr as measured absolutely by an MKS Baratron. The exit slit of the chamber is the entrance slit to a McPherson 1-m vacuum ultraviolet monochromator. L_α and L_β radiation was detected by a Bendix Channeltron and an EMR 541-F photon counter, respectively. The detectors are coupled to an SSR pulse counter. The radiation detected is in line with the direction of the ion beam. Cross section determinations assume isotropic emission of radiation from the reaction zone and neglect polarization.

The quantum efficiencies of the detectors were interpolated from the data supplied by the manufacturer. The method of estimating grating reflectance has been outlined previously.[2]

Results and Discussion

A spectral scan of the vacuum-ultraviolet (VUV) region for the reaction of 100 eV, lab He^+ ions with hydrogen sulfide is shown in Fig. 1.

The first three members of the Lyman series are indicated in the figure. Because of intensity considerations, cross sections only for L_α and L_β are reported. The emission cross section for a series of reactions of 100 eV, lab He^+ ions are summarized in Table I. In each case L_α and L_β emission lines are the dominant features of the VUV region. No corrections for cascading have been applied. The relative intensities, however, imply that these effects would be negligible for these systems. It should be pointed out that only emissions from short-lived (< 1 μs) excited species would be monitored by this apparatus. The metastable state H(2s) would not be detected. Only in the case of the hydrogen reaction are absolute cross-section data available in the literature. As discussed in the previous study on hydrogen,[2] the cross section for L_α emission is in excellent agreement with the data of Dunn, et al.[3] The cross section for L_β is approximately 2.5 times smaller than the value determined by Gusev, et al.[8] For all of the polyatomics studied, the cross section for L_α emission exceeds that for L_β emission by a factor ranging from 5 to 25. The level H(3) lies 1.89 eV above H(2) for an isolated H atom. The differences in the cross sections reflect the probability of producing H(3) and H(2) in a reaction at 100 eV.

In general, the larger polyatomics exhibit considerably smaller cross sections for H-atom excitation. Overlooking hydrogen which has been treated previously,[2] the largest cross sections for L_α emission arise from the reactions with H_2S, H_2O, NH_3 and CH_4. The kinetic energy behavior of the cross section for Lyman alpha production in these four reactions is displayed in Figs. 2-5. All of these reactions exhibit similar kinetic energy dependence in that there is a threshold region below which the

reaction is of low probability and above which the reaction cross section increases monotonically to the highest energy studied. The cross section for Lyman alpha emission in the reaction with H_2S appears to remain approximately constant in the vicinity of 100-150 eV, lab. The cross sectional dependence of the Lyman beta emission shown in Fig. 2 displays a similar kinetic energy dependence.

Two factors combine to make a precise kinetic energy threshold determination difficult except in favorable cases. First, below 10 eV, lab there is a gradual decrease in ion flux through the collision region, resulting in large correction to the observed counting rate. The second effect is related to the instrument geometry. The in-line geometry allows the detection of some reactive events occurring in the deceleration lens which is adjacent to the collision chamber. Corrections[9] for this usually amount to ~ 20-40% of the observed count rate for 100 eV He^+ ion impact. The absolute magnitude of this correction does not change appreciably over the entire kinetic energy region; however, this results in a very poor signal-to-noise ratio at kinetic energies in the vicinity of the onset. This necessitates longer counting intervals. The kinetic energy thresholds, estimated from Figs. 2-5, are summarized in Table II. No attempt to correct for the doppler effect or the primary-ion energy spread has been made. Because of the relative masses of the reactants, calculated enthalpy changes are listed in Table II for two possible excitation reaction steps

$$He^+ + R\text{-}H \rightarrow R^+ + H(2p) + He \qquad (1)$$

$$He^+ + R^1\text{-}H_2 \rightarrow R^{1+} + H(2p) + H + He \qquad (2)$$

It is not possible in these experiments to distinguish between Reactions (1) and (2). For example, interaction of 30 eV, lab He^+ ions with CH_4 produce CH_4^+, CH_3^+, CH_2^+, CH^+, and C^+ ionic products.[12] Although CH_2^+ is the most abundant ion product, no direct correlation between H(2p) and a specific ion product can be made. For 100-eV ions striking CH_4, the cross section for Lyman alpha production is 0.2 $Å^2$; this may or may not be comparable to the cross section for CH_2^+ or CH_3^+ formation. There is no absolute data available in this energy range.

A strong analogy exists between the results of this study and the He^+/H_2 system.[2] All of the kinetic studies indicate endoergic excitation processes. In these systems the transfer of kinetic into reaction energy to produce excited product species is important. Very selective reaction channels appear to be available which are determined by symmetry considerations. As more data become available on the partitioning of kinetic energy into reaction channels, it becomes quite clear that frequently the most probable channels involve excited electronic states of the products.

REFERENCES

1. A. R. Turner-Smith, J. M. Green, and C. E. Webb, J. Phys. (B):Atom. Molec. Phys. 6, 114 (1973).
2. B. M. Hughes, E. G. Jones, D. G. Hopper. and T. O. Tiernan, submitted for publication.
3. G. H. Dunn, R. Ceballe, and D. Pretzer, Phys. Rev. 128, 2200 (1962).
4. J. W. McGowan and J. F. Williams, Abstracts of VI International Conference on the Physics of Electronic and Atomic Collisions (MIT Press, Cambridge, Mass., 1969).
5. J. W. McGowan, J. F. Williams, and D. A. Vroom, Chem. Phys. Lett. 3, 614 (1969).
6. D. A. Vroom and F. J. de Heer, J. Chem. Phys. 50, 1883 (1969) and references therein.
7. B. M. Hughes, E. G. Jones, and T. O. Tiernan in Abstracts of VIII International Conference on the Physics of Electronic and Atomic Collisions. Vol. I (B. C. Cobic and M. V. Knsepa, Eds.) (Institute of Physics, Beograd, Yugoslavia, 1973) p. 223.
8. V. A. Gusev, G. N. Polyakova, V. F. Erko, Ya. M. Fogel, and A. V. Zats in Abstracts of the VI International Conference on the Physics of Electronic and Atomic Collisions (MIT Press, Cambridge, Mass., 1969).
9. E. G. Jones, B. M. Hughes, D. C. Fee, and T. O. Tiernan, submitted to Chem. Phys. Lett.
10. H. A. Bethe, Rev. Mod. Phys. 9, 69 (1937).
11. J. L. Franklin, J. G. Dillard, H. M. Rosenstock, J. T. Herron, K. Draxl, and F. H. Field, National Bureau of Standards Report NSRDS-NBS 26, 1969.
12. H. Von Koch, Arkiv Fysik 28, 529 (1965).

20<

Table 1

EMISSION CROSS SECTIONS, 100 eV He^+

$He^+ + M \rightarrow L_\alpha, L_\beta$

Species	Cross Section $\sigma(cm^2)$ $L_\alpha (\times 10^{16})$	$L_\beta (\times 10^{18})$	Ratio $L_\beta/L_\alpha \times 10^2$
H_2	0.46	1.7	3.7
D_2	0.69	2.7	3.9
H_2S	0.54	3.1	5.7
H_2O	0.31	1.6	5.2
NH_3	0.23	1.5	6.5
CH_4	0.20	2.0	10.0
CD_4	0.20	1.7	8.5
C_2H_2	0.09	1.3	14.0
C_3H_8	0.039	0.51	13.0
$C\text{-}C_4H_8$	0.037	0.67	18.0
C_6H_6	0.013	0.15	12.0

Table II

KINETIC ENERGY THRESHOLDS FOR LYMAN ALPHA EMISSIONS

System	Kinetic Energy Threshold (eV)	Enthalpy Change[a] to Form H(2p) (eV)
$He^+ + CH_4$	5 ± 1.6	-0.08[b]; +5.34[c]
$He^+ + H_2S$	5 ± 1.8	+0.05[b]; +3.61[c]
$He^+ + NH_3$	2.6 ± 1.6	+1.39[b]; +3.65[c]
$He^+ + H_2O$	6.1 ± 1.6	+3.91[b]; +8.85[c]

[a]Heats of formation based on tabulations of Ref. 11.

[b]Calculation assumes reaction of the form

$$He^+ + R\text{-}H \rightarrow R^+ + H(2p) + He$$

[c]Calculation assumes reaction of the form

$$He^+ + R'\text{-}H_2 \rightarrow R'^+ + H + H(2p) + He$$

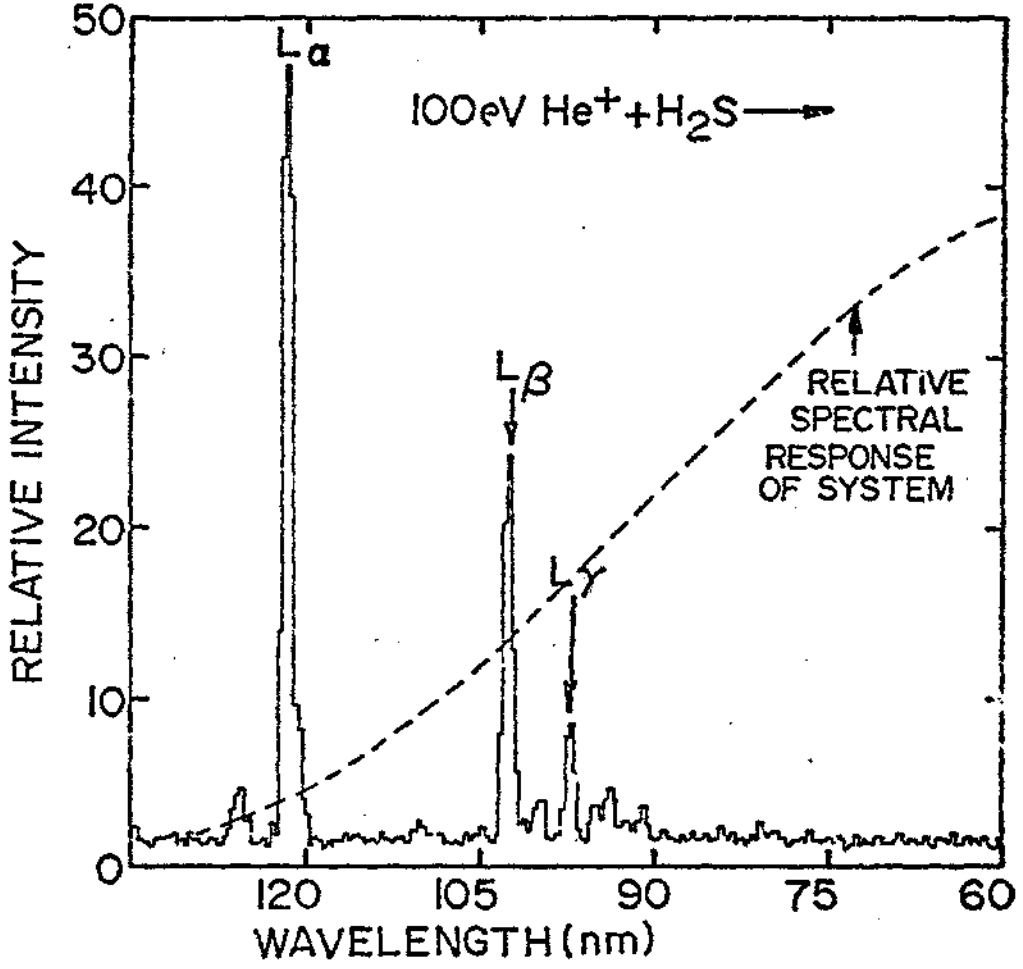
50
40
30
20
10
0
RELATIVE INTENSITY
Lα
100eV He+ + H2S
Lβ
Lγ
RELATIVE SPECTRAL RESPONSE OF SYSTEM
120
105
90
75
60
WAVELENGTH (nm)

COLLISION-INDUCED DISSOCIATION OF CO_3^-

Richard L. C. Wu

Systems Research Laboratories, Inc.
2800 Indian Ripple Road
Dayton, Ohio 45440

T. O. Tiernan

Aerospace Research Laboratories
Chemistry Research Laboratory
Wright Patterson Air Force Base, Ohio 45433

ABSTRACT

Collision-induced dissociation reactions of the molecular negative ion CO_3^- impacted on various target gases (He, Ne, Ar, Kr, Ne, N_2, O_2 and NO_2) have been investigated in an in-line tandem mass spectrometer. These processes exhibit endothermic thresholds. The energy dependences of the cross sections are compared with these predicted by the statistical theory. The dissociation energy of the molecular ion CO_3^- was determined from the measured energy threshold and was used to calculate the electron affinity of CO_3 molecule.

INTRODUCTION

Recently, the collisional phenomena and thermochemistry of the CO_3^- ion have been subjects of extensive investigation because of their importance in the fields of aeronomy[1,2] and radiation chemistry.[3,4] The dissociation energy of $O^- - CO_2$ has been measured by various researchers[5,6,7] and found to vary from 1.8 to 2.0 eV and the electron affinity of CO_3 has been calculated and found to range from 1.8[8] to > 2.9[7] eV. The techniques used in the experiments reported above were photodetachment, photodissociation, and flowing afterglow processes.

In the present study, the tandem mass spectrometer was used to study the energy dependence of the cross section for collision-induced dissociation (CID) of CO_3^- upon various target molecules. The post-threshold behavior of these processes was compared with the prediction of the statistical theory of Robick and Levine.[9] The energy dependence of the cross section is assumed to have the form $A(E_t-E_o)^n/E_{rel}$, where E_t and E_{rel} are respectively the total energy and the relative translational energy of the reactants and E_o is the threshold energy. The exponent n depends upon the mechanism of the process, with $1.9 < n < 2.2$ for a "direct" mechanism and $1.5 < n < 1.8$ for an "indirect" mechanism. For a given CID reaction, the calculated threshold function was convoluted, with the calculated center of mass energy distribution arising from the thermal motion of the target molecules and the energy spread of the incident-ion beam. The calculated curves were then fitted to the experimental cross section to obtain the true energy threshold and the appropriate values of n. The dissociation energy of CO_3^- was then determined from the energy thresholds and was used to calculate the electron affinity of the CO_3 molecule.

EXPERIMENTAL

The experiments were conducted using a recently modified in-line tandem mass spectrometer. The instrument has been described previously.[10,11,12] As a result of the installation of a 1000 ℓ/sec oil diffusion pump and the reduction of the size of the electron-entrance and ion-exit slits, sufficiently high pressures can be achieved in the first-stage ion source to generate the secondary or high-order ion products of ion-neutral collisions. The mass- and energy-analyzed primary ions were injected into the field-free collision chamber containing various target molecules. The product ion was then analyzed by the second-stage mass spectrometer which was fixed at 0° scattering angle. Pulse-counting techniques were used to measure the product ion currents. The temperature of the collision chamber was maintained at 160°C in the experiments reported. The energy spread of the ion beam was about 0.3 eV (lab) over the energy range 0.3-180 eV.

The primary ion of CO_3^- was formed by electron impact on a gaseous mixture of CO_2 and N_2O at high pressures. Currents of CO_3^- generated in this manner were on the order of 50-200 PA. In order to ascertain whether a single collision had occurred in the collision chamber, the pressure of the target molecules was varied from 10-50 μ. All reactions showed a linearity over this pressure range. The experiments were carried out at a pressure of 50 μ in order to obtain reliable cross sections. All cross sections were evaluated relative to the absolute cross section of 63 $Å^2$ at 0.3 eV O^- energy for the O^-/NO_2 charge-transfer.[13]

ANALYSIS OF DATA

Threshold Behavior

Theoretical predictions[9,14] as well as experimental studies[15,16] of the threshold behavior for CID reactions involving a colliding pair (A + BC) which yields three products (A+B+C) have shown this behavior to have the form

$$\sigma = A(E_t - E_o)^n/E_{rel} \qquad (1)$$

E_t, E_{rel}, and E_o having been defined previously and A being a function of the internal energy of the reactant (BC). Thus, the cross section would be zero at the threshold and would increase monotonically with the kinetic energy of the reactant according to the mechanism of the process. If the experiment were carried out at an infinite translational energy resolution, the experimental data could be parameterized according to Eq (1), from which the values of A, E, and E_o would be obtained. However, in the present study a distribution exists in the effective center of mass energy. Hence, the results were treated as described below.

Corrections for Energy Resolutions

Two factors limit the energy resolution in the present experiments -- principally, the thermal motion of the target molecules and the ion energy spread of the incident ion beam. The former effect is well-known as Doppler broadening.[17] The energy distribution caused by the thermal motion of the target molecules in a system where the monoenergetic ion beam collides with target molecules having a Maxwellian distribution has been discussed and derived in detail by Tiernan, Hughes, and Lifshitz.[18]

The effective energy distribution in the laboratory system is expressed by

$$W(E'/E_i) = \frac{1}{(\pi)^{1/2}} \frac{1}{\Delta} \exp\left[-\frac{(E' - E_i)^2}{\Delta^2}\right] \qquad (2)$$

where $\Delta = 2(mE_iKT/M)^{1/2}$ is the Doppler width as well as the half-width of the probability distribution at 1/e of the maximum height, m and M are the masses of the ion and target molecules, respectively, T is the temperature of the target molecules, E_i is the translational energy of the ion beam, and K is the Boltzmann's constant. However, in the tandem mass spectrometer used in this study the distribution of the energy spread in the incident ion E_i has been found to be a Gaussian function with a full-width at half-maximum (FWHM) of ~ 0.3 eV. Thus the energy distribution of E_i is assumed to be

$$W(E_i) = \frac{1}{(\pi)^{1/2}} \frac{1}{0.2} \exp\left[-\frac{(E_i - E_{io})^2}{0.2^2}\right] \qquad (3)$$

with the most probable value being $E_i = E_{io}$. Therefore, the effective energy distribution in the laboratory system arising from both the thermal motion of the target molecules and the energy spread of the incident ion beam becomes

$$W(E') = \int_{-\infty}^{+\infty} W(E'/E_i)\, W(E_i)\, dE_i \qquad (4)$$

The distribution of Eq (4) is, in general, broader than that of Eq (2). It is notable that those collisions which involve a relatively heavy ion and light target molecules are those for which Doppler broadening is most severe, e.g., for the CO_3^-/Ne collision, the effective energy

28

distribution of Eq (4) is nearly the same as that of Eq (2). On the other hand, for the reaction of a relatively light ion with a heavier neutral target such as CO_3^-/Xe, the ion energy spread [Eq (2)] will play a more important role in the final evaluation of the energy distribution in the system.

Typical results obtained from the calculation described are illustrated in Fig. 1 for the CO_3^-/Xe collision at an CO_3^- laboratory energy of 3.6 eV and a temperature of 160°C. Fig. 1(a) shows the energy distributions of Eq (2) (solid lines) and Eq (4) (dashed lines). Figure 1(b) shows the ion energy spread of Eq (3). It is shown that the effect of the ion energy spread on the total effective energy distribution is less important than that of the Doppler broadening in this study. The FWHM of the effective energy distribution in the laboratory energy for the CID reactions of CO_3^- are found to be 0.88, 1.25, 2.13, 3.50, 2.69 and 2.75 eV, respectively, for the target molecules of Xe, Kr, Ar, Ne, O_2 and N_2.

Techniques Used

A convolution technique was utilized in the analysis given below. The energy dependences of cross sections was computed by convoluting the above effective energy distribution [Eq (4)] with the assumed threshold function f(E') according to

$$f(E)\, dE = \int_{-\infty}^{+\infty} f(E')\, W(E')\, dE' \qquad (5)$$

In the present study the statistical theory was adopted in order to describe the behavior of the cross section (zero value at threshold—no step). The reactants and the products were assumed to be in the ground state and A to be independent of the CO_3^- initial state; therefore, the assumed threshold function f(E') is simply

$$f(E') = A(E' - E_o)^n/E' \qquad (6)$$

For a given CID process using Eq (6), the computed threshold functions having different values of E_o and n were then convoluted with the calculated effective energy distribution [Eq (4)]. These calculated curves were then compared with the experimental results to obtain the true threshold energy (E_o) and the appropriate value of n.

RESULTS AND DISCUSSION

Translational Energy Dependence of the Cross Section

The cross section for the CID reaction

$$CO_3^- + X \rightarrow O^- + CO_2 + X \qquad (7)$$

was studied as a function of CO_3^- ion translational energy for various target molecules, and results are shown in Fig. 2. In these reactions, typical endothermic behavior is exhibited. In the region near the threshold (~ 1.8 eV), the energy dependence shows an exponential increase (no sharp step) followed by a linear rise to a maximum (~ 6 eV (CM)) and then a gradual decrease. Thus, the statistical prediction of the threshold behavior was utilized to describe the experimental observations.

Figure 3 shows the calculated cross section as a function of laboratory energy (solid line) for the CID of CO_3^- impacted on various target molecules. These curves were obtained by convoluting the energy-distribution functions with the assumed statistical threshold functions (dashed lines); experimental data points are also shown. It was found that a good fit to the experimental results could be obtained over the entire energy range of 2-6 eV (CM) with appropriately chosen E_o and n. The uncertainty of the values of E_o and n is on the order of $\pm$ 0.1. Table I contains the values of E_o and n which give the best fit to the experimental data. Values of E_o obtained from photodissociation measurements made by various researchers are also included for comparison purposes. The exponent n given in Table I varied from 2.0 to 2.5; according to the statistical theory, these CID processes are direct mechanisms--not totally unexpected in view of the structure of the CO_3^- ion. The ground state of CO_3^- is believed to be a trigonal structure having C_{2v} symmetry with an O-C-O valence angle of ~ 120°.[18] Hence, it is unlikely that an intermediate complex is formed during the collision process.

The dependence of the coefficient A in Eq (1) upon internal energy of the reactant has been shown to affect remarkedly the CID reaction cross sections.[9,19] In general, the cross sections should increase and the translational energy threshold decrease as the reactant vibrational excitation increases. In recent photodissociation experiment by Cosby and Moseley,[20] the possibility of the existence of some vibrational excited states of the CO_3^- was discussed. However, as shown in Fig. 3, excellent fit to the experimental data was obtained for various

target molecules by assuming A to be equal to a constant and no apparent lower the translational energy threshold was observed. Thus, the effect on coefficient A due to the vibrational excitation of the initial CO_3^- ion, if any, may not be important in the present study.

Thermochemistry

It is assumed that neither the reactants nor products are in the excited states at the threshold. The average bond dissociation energy of O^--CO_2 was calculated to be 1.95 ± 0.1 eV from a total of six experiment involving various target molecules. This value is in excellent agreement with the photodissociation values of ~ 1.8 eV found by Beaty et al.,[5] 1.86 ± 0.01 eV by Vestal et al.,[6] 1.93 by Cosby et al.,[20] and ~ 2.0 eV by Moseley et al.[21] This value is also in excellent agreement with the flowing afterflow value of 2.0 ± 0.2 eV found by Ferguson et al.[7]

In the present study, the formation of CO_3^- takes place by electron impact on the gaseous mixtures of N_2O and CO_2, whereas, in a number of photodissociation experiments, it takes place by electron impact on pure CO_2 (Vestal[6] and Moseley[21]) and by electrical discharge on the gaseous mixture of CO_2 and O_2 (Beaty[5]). Although the source of the formation of the CO_3^- ion is different in these experiments, the observed thresholds are the same within experimental error. This leads to the conclusion that the CO_3^- ion formed in the present experiment is indeed in the ground state.

The heat of formation of CO_3^- can be calculated from the thermodynamic cycle as follows

$$CO_3^- + X \rightarrow O^- + CO_2 + X \quad \Delta H_R = 1.95 \qquad (8)$$

then, $\Delta H_R = \Delta H_f(O^-) + \Delta H_f(CO_2) - \Delta H_f(CO_3^-)$.

Thus,

$$\Delta H_f(CO_3^-) = \Delta H_f(O^-) + \Delta H_f(CO_2) - \Delta H_R$$

$$= 1.053^{22} - 4.078^{22} - 1.95$$

$$= -4.98 \pm 0.1 \text{ eV}$$

The heat of formation of the CO_3 molecules is equal to -43 ± 5 kcal/mole (-1.864 ± 0.22 eV).[7] Thus, the electron affinity of CO_3 may be calculated from

$$EA(CO_3) = \Delta H_f(CO_3) - \Delta H_f(CO_3^-) \qquad (9)$$

$$= -1.864 + 4.98 = 3.1 \pm 0.2 \text{ eV}$$

which is comparable to the lower-limit value of 2.9 eV reported by Ferguson et al.[7] who used the flow-afterglow technique, and to the lower-limit value of ~ 2.7 eV reported by Moseley et al.[21] who used the photodetachment technique. The value of 1.8 eV reported by Burt[8] is believed to be too low for the same reason given by Ferguson et al.[7] who suggested that photodissociation instead of photodetachment may have occurred in Burt's experiment. Ferguson's argument has been confirmed by Moseley et al.[21] who recently repeated Burt's experiment.

The charge-transfer process,

$$CO^- + NO \rightarrow NO_2^- + \text{products} \quad \Delta H_R = 1.3 \pm 0.2$$

was also found in the present investigation to be endothermic by 1.3 ± 0.2 eV, as shown in Fig. 4. By assuming the reaction according to

$$CO_3^- + NO_2 \rightarrow NO_2^- + CO_3 \qquad \Delta H_R = 1.3 \tag{11}$$

and taking the electron affinity of NO_2 to be 2.3 eV,[23] the electron affinity of CO_3 was calculated to be

$$EA(CO_3) = EA(NO_2) + \Delta H_R$$

$$= 3.6 \pm 0.2 \text{ eV}$$

which is greater (by 0.5 eV) than the value of 3.1 ± 0.2 eV found from the dissociation energy of CO_3^-. However, if the above charge-transfer reaction occurs as

$$CO_3^- + NO_2 \rightarrow NO_2^- + O + CO_2 \qquad \Delta H_R = 1.3 \tag{12}$$

then, the heat of formation of CO_3^- is calculated to be -5.0 ± 0.2 eV, which is in excellent agreement with the value of -4.98 ± 0.1 eV determined from Eq (8) in the present study. This provides an internal check on the thermochemical process. The heat of formation of CO_3 is ΔH_f = -1.864 ± 0.2 eV, which leads to $D(O - CO_2) = 0.39 \pm 0.22$ eV; for the above charge-transfer process (10), the reaction (12) is probably more favorable than the reaction (11).

CONCLUSIONS

The collision-induced dissociation of CO_3^- has been shown to exhibit endothermic thresholds. The threshold behavior agrees well with the prediction of the statistical theory, the exponent n ranging from 2.0 to 2.5. These processes proceed through a direct mechanism. The bond-dissociation energy and heat of formation of CO_3^- are determined to be 1.95 ± 0.1 and -4.98 ± 0.1 eV, respectively, and the electron affinity of CO_3 is calculated to be 3.1 ± 0.2 eV.

34

REFERENCES

1. D. K. Bohme, D. B. Dunkin, F. C. Fehsenfeld, and E. E. Ferguson, J. Chem. Phys. 51, 863 (1969).
2. N. G. Adams, D. K. Bohme, D. B. Dunkin, F. C. Fehsenfeld, and E. E. Ferguson, J. Chem. Phys. 52, 3133 (1970).
3. D. A. Parkes, J. C. S. Faraday I 68, 627 (1972).
4. A. R. Anderson and J. V. F. Best, Radiat. Chem. 2, 231 (1968).
5. Beaty, Mitchell and Woo, private communication.
6. M. J. Vestal and J. Futrell, private communication.
7. E. E. Ferguson, F. C. Fehsenfeld and A. V. Phelps, J. Chem. Phys. 59, 1565 (1973).
8. J. A. Burt, J. Chem. Phys. 57, 4649 (1972).
9. C. Rebick and R. D. Levine, J. Chem. Phys. 58, 3942 (1973).
10. J. H. Futrell and C. D. Miller, Rev. Sci. Instr. 37, 1521 (1966).
11. B. M. Hughes and T. O. Tiernan, J. Chem. Phys. 55, 3419 (1971).
12. T. O. Tiernan and R. E. Marcotte, J. Chem. Phys. 53, 2107 (1970).
13. J. L. Paulson, Advan. Chem. Ser. 58, 28 (1966).
14. R. D. Levine and R. B. Bernstein, Chem. Phys. Lett. 11, 552 (1971).
15. E. K. Parkes, A. Wagner and S. Wexler, J. Chem. Phys. 58, 5522 (1973).
16. W. B. Maier, J. Chem. Phys. 41, 2174 (1964); J. Chem. Phys. 42, 1790 (1965).
17. P. J. Chantry, Bull. Am. Phys. Soc. 16, 212 (1971); J. Chem. Phys. 55, 2746 (1971).

35

18. M. E. Jacox and D. A. Milligan, J. Mol. Spectrosc. 52, 363 (1974).

19. E. K. Parkes, A. Wagner, and S. Wexler, J. Chem. Phys. 58, 5502 (1973).

20. P. C. Cosby and J. T. Moseley, to be published in Phys. Rev. Lett.

21. J. T. Moseley, P. C. Cosby, R. A. Bennett, and J. R. Peterson, to be published in J. Chem. Phys.

22. J. L. Franklin, J. G. Dillard, H. M. Rosenstock, J. T. Herron, K. Draxl, and F. H. Field, Ionization Potentials, Appearance Potentials, and Heats of Formation of Gaseous Positive Ions (U.S. Dept. of Commerce, National Bureau of Standards, Washington, D.C., 1969).

23. B. M. Hughes, C. Lifshiftz, and T. O. Tiernan, J. Chem. Phys. 59, 3162 (1973).

FIGURE CAPTIONS

Fig. 1. (a) Calculated relative energy distributions, $W(E'/E_1)$ (solid line) and $W(E')$ (dashed line), for the reaction pair CO_3^-/Xe at 3.6 eV CO_3^- laboratory energy at 433°K. (b) Calculated relative energy distribution, $W(E_1)$, for the incident ion energy spread.

Fig. 2. Energy dependence of the cross section for the collision-induced dissociation reaction of CO_3^- with rare gas atomic and molecular targets. The base lines for some experiments are shifted as indicated in the graph.

Fig. 3. Calculated cross section as a function of laboratory energy (solid line) for CID reaction of CO_3^- on various target molecules at 433°K; obtained by convoluting appropriate energy distribution functions with statistical threshold functions (dashed line). Points are experimental data.

Fig. 4. CRoss section (arbitrary units) as a function of nominal center of mass energy (eV) for the reaction $CO_3^- + NO_2 \rightarrow NO_2^- +$ products.

Table I

Best fit values of E_o and n obtained by convoluting $\sigma = A(E - E_o)^n/E$ with the energy distribution for the collision-induced dissociation of

$$CO_3^- + X \rightarrow O^- + CO_2 + X$$

Target Gas	n (± 0.1)	E_o (± 0.1 eV)	E_o (Lit.)
Xe	2.2	1.9	1.8[5]
Kr	2.0	1.9	1.86 ± 0.01[6]
Ar	2.2	1.9	~ 1.93[20]
Ne	2.0	2.0	~ 2.0[21]
O_2	2.4	2.0	2.0 ± 0.2[7]
N_2	2.5	2.0	
		Ave. 1.95	

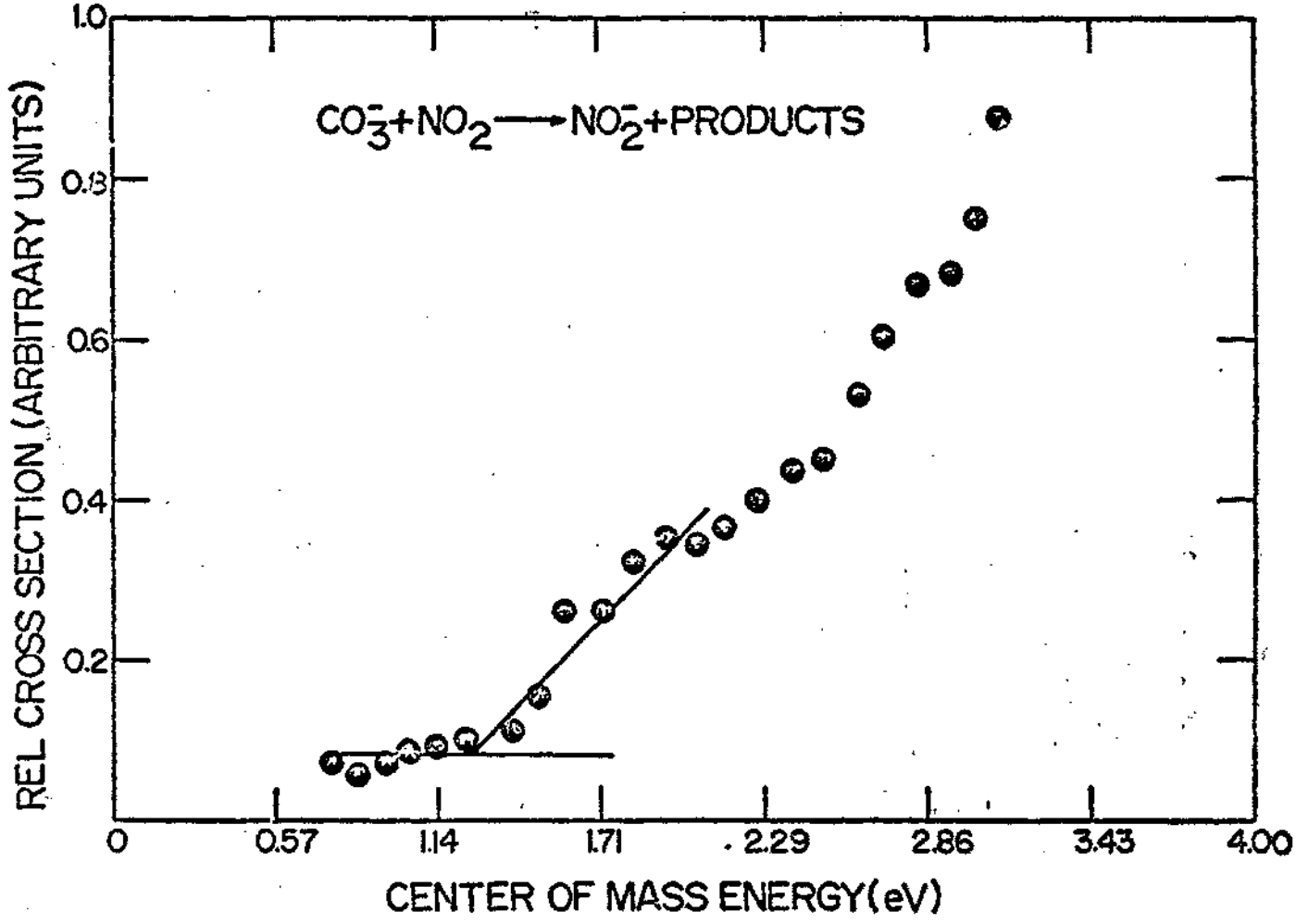
$CO_3^- + NO_2 \longrightarrow NO_2^- + PRODUCTS$
REL CROSS SECTION (ARBITRARY UNITS)
1.0
0.8
0.6
0.4
0.2
0
0.57
1.14
1.71
2.29
2.86
3.43
4.00
CENTER OF MASS ENERGY(eV)

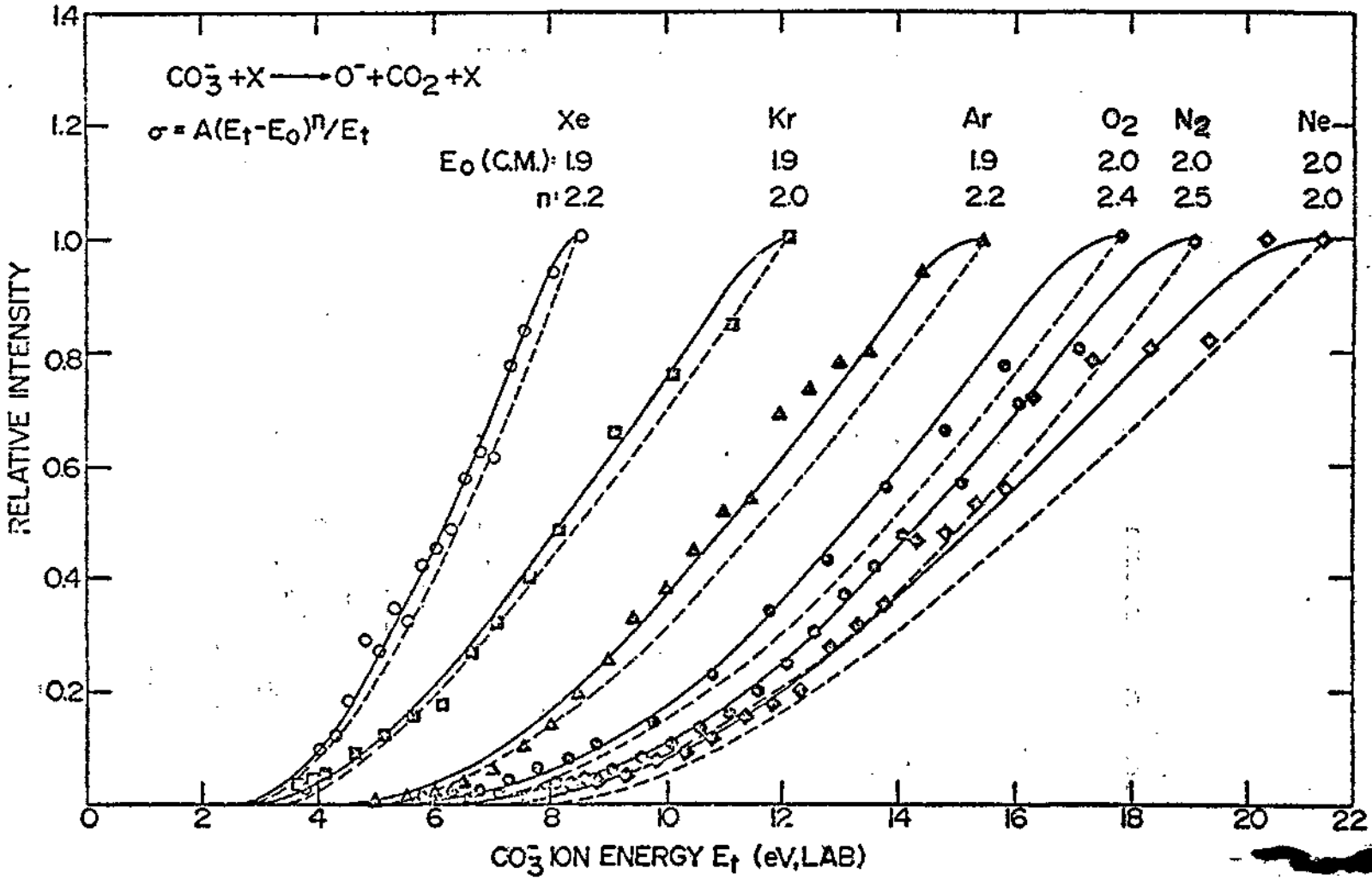
$CO_3^- + X \longrightarrow O^- + CO_2 + X$
$\sigma = A(E_t - E_0)^n / E_t$
Xe
Kr
Ar
O_2
N_2
Ne
E_0 (C.M.): 1.9 1.9 1.9 2.0 2.0 2.0
n: 2.2 2.0 2.2 2.4 2.5 2.0
RELATIVE INTENSITY
CO_3^- ION ENERGY E_t (eV, LAB)
0 2 4 6 8 10 12 14 16 18 20 22
0.2 0.4 0.6 0.8 1.0 1.2 1.4

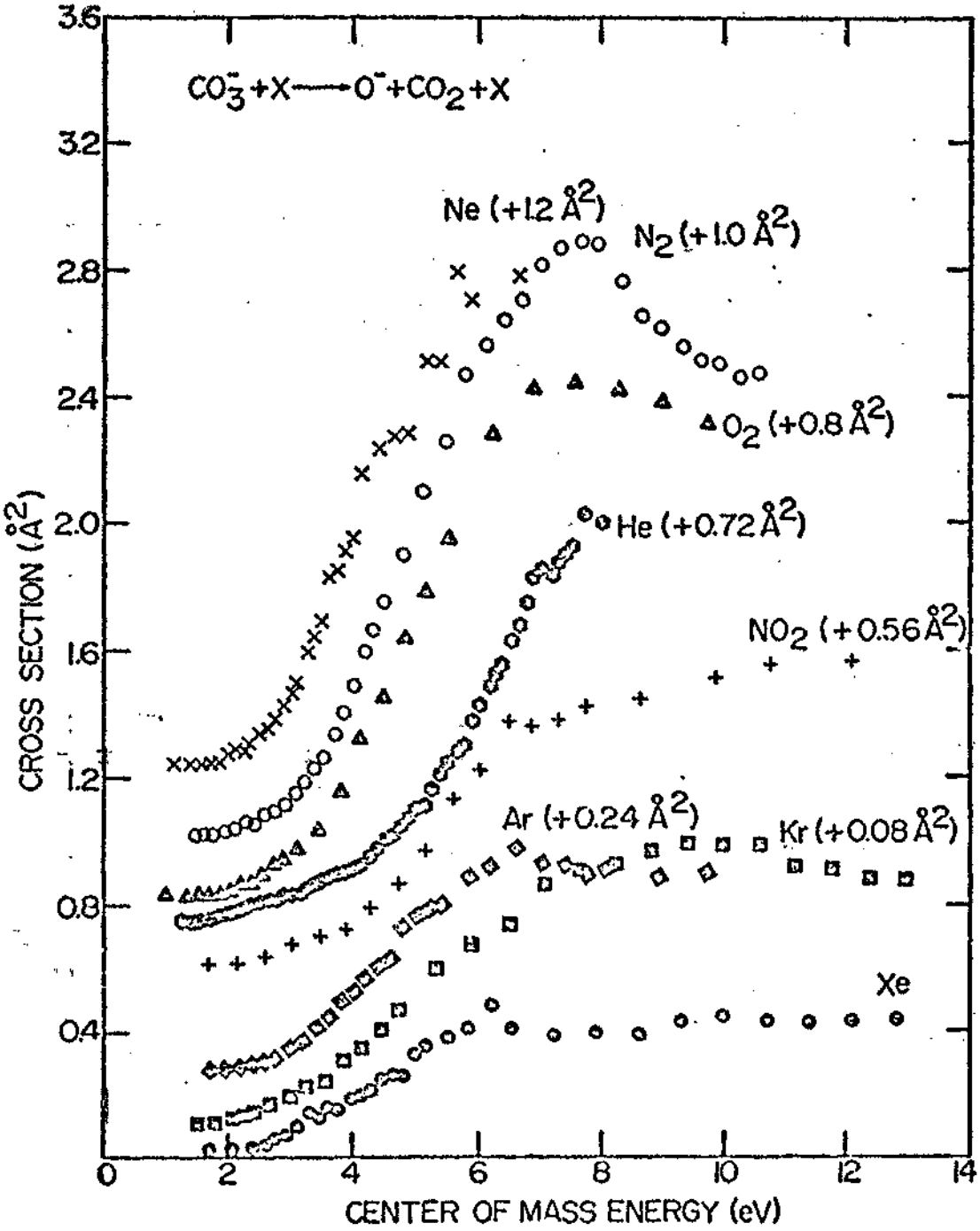
$CO_3^- + X \longrightarrow O^- + CO_2 + X$
Ne (+1.2 Å²)
N₂ (+1.0 Å²)
O₂ (+0.8 Å²)
He (+0.72 Å²)
NO₂ (+0.56 Å²)
Ar (+0.24 Å²)
Kr (+0.08 Å²)
Xe
CROSS SECTION (Å²)
CENTER OF MASS ENERGY (eV)
0
2
4
6
8
10
12
14
0.4
0.8
1.2
1.6
2.0
2.4
2.8
3.2
3.6

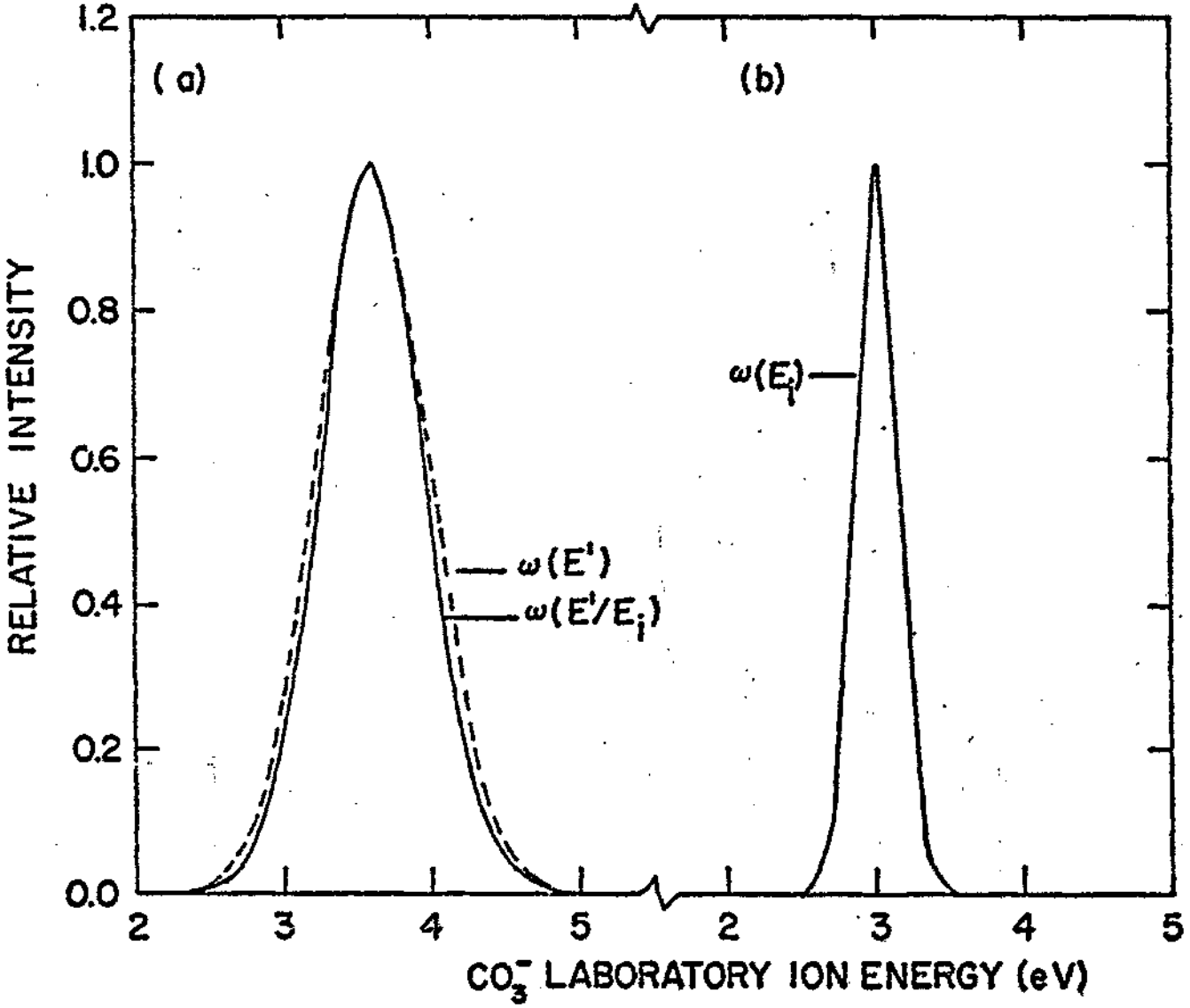
1.2
1.0
0.8
0.6
0.4
0.2
0.0
RELATIVE INTENSITY
(a)
(b)
ω(E')
ω(E'/E_i)
ω(E_i)
2
3
4
5
2
3
4
5
CO3- LABORATORY ION ENERGY (eV)

CHARACTERIZATION OF THE POTENTIAL ENERGY SURFACE OF THE $X^2A'(^2\Pi)$ STATE OF N_2O^-.*

Richard L. C. Wu†

Systems Research Laboratories, Inc.
2800 Indian Ripple Road
Dayton, Ohio 45440

T. O. Tiernan†

Aerospace Research Laboratories (LJ)
Wright Patterson Air Force Base, Ohio 45433

D. G. Hopper and A. C. Wahl

Chemistry Division
Argonne National Laboratory
Argonne, Illinois 60439

*Work partially performed under the auspices of USERDA and Air Force Contract MIPR899474 00117, Amendment 1.

†Present address: Department of Chemistry, Wright State University, Dayton, Ohio 45431.

43<

ABSTRACT

Collision-induced dissociation of N_2O^- by six rare gas and diatomic target gases yields an average value of 0.43 ± 0.1 eV for the dissociation energy $D(N_2—O^-)$. This measurement along with literature values for other quantities leads to an electron affinity of 0.22 ± 0.1 eV and a bond dissociation energy $D(N-NO^-)$ of 5.13 ± 0.1 eV. These values pertain to the X^2A' ground state of N_2O^-. Ab initio LCCG-MO SCF and OVC-MCSCF calculations on the potential energy surface of this state show that it has a minimum in C_s symmetry with an N-N-O angle near 125°. The geometry of each minimum has N-N and N-O bond lengths that are approximately 5 and 15% greater, respectively, than the bond lengths in neutral N_2O ($X^1\Sigma^+$). The computed minimum energy geometry at the SCF level with a better than double-zeta quality basis set is, within a precision of 2%, $R_{NN} = 1.20$ Å, $R_{NO} = 1.38$ Å, $\theta_{NNO} = 124°$. The valence force field force constants for N-N stretch, for N-O stretch, and for bending are found to be 11.5, 3.9, and 0.65 md/Å, respectively, at this geometry.

I. INTRODUCTION

The potential energy surface of the $X^2A'(^2\Pi)$ ground state of the nitrous oxide negative ion N_2O^- has been of some concern in recent years.[1-11] This molecular system is interesting in that the possible ionospheric associative detachment reaction

$$O^-(^2P) + N_2(X^1\Sigma_g^+) \rightarrow N_2O(X^1\Sigma^+) + e + 0.21\ eV \qquad (1)$$

is not observed in laboratory experiments at 300°K.[2-6] The upper bound to the thermal rate constant has been placed at 10 to 1×10^{-13} cm^3/s by various experiments.[2,3,5] The origin of the low thermal rate for this exothermic reaction may be discussed in terms of the characteristics of this X^2A' ground state potential energy surface. This surface connects adiabatically to the reagent asymptote, $O^-(^2P)$, $N_2(X^1\Sigma_g^+)$.[11] The effects of increased vibrational temperature, which is common in the ionosphere but which has not been investigated in laboratory experiments, can also be discussed in terms of this potential surface. Knowledge of this surface can also contribute to the understanding of the recombination reaction

$$O^-(^2P) + N_2(X^1\Sigma_g^+) \overset{M}{\rightarrow} N_2O^-(X^2A') \qquad (2)$$

and the dissociative attachment reaction[8]

$$N_2O(X^1\Sigma^+) + e \rightarrow N_2(X^1\Sigma_g^+) + O^-(^2P) \qquad (3)$$

This paper presents some experimental and theoretical studies conducted to characterize the $N_2O^-(X^2A')$ potential energy surface. The results of collision-induced dissociation experiments including corrections for Doppler motion and ion energy spread are presented in Section 2,

followed by a presentation of ab initio LCBF-MO-SCF and OVC-MCSCF calculations in Section 3. Section 4 is a discussion of the present results including comparisons with previous work. Conclusions are then made in Section 5.

2. COLLISION-INDUCED DISSOCIATION AND CHARGE-EXCHANGE EXPERIMENTS WITH N_2O^-

A. Apparatus

The ARL in-line tandem mass spectrometer was utilized in this study. The instrument has been described previously.[12,13] In brief, it consists of two double-focusing mass spectrometers connected by a field-free collision chamber. The primary ion is formed in the ion source of the first stage mass spectrometer which produces a mass and energy analyzed beam. In this study the primary ion of N_2O^- was formed by electron impact on N_2O molecules at high pressures (~ 0.1 μ):

$$N_2O(X^1\Sigma^+) + e \rightarrow N_2O^{-*}(X^2A') \xrightarrow{N_2O} \xrightarrow{N_2O} \cdots \xrightarrow{N_2O} N_2O^-(X^2A') \quad (4)$$

It is estimated that N_2O^{-*} suffered approximately ten collisions within the source chamber and that exiting N_2O^- was, thus, predominately in the ground vibrational state. The energy spread of the ion beam is about ± 0.3 eV (LAB) over the ion energy range 0.3 to 180 eV (LAB).[12,13] The second stage mass spectrometer was used to analyze the masses of the product ions formed in the collision chamber. Pulse counting techniques were used to measure the product ion currents. The collection stage in this instrument is fixed at 0° (LAB) scattering angle. The temperature of the collision chamber was maintained at 160°C and the pressure was varied from 10 to 40 μ. The product ion O^- signal intensity was linear over this target gas pressure range indicating that single bimolecular collision events $N_2O^- + M$ prevailed. The experiments with the various target gases were, thus, carried out at a target gas pressure of 40 μ

in the collision chamber in order to obtain a high O^- product ion intensity while yet maintaining single collision conditions. Production intensity I_p was converted to an observed cross section σ_{obs} via the relationship

$$\sigma_{obs}(E_{io}) = a\, I_p(E_{io})/I_i(E_{io})\, n \tag{5}$$

where $I_i(E_{io})$ is the primary ion intensity and n is the target pressure. The conversion factor a was determined from the reported absolute cross section (63 $Å^2$, Reference 14) and the observed product ion intensity at 0.3 eV reactant ion energy E_{io} (LAB) for the charge transfer reaction

$$O^-(^2P) + NO_2(X^2A_1) \rightarrow O(^3P) + NO_2^-(X^1A_1) + 0.81\ eV \tag{6}$$

See Fig. 1.

B. Threshold Behavior and Corrections for the Ion Energy Distribution and Doppler Motion

The threshold behavior of the total cross section σ_n for collision induced dissociation reactions

$$RS + M \rightarrow M + R + S \tag{7}$$

is known from theoretical considerations[15] and experimental studies[16-19] to be well approximated by the functional form

$$\sigma(E_{rel}) = A(E_t - E_o)^n/E_{rel} \tag{8}$$

In Eq (8) E_t is the total energy (C.O.M.) and E_{rel} the relative translational energy of the reactants; E_o is the threshold total energy. The exponent n depends upon the mechanism of Reaction (7): the range

$1.9 < n < 2.2$ corresponds to a direct process, and the range $1.5 < n < 1.8$ to an indirect process.[15] The coefficient A is a function of the internal energy of the reactant RS.[15]

In the present beam-chamber experiments the observed cross section is related to the absolute cross section by the integral equation

$$\sigma_{obs}(E_{io}) = \int_0^{\infty} dE_i \int_{-\infty}^{+\infty} du_m \, f(E_i|E_{io}) \, f(u_m) \, \sigma(E_{rel}) \tag{9}$$

where E_{io} is the set-point of the ion beam energy in the laboratory frame, E_i is the laboratory energy of the ions moving along the axis directed through the collision chamber, u_m is the speed of the target molecule M along the same axis, and $f(E_i|E_{io})$ is the distribution function for the ion energy about the set-point E_{io}. The latter function is assumed to be of the form

$$f(E_i|E_{io}) = (a\pi)^{-1} \exp[-(E_i - E_{io})^2/a^2] \, dE_i \tag{10}$$

where the parameter a is determined to be 0.2 by the requirement that the half-width-at-half-maximum be 0.3 eV. It is further assumed in Eq (9) that $f(u_m)$ is the one-dimensional Maxwellian distribution of target gas molecular speed u_m

$$f(u_m) = (m_m/2\pi kT_m)^{1/2} \exp(-\tfrac{1}{2} m_m u_m^2/kT_m) \, du_m \tag{11}$$

with m_m being the mass of the target molecule, k, Boltzman's constant, and T_m the target gas temperature. Lastly in Eq (9), E_{rel} is the center-of-mass collision energy

$$E_{rel} = \tfrac{1}{2} \mu (u_i - u_m)^2 \tag{12}$$

with the reduced mass μ and ion speed u_i being

$$\mu = m_i\, m_m/(m_i + m_m) \tag{13}$$

$$u_i = (2E_i/m_i)^{1/2} \tag{14}$$

and m_i being the ion mass. The ion energy distribution function of $f(E_i|E_{io})$ given in Eq (10) has been previously established for the ARL tandem mass spectrometer.[12,13] The absolute cross section $\sigma_{obs}(E_{rel})$ is assumed to have the form of Eq (8); since the reagent molecules are taken to have no internal excitation the total energy E_t reduces to E_{rel}. In some places this function is compared to experiment on the laboratory energy scale with all energy of motion attributed to the ion

$$E_i' = ((m_i + m_m)/m_i)\, E_{rel} \tag{15}$$

in which case the mass factor is raised to the $(n-1)$ power multiplied into the constant factor A to form a new constant A'.

$$\sigma(E_i') = A'(E_i' - E_o)^n/E_i' \tag{16}$$

In this case, of course, E_o is obtained in the laboratory scale. Optimum values of the parameters E_o and n are determined for each target gas by means of a grid search procedure. Visual comparisons of plots of $\sigma_{obs}(E_{io})$ as evaluated from Eqs (8)-(14) with the observed data were made for all combinations of n = 2.1, 2.2, 2.3, 2.4, and 2.5 for E_o(COM) = 0.3, 0.4, 0.5, 0.6 eV.

C. Results

A lower bound of greater than zero for the electron affinity for N_2O was established by the observation of m/e = 44 negative ions from electron impact on N_2O gas.

An upper bound to the electron affinity of N_2O was established by a study of the cross section for the charge transfer reaction

$$N_2O^-(X^2A') + O_2(X^3\Sigma_g^-) \rightarrow O_2^-(X^2\Pi_g) + N_2O(X^1\Sigma^+) \qquad (17)$$

The results are shown in Fig. 1 along with the standard charge transfer Reaction (6). The cross section for Reaction (17) was found to decrease monotonically with the translational energy of the incident N_2O^- ion from the lowest energy obtainable, 0.3 eV, to above 8 eV. This result indicates that Reaction (17) is exothermic and that the electron affinity of N_2O is smaller than the electron affinity of O_2. The electron affinity of O_2 has been determined to be 0.45 ± 0.1 eV by various researchers using differing techniques.[20]

Direct determinations of the N_2-O^- bond dissociation energy -- and, thence, the electron affinity and the N-NO^- bond dissociation energy were then undertaken. The cross section $\sigma(E_{io})$ the collision-induced dissociation Reaction (/), where R = N_2 and S = O^-, was measured as a function of the nominal ion energy E_{io} for each of various target molecules M = Xe, Kr, Ar, Ne, He, and N_2. The results are shown in Fig. 2. All of these reactions exhibit thresholds and, thus, may be expected to be endoergic. In the threshold region the cross sections show exponential increase, followed by a linear rise to a maximum, and then a gradual decrease. In order to obtain the true energy threshold for each reaction the convolution

technique described above in Eqs (8)-(14) was employed to resolve the energy distribution resulting from the thermal motion of the target molecules M (Doppler correction) and the energy spread of the incident ion beam. In Fig. 3 the calculated cross sections [Eq (9)] for O^- from N_2O^- + Ne at 433°K are drawn as solid lines for various combinations of E_o and n. Visual comparisons with the data, which are shown as solid points, show that the computed curve with $E_o = 0.4$ eV and $n = 2.3$ is the best fit. The uncertainty in the values of E_o and n is on the order of $\pm$ 0.1; these error limits are estimated from the ranges of E_o and n which yielded a good fit to the experimental data. Figure 4 compares the best fit curves [Eq (9)] for all of the target molecules The values of E_o and n defining these best fits are tabulated in Table I. The dashed lines in Figs. 3 and 4 are the unconvoluted cross section functions [Eq (16)].

From Table I the average value for the bond dissociation energy $D(N_2\text{-}O^-)$ is 0.43 $\pm$ 0.1 eV. This result is based on the assumption mentioned above that neither the reagent nor the product molecules are internally excited near threshold. The electron affinity of $O(^3P)$ is 1.47 eV[20] and the dissociation energy $D(N_2\text{-}O)$ is 1.68 eV.[21] From these values the electron affinity of $N_2O(X^1\Sigma^+)$ is 0.22 $\pm$ 0.1 eV. The bond dissociation energy D(N-NO) and the electron affinity of $NO(^2\Pi)$ are 4.93 eV[21] and 0.02 eV,[20] respectively. Thus, the bond dissociation energy $D(N\text{-}NO^-)$ is 5.13 $\pm$ 0.1 eV.

5i-

3. AB INITIO DETERMINATION OF THE EQUILIBRIUM GEOMETRY AND FORCE CONSTANTS OF N_2O^-

A. Method of Calculation

Calculations on the potential energy surface of the $X^2A'(^2\Pi)$ state of N_2O^- were carried out with both a single (SCF) and a multi-configuration (MCSCF) wave function. The calculations were made with the BISONMC and POLYINT codes[22,23] with 4s3p contracted[24] Gaussian basis sets.[25] The SCF determinant was

$$\begin{aligned} C_s&: 1a'^2 2a'^2 3a'^2 4a'^2 5a'^2 6a'^2 7a'^2 8a'^2 9a'^2 10a'^2 1a''^2 2a''^2 \\ C_{\infty v}&: 1\sigma^2 2\sigma^2 3\sigma^2 4\sigma^2 5\sigma^2 6\sigma^2 1\pi_x^2 7\sigma^2 2\pi_x^2 3\pi_x 1\pi_y^2 2\pi_y^2 \end{aligned} \qquad (18)$$

The MCSCF wave function was developed for the linear π state by the sequential consideration of doubly excited configurations to correlate the 8σ, 9σ, and 3π orbitals. The 15 configurations of the present MCSCF wave function are listed in Table II along with their weighting coefficients at selected geometries. While the MCSCF configuration list has not been optimized at a geometry near the minimum of the X^2A' potential surface, it should be indicative of the effects of correlation upon the minimum located in the extensive scan with the single determinant wave function. The MCSCF molecular orbitals are presented in Tables IIIa and IIIb at the first and third geometries of Table II.

B. SCF Equilibrium Geometry and Force Constants

The SCF bending curves at various combinations of bond lengths (R_{NN}, R_{NO}) are displayed in Fig. 5(a). These results, along with an examination of those of Fig. 5(b) as they were obtained, indicate an equilibrium geometry near 125° with $R_{NN} \simeq 1.05\ R^r_{NN}$ and $R^r_{NO} \simeq 1.15\ R^r_{NO}$,

where R_{NN}^{r} and R_{NO}^{r} are the equilibrium values for $N_2O(X^1\Sigma^+)$. Figs. 5(b) and 5(c) give the SCF minimum at $R_{NN} = 2.27$ a.u., $R_{NO} = 2.60$ a.u., and $\theta_{NNO} = 124°$. The valence field force constants at this geometry are shown in Table IV. The bending force constant is computed as the second derivative of the bending potential in Fig. 5(c) divided by the bond lengths given above from Fig. 5(b). The bond stretch force constants were computed as the second derivative of the potential curves given in Fig. 5(b).

C. MCSCF Bending Curves

The bending curves obtained with the above described 15 configuration MCSCF wave function are shown in Fig. 6. Comparison of these curves with the corresponding SCF curves in Fig. 5(a) shows that the correlation energy added by the 14 extra configurations in the present MCSCF wave function do not have a strong effect on the geometry and shape of the potential minimum. This is, of course, to be expected from the high coefficient of the main configuration. See Table II. The MCSCF and SCF potential energy surfaces are compared in Table IV.

4. DISCUSSION

A. Interpretation of the Collision-Induced Dissociation Results in Terms of Theory

The statistical theory derived by Rebick and Levine[15] is found to satisfactorily describe the threshold behavior of the collision-induced dissociation reactions of N_2O^- impacted on five rare gas and N_2 diatomic molecules. The exponent n given in Table I ranges from 2.3 to 2.5 for the various target gases. This range is larger than the upper limit of 2.2 given by Rebick and Levine, but it is contained by the upper limit

derived by Levine and Bernstein.[26] By comparison a range 1.4 to 2.3 was reported by Maier[16] and by Parks, Wagner, and Wexler[18] from their studies of the collision-induced dissociation of positive ions. According to the statistical theory leading to Eq (9) the collision-induced dissociation reactions of N_2O^- examined in the present work are direct processes. That these processes do not involve the formation of an intermediate collision complex is not totally unexpected since the target gases employed were composed of closed shell molecules of essentially zero electron affinity.

B. Electron Affinity of N_2O

The electron affinity of the N_2O molecule has been determined by various groups using different experimental techniques. A tabulation of these studies is displayed in Table V. That the adiabatic electron affinity might be positive while the vertical electron affinity remained negative was suggested in 1967 by Ferguson, Fehsenfeld and Schmeltekopf.[4] Bardsley[7] concurred in his molecular orbital analysis in 1969. In 1971 Wentworth, Chen and Freeman[8] reported an adiabatic electron affinity of 0.3 ± 0.2 eV from thermal electron attachment rate experiment. Malley et al.[9] reported a lower bond of -0.15 ± 0.1 eV from their cesium collisional ionization experiments in 1973. Tiernan and Clow[10] report 0.6 eV from collision-induced dissociation experiments, but they made no correction for the ion or the target ion velocity distributions. From the present experiments one can see that N_2O^- is not metastable since its detection in the second stage mass spectrometer implies a lifetime of greater than 50 μsec. Also, as discussed previously, observation of the

charge transfer Reaction (6) establishes the electron affinity as less than that of O_2, 0.45 $\pm$ 0.1 eV. The present collision induced dissociation result of 0.22 $\pm$ 0.1 eV, which has been corrected for the ion and product molecule energy distribution, is in excellent agreement with the result of Wentworth et al.[8]

C. Equilibrium Geometry of the X^2A' State of N_2O^-

The presently reported equilibrium geometry (Table IV) is the best available to date. A suggestion[4] that the equilibrium angle would be close to that of the isoelectronic neutral molecule NO_2 - 134° - is about 10° too high. From Figs. 5(a) and 6 this latter overestimate may be seen to be attributable to an approximately 10° decrease in the bending potential minimum upon stretching the N-N and N-O bond elengths about 10% each from the neutral equilibrium values.

The statement by Wentworth et al.[8] in the abstract of their paper that they determined the equilibrium angle to be about 160° appears to be an inadvertent error. These authors actually assume an equilibrium value of 134° in the analysis of their data to determine the electron affinity tabulated in Table V. From the text of their paper the 160° figure corresponds to the threshold bending angle for thermal electron attachment -- i.e., for a crossing of the $N_2O(X'\Sigma)$ and $N_2O^-(X^2A')$ potential energy surfaces at near neutral equilibrium values for the bond lengths.

D. Contour Plots of $V(R_{NO}, \theta_{NNO}|R_{NN})$ for $N_2O^-(X^2A')$ and $N_2O(X^1\Sigma^+)$

Wentworth, Chen, and Freeman[8] employed a parameterized Morse function which may be written

$$V(R_{NO}, \theta_{NNO} | R_{NN}) = D_{NN-O} \{ -2 \exp[-\beta(R_{NO} - R_{NO}^e)] f(\theta_{NNO}) + \exp[-2\beta(R_{NO} - R_{NO}^e)] + 1 \} \quad (19)$$

where $f(\theta)$ is determined from the assumption that

$$V(R_{NO}^e, \theta_{NNO} | R_{NN}^e) - D_{NN-O} = \frac{1}{2} k (\theta_{NNO} - \theta_{NNO}^e)^2 \quad (20)$$

and the parameters D_{NN-O}, β, and k depend, in turn, implicitly upon $R_{NN}^e(X^1\Sigma^+)$. Wentworth et al. wroteone such Eq (19) for $N_2O(X^1\Sigma^+)$ and one for $N_2O^-(X^2A')$, took literature values for the N_2O parameters,[21] assumed $\theta_{NNO}^e = 134°$ for N_2O^-, $D_{NN-O^-} = D_{NN-O} = 3.64$ eV and determined k for N_2O^- by requiring that the lowest crossing point $(R_{NO}, \theta_{NNO})_{threshold}$ of the two surfaces occur at an energy 0.45 ± 0.02 eV above the zero point energy of N_2O. The latter energy is the activation energy that Wentworth et al.[8] determined from their measurement of the temperature dependence of the rate of Reaction (3) in the range -66 to 215°C. The results of the present study can be employed to establish all the parameters in the Eqs. (19-20) as written for N_2O^- and to determine the crossing threshold locu $(R_{NO}, \theta_{NNO})_{threshold}$ and activation energy with respect to zero point N_2O independently of the experimental determination of Wentworth et al. A comparison between the predicted and measured thresholds will then serve as a check on the appropriateness of the parametric potential function form given by Eqs. (19-20). The implicit treatment given R_{NN} in Eq.(19) may be justified on the grounds that it increases but 5% in going from N_2O to N_2O^-, and the decreases to 2% less than the N_2O equilibrium value on decomposition to $N_2 + O^-$. The parameters are summarized in Table VI. The

functions $f(\theta_{NNO})$ have been fit to the functional form $a + b\theta + c\theta^2$, where the constants a, b, and c are included in Table VI. Figure 7 is a combined contour map with the function $V(R_{NO}, \theta_{NNO}|R_{NN})$ for $N_2O^-(X^2A')$ (dashed contour lines) on top of that for $N_2O(X^1\Sigma^+)$ (solid contour lines). The crossing locus is shown by the symmetric pair of dash-dot lines.

5. CONCLUSION

The potential energy surface of the $X^2A'(^2\Pi)$ state of N_2O^- is stable in its equilibrium region with respect to either dissociation or detachment. The key quantities required to characterize this surface have been determined and are summarized in Table VII. In addition a value of 0.22 ± 0.1 eV was established for the adiabatic electron affinity of N_2O.

REFERENCES

1. J. F. Paulson, Adv. Chem. Ser. 58, 28 (1966).
2. F. C. Fehsenfeld, E. E. Ferguson, and A. L. Schmeltekopf, J. Chem. Phys. 45, 1844 (1966).
3. F. Kaufman, J. Chem. Phys. 46, 2449 (1967).
4. E. E. Ferguson, F. C. Fehsenfeld, and A. L. Schmeltekopf, J. Chem. Phys. 47, 3085 (1967).
5. J. L. Moruzzi, J. W. Ekin, and A. V. Phelps, J. Chem. Phys. 48, 3070 (1968).
6. P. J. Chantry, J. Chem. Phys. 51, 3380 (1969).
7. J. N. Bardsley, J. Chem. Phys. 51, 3384 (1969).
8. W. E. Wentworth, E. Chen, and R. Freeman, J. Chem. Phys. 55, 2075 (1971).
9. S. J. Nalley, R. N. Compton, H. C. Schweinler, and V. E. Anderson, J. Chem. Phys. 59, 4125 (1973).
10. T. O. Tiernan and R. P. Clow, Adv. Mass Spect. 6, 295 (1974).
11. M. Krauss, D. G. Hopper, P. J. Fortune, A. C. Wahl, and T. O. Tiernan, "Potential Energy Surfaces for Air Triatomics. Volume I. Literature Review," ARL TR 202, Vol. I, Air Force Systems Command, June 1975. Available from the National Technical Information Service, U.S. Department of Commerce, Springfield, Va. 22151.
12. T. O. Tiernan and R. E. Marcotte, J. Chem. Phys. 53, 2107 (1970).
13. B. M. Hughes and T. O. Tiernan, J. Chem. Phys. 55, 3419 (1971).

14. This value has been deduced from the thermal rate constant of 1.2×10^{-9} cm^3/molecule-sec reported in Reference 1 from the equation $k = \bar{\sigma v}$. The $^{16}O^-$ velocity was computed as $\bar{v} = (2E/m)^{1/2}$ at E = 0.3 eV (LAB).

15. C. Rebick and R. D. Levine, J. Chem. Phys. 58, 3942 (1973).

16. W. B. Maier II, J. Chem. Phys. 41, 2174 (1964).

17. W. B. Maier II, J. Chem. Phys. 42, 1790 (1965).

18. E. K. Parks, A. F. Wagner, and S. Wexler, J. Chem. Phys. 58, 5522 (1973).

19. R. L. C. Wu and T. O. Tiernan, "Collision-Induced Dissociation of CO_3^-," in preparation (1975).

20. CRC Handbook of Chemistry and Physics, 55th Edition, edited by R. C. Weast, CRC Press, Cleveland, 1974-1975, and references listed therein.

21. G. Herzberg, Electronic Spectra and Electronic Structure of Polyatomic Molecules, Van Nostrand, Princeton, 1966.

22. G. Das and A. C. Wahl, "BISON-MC" A FORTRAN Computing System for Multiconfiguration Self-Consistent-Field (MCSCF) Calculations on Atoms, Diatoms, and Polyatoms," Argonne National Laboratory Technical Report, ANL-7955 (1972). For availability, see Reference 11.

23. D. Neuman et al., "POLYATOM (Version 2)," Quantum Chemistry Program Exchange Indiana U., Bloomington, Indiana. PA300 was modified and linked to BISON-MC by A. Hinds of Argonne National Laboratory. The modified version, which generates canonical lists of integrals and no labels, is referred to as POLYINT.

24. T. H. Dunning, Jr., J. Chem. Phys. 55, 3958 (1971).

25. S. Huzinaga, J. Chem. Phys. 42, 1293 (1965).

26. R. D. Levine and R. B. Bernstein, Chem. Phys. Lett. 11, 552 (1971).

27. E. B. Wilson, J. C. Decius, and P. C. Cross, Molecular Vibrations. The Theory of Infrared and Raman Vibrational Spectra, McGraw-Hill, New York, 1955, p. 176.

60

FIGURE CAPTIONS

Figure 1. Charge transfer cross sections for O^-/NO_2 (●) and N_2O^-/O_2 (■).

Figure 2. Collision-induced dissociation cross sections of N_2O^- to $N_2 + O^-$ by target gas molecules X = Xe, Kr, Ar, Ne, He, and N_2.

Figure 3. Optimization of the parameters E_o and n for m = Ne. The effect of the variation of n is shown for three values of E_o. The curves for $E_o = 0.3$ and $E_o = 0.5$ are off-set 4 and 8 eV, respectively, on the energy scale for clarity of presentation. The solid points are the data from Figure 3. The dashed lines are for Eq (16). The solid lines are for Eq (9). The near Gaussian distribution curve centered about $E_{io} \simeq 3$ eV (LAB) is for the combined distribution function $f_o = f(E_i/E_{io})\ f(u_m)$ with which Eq (16) is convoluted in Eq (9) in order to compute an "observed" cross section for direct comparison with the unadjusted experimental data.

Figure 4. Comparison of the Eq (9) optimum computed values (solid lines) for $\sigma_{obs}(E_{io})$ with the uncorrected experimental values (solid symbols) for target gases Xe (●), Kr (■), Ar (◆), N_2 (▲), and He (⊛). The optimized values for E_o and n in Eq (16) are shown for each collision gas. The dashed lines are from Eq (16). Comparison of the solid and dashed lines provides a visual indication of the importance of the combined Doppler and ion energy spread effects upon the cross section for the various target gases.

6i

Figure 5. (a) Bending potential energy curves for $N_2O^-(X^2A')$ with an SCF wave function and a 4s3p basis set. Curves are drawn for combinations of the two bond lengths ranging from 100 to 130% of their respective equilibrium values for $N_2O(X^1\Sigma^+)$.

(b) SCF bend stretching potential energy curves for $N_2O^-(X^2A')$ at 125°.

(c) SCF bending potential energy curve for $N_2O^-(X^2A')$ at near equilibrium bond lengths $R_{NN} = 2.2745$ a.u. and $R_{NO} = 2.6011$ a.u.

Figure 6. MCSCF bending curves for N_2O^- with the $N_2O(X^1\Sigma^+)$ bond lengths and with 10% greater values.

Figure 7. Contour plot of Eq (19) written for $N_2O^-(X^2A')$ (dashed contours) over the same equation with parameters for $N_2O(X^1\Sigma^+)$. The dot-dash line is the intersection locus.

62

Table I

Best-fit values of E_o and n obtained by combining $\sigma = A(E - E_o)^n/E$ with the energy distribution for the collision-induced dissociation of

$$N_2O^- + X \rightarrow O^- + N_2 + X$$

Target Gas	n (± 0.1)	E_o (± 0.1 eV, C.O.M.)
Xe	2.5	0.5
Kr	2.3	0.4
Ar	2.4	0.4
Ne	2.3	0.4
He	2.4	0.4
N_2	2.5	0.5
Average Values	2.4	0.43

Table II

Configurations of the MCSCF wave function for N_2O^- in its $X^2A'(^2\Pi)$ state and their weighting coefficients at selected geometries

No.	Orbital Occupancy[a]												Spin Coupling[b]	Weighting Coefficient		
	4a'	5a'	6a'	7a'	8a'	9a'	10a'	11a'	12a'	1a''	2a''	3a''		R_{NN}	2.132	2.132	2.345
	4σ	5σ	6σ	$1\pi_x$	7σ	$2\pi_x$	$3\pi_x$	8σ	9σ	$1\pi_y$	$2\pi_y$	$3\pi_y$		R_{NO}	2.238	2.238	2.462
														θ_{NNO}	180°	130°	130°
1.	2	2	2	2	2	2	1	0	0	2	2	0	D		0.973	0.972	0.963
2.	2	2	2	1	2	2	0	0	2	2	2	0	D		0.009	0.005	0.007
3.	2	2	2	:	2	1	0	0	2	2	2	0	D		0.000	0.000	0.001
4.	2	2	2	2	2	2	1	0	0	0	2	2	D		-0.145	-0.147	-0.175
5.	2	2	2	2	2	2	1	0	0	2	0	2	D		-0.042	-0.048	-0.045
6.	2	2	2	2	0	2	1	2	0	2	2	0	D		-0.052	-0.055	-0.068
7.	2	2	2	2	0	2	1	0	2	2	2	0	D		-0.005	-0.005	-0.006
8.	2	2	2	2	:	1	2	0	0	2	1	1	TD		0.037	0.030	0.025
9.	2	2	2	2	2	1	2	0	0	2	1	1	SD		-0.026	-0.023	-0.018
10.	2	2	2	:	2	2	2	0	0	1	2	1	TD		0.104	0.107	0.110
11.	2	2	2	1	2	2	2	0	0	1	2	1	SD		-0.088	-0.104	-0.114
12.	2	2	0	2	2	2	1	2	0	2	2	0	D		-0.012	-0.010	-0.013
13.	0	2	2	2	2	2	1	0	2	2	2	0	D		-0.077	-0.071	-0.089
14.	2	0	2	2	2	2	1	0	2	2	2	0	D		-0.018	-0.014	-0.019
15.	2	2	2	2	2	1	2	0	0	2	0	2	D		0.008	0.007	0.007
Total Energy + 183 (a.u.), SCF															-0.5184	-0.5661	-0.6027
Total Energy + 183 (a.u.), MCSCF															-0.6020	-0.6461	-0.6930

[a] The core $1a'^2 2a'^2 3a'^2$ is assumed.

[b] Cumulative spin, coupling from the left: D, doublet; T, triplet.

TABLE IIIa

Molecular Orbitals for the $N_2O^-(X^2A')$ MCSCF Wavefunction at R_{NN} = 2.132 a.u., R_{NO} = 2.238 a.u., θ_{NNO} = 180°[a]

ORBITALS -- Block 1

BF	Type	Zeta	Center	1σ	2σ	3σ	4σ	5σ	6σ	7σ	8σ	9σ	$1\pi_x$	$2\pi_x$	$3\pi_x$
1	S	5909.440	N1	-0.001	-0.001	0.604	0.012	0.001	0.078	-0.020	-0.061	0.002	0.018	-0.001	0.008
2	S	7.193	N1	-0.001	-0.001	0.461	0.017	0.000	0.140	-0.027	-0.088	0.003	0.026	-0.013	0.012
3	S	0.700	N1	0.001	0.003	-0.046	-0.040	0.005	-0.508	0.092	0.392	0.010	-0.089	0.036	-0.060
4	S	0.213	N1	0.003	0.005	-0.054	-0.162	-0.027	-0.580	-0.170	0.049	-0.052	-0.114	-0.241	0.059
5	Z	26.786	N1	-0.000	-0.002	0.012	-0.040	-0.003	0.093	0.248	0.471	-0.012	-0.009	-0.015	-0.072
6	Z	0.531	N1	0.000	-0.001	0.007	-0.058	-0.006	0.091	0.291	0.476	-0.016	-0.036	-0.047	-0.106
7	Z	0.165	N1	0.001	-0.001	0.012	-0.069	-0.020	0.114	0.120	0.005	-0.022	-0.026	-0.035	-0.038
8	S	5909.440	N2	-0.001	0.594	0.002	-0.075	0.016	0.022	-0.079	0.091	-0.081	-0.056	0.039	-0.029
9	S	7.193	N2	-0.001	0.447	0.002	-0.103	0.020	0.025	-0.111	0.122	-0.112	-0.076	0.053	-0.039
10	S	0.700	N2	0.002	-0.000	-0.004	0.318	-0.044	-0.051	0.346	-0.690	0.559	0.216	-0.168	0.095
11	S	0.213	N2	-0.001	-0.001	0.003	0.276	0.032	0.032	0.187	0.131	0.034	0.312	-0.072	0.339
12	Z	26.786	N2	0.001	-0.001	0.001	0.138	-0.021	0.018	-0.205	0.479	0.264	0.072	-0.068	0.091
13	Z	0.531	N2	0.000	0.001	-0.001	0.199	-0.011	-0.004	-0.285	0.455	0.285	0.078	-0.103	0.112
14	Z	0.165	N2	0.002	0.000	-0.002	-0.080	-0.018	-0.025	-0.016	-0.111	-0.122	0.027	-0.077	0.156
15	S	7816.540	O	-0.588	-0.001	-0.001	0.005	0.109	-0.002	0.008	0.001	0.039	0.004	-0.007	0.010
16	S	9.532	O	-0.471	-0.001	-0.001	-0.007	0.169	-0.001	0.011	0.001	0.057	0.007	-0.010	0.014
17	S	0.940	O	0.030	0.002	0.002	-0.025	-0.547	0.003	-0.024	-0.013	-0.193	-0.032	0.028	-0.040
18	S	0.285	O	0.027	0.002	-0.000	-0.134	-0.547	-0.013	-0.093	-0.014	-0.190	0.061	0.071	-0.077
19	Z	35.183	O	0.004	0.001	-0.001	-0.203	-0.038	-0.012	0.016	-0.022	0.298	-0.077	-0.224	0.001
20	Z	0.717	O	0.001	0.001	-0.001	-0.259	-0.027	-0.017	0.023	-0.042	0.345	-0.104	-0.287	0.021

TABLE IIIa (Continued)

BF	Type	Zeta	Center	1σ	2σ	3σ	4σ	5σ	6σ	7σ	8σ	9σ	$1\pi_x$	$2\pi_x$	$3\pi_x$
21	Z	0.214	O	0.004	0.001	0.000	-0.164	-0.055	-0.000	0.053	-0.028	0.025	-0.138	-0.259	-0.019
22	X	26.786	N1	-0.000	-0.001	0.002	0.022	0.005	0.020	0.050	0.054	-0.047	-0.185	-0.005	0.295
23	X	0.531	N1	-0.001	-0.001	0.002	0.020	0.011	0.025	0.070	0.023	-0.083	-0.250	-0.011	0.397
24	X	0.165	N1	-0.000	-0.000	0.002	0.013	0.002	0.020	0.039	-0.039	-0.083	-0.148	-0.024	0.386
25	X	26.786	N2	0.001	0.001	0.001	0.140	-0.023	0.013	0.017	-0.027	0.325	-0.216	0.068	-0.174
26	X	0.531	N2	0.000	-0.002	0.002	0.219	-0.013	0.017	0.027	-0.012	0.383	-0.298	0.091	-0.230
27	X	0.165	N2	0.000	-0.000	0.002	-0.001	0.006	0.023	0.058	-0.026	0.018	-0.216	0.036	-0.203
28	X	35.183	O	0.004	-0.000	0.002	-0.129	-0.032	0.019	0.022	0.021	0.276	0.129	0.227	0.115
29	X	0.717	O	0.000	-0.000	0.002	-0.162	-0.018	0.027	0.028	0.028	0.361	0.128	0.289	0.159
30	X	0.214	O	0.004	-0.000	0.002	-0.087	-0.055	0.022	0.026	0.028	0.086	0.142	0.233	0.190

ORBITALS -- Block 2

BF	Type	Zeta	Center	$1\pi_y$	$2\pi_y$	$3\pi_y$
31	Y	26.786	N1	-0.250	-0.008	0.318
32	Y	0.531	N1	-0.338	-0.014	0.423
33	Y	0.165	N1	-0.251	-0.061	0.170
34	Y	26.786	N2	-0.203	0.129	-0.317
35	Y	0.531	N2	-0.287	0.182	-0.436
36	Y	0.165	N2	-0.172	0.104	-0.245
37	Y	35.183	O	0.109	0.311	0.154
38	Y	0.717	O	0.134	0.400	0.191
39	Y	0.214	O	0.193	0.356	0.163

[a]Basis Set: Dunning's 4s3p contraction, Reference 24.

TABLE IIIb

Molecular Orbitals for the $N_2O^-(X^2A')$ MCSCF Wavefunction at

R_{NN} = 2.345 a.u., R_{NO} = 2.462 a.u., θ_{NNO} = 130°[a]

ORBITALS -- Block 1

BF	Type	Zeta	Center	1a' 1σ	2a' 2σ	3a' 3σ	4a' 4σ	5a' 5σ	6a' 6σ	8a' 7σ	11a' 8σ	12a' 9σ	7a' $1\pi_x$	9a' $2\pi_x$	10a' $3\pi_x$
1	S	5909.440	N1	-0.001	-0.001	0.603	0.013	0.002	0.079	-0.023	-0.066	0.006	-0.000	-0.000	-0.000
2	S	7.193	N1	-0.001	-0.002	0.460	0.016	0.003	0.139	-0.028	-0.099	0.007	-0.000	-0.000	-0.000
3	S	0.700	N1	0.001	0.006	-0.425	-0.026	-0.005	-0.496	0.078	0.474	0.006	0.000	-0.000	0.000
4	S	0.213	N1	0.008	0.008	-0.053	-0.132	-0.103	-0.566	-0.268	0.156	0.125	0.000	0.000	-0.000
5	Z	26.7860	N1	0.000	-0.002	0.014	-0.045	-0.003	0.098	0.256	0.518	-0.042	0.000	-0.000	0.000
6	Z	0.531	N1	0.001	-0.002	0.008	-0.017	-0.021	0.099	0.238	0.577	0.038	0.000	-0.000	0.000
7	Z	0.165	N1	0.002	-0.002	0.013	-0.066	-0.033	0.132	0.100	-0.001	0.007	0.000	0.000	-0.000
8	S	5909.440	N2	-0.001	0.593	0.001	-0.082	0.019	0.023	-0.099	0.112	-0.098	-0.000	0.000	-0.000
9	S	7.193	N2	-0.001	0.446	0.001	-0.113	0.023	0.025	-0.137	0.140	-0.133	-0.000	0.000	-0.000
10	S	0.700	N2	0.002	0.002	-0.000	0.344	-0.048	-0.034	0.421	-0.871	0.659	0.000	-0.000	0.000
11	S	0.213	N2	-0.004	-0.002	0.006	0.241	0.077	0.052	0.249	0.184	0.079	-0.000	-0.000	0.000
12	Z	26.786	N2	0.002	0.000	0.002	0.199	-0.033	0.031	-0.191	0.488	0.410	-0.000	-0.000	0.000
13	Z	0.531	N2	0.000	-0.000	-0.001	0.306	-0.022	0.009	-0.275	0.513	0.509	0.000	-0.000	0.000
14	Z	0.165	N2	0.006	0.000	0.000	-0.100	-0.074	0.017	-0.030	-0.054	0.017	0.000	0.000	-0.000
15	S	7816.540	O	-0.589	-0.000	-0.000	-0.002	0.102	-0.001	0.009	0.003	0.049	0.000	-0.000	0.000
16	S	9.532	O	-0.473	-0.001	-0.000	-0.002	0.163	-0.001	0.013	0.004	0.073	0.000	-0.000	0.000
17	S	0.940	O	0.036	0.002	0.001	-0.002	-0.552	0.002	-0.037	-0.020	-0.265	-0.000	0.000	-0.000
18	S	0.285	O	0.030	0.002	-0.002	-0.143	-0.499	-0.036	-0.022	-0.160	-0.346	-0.000	0.000	-0.000
19	Z	35.183	O	0.007	0.000	0.001	-0.252	-0.062	0.006	0.029	-0.001	0.448	0.000	-0.000	0.000
20	Z	0.717	O	0.002	0.000	0.001	-0.295	-0.053	0.013	0.007	0.058	0.571	0.000	-0.000	0.000

TABLE IIIb (continued)

BF	Type	Zeta	Center	1a' 1σ	2a' 2σ	3a' 3σ	4a' 4σ	5a' 5σ	6a' 6σ	8a' 7σ	11a' 8σ	12a' 9σ	7a' $1\pi_x$	9a' $2\pi_x$	10a' $3\pi_x$
21	Z	0.214	O	0.008	0.000	0.002	-0.154	-0.100	0.021	0.025	0.042	0.088	0.000	-0.000	0.000
22	X	26.786	N1	0.000	-0.000	0.000	-0.000	0.000	0.000	0.000	-0.000	0.000	-0.250	0.012	0.255
23	X	0.531	N1	-0.000	0.000	-0.000	0.000	-0.000	-0.000	-0.000	0.000	-0.000	-0.330	0.003	0.338
24	X	0.165	N1	0.000	-0.000	-0.000	-0.000	0.000	0.000	0.000	0.000	0.000	-0.230	-0.038	0.527
25	X	26.786	N2	0.000	0.000	-0.000	-0.000	0.000	0.000	0.000	0.000	0.000	-0.207	0.149	-0.306
26	X	0.531	N2	0.000	-0.000	-0.000	-0.000	-0.000	0.000	0.000	0.000	0.000	-0.290	0.204	-0.453
27	X	0.165	N2	-0.000	0.000	0.000	0.000	-0.000	-0.000	-0.000	-0.000	-0.000	-0.158	0.074	-0.500
28	X	35.183	O	0.000	-0.000	-0.000	0.000	-0.000	0.000	-0.000	0.000	0.000	0.131	0.314	0.147
29	X	0.717	O	-0.000	0.000	-0.000	0.000	-0.000	-0.000	0.000	-0.000	0.000	0.168	0.496	0.179
30	X	0.214	O	-0.000	-0.000	0.000	-0.000	0.000	-0.000	0.000	-0.000	-0.000	0.221	0.321	0.306

ORBITALS -- Block 2

BF	Type	Zeta	Center	1a" $1\pi_y$	2a" $2\pi_y$	3a" $3\pi_y$
31	Y	26.786	N1	-0.246	0.007	0.332
32	Y	0.531	N1	-0.333	-0.003	0.439
33	Y	0.165	N1	-0.226	-0.059	0.193
34	Y	26.786	N2	-0.200	0.150	-0.322
35	Y	0.531	N2	-0.288	0.215	-0.462
36	Y	0.165	N2	-0.171	0.102	-0.244
37	Y	35.183	O	0.130	0.304	0.183
38	Y	0.717	O	0.167	0.397	0.224
39	Y	0.214	O	0.233	0.316	0.152

[a]Basis Set: Dunning's 4s3p construction, Reference 24.

Table IV

Computed equilibrium minimum

	Wave Function		
Parameter	SCF	MCSCF	MCSCFCI
R_{NN} (Å)	1.203		
R_{NO} (Å)	1.376		
θ_{NNO} (deg)	123.6		
k_{NN} (md/Å)	11.54		
k_{NO} (md/Å)	3.93		
k_{NNO} (md/Å)	0.645		
E_T (2.132, 2.238, 180)			
$-E_T$ (2.132, 2.238, 130°)			
a.u. (eV)	0.0477 (1.30)	0.0441 (1.20)	
E_T (2.132, 2.238, 130°)			
$-E_T$ (2.345, 2.462, 130°)			
a.u. (eV)	0.0366 (1.00)	0.0469 (1.28)	

Table V

Electron affinity of N_2O

Paper	Electron Affinity (eV)	Method
Wentworth, Chen, Freeman (1971)[a]	0.3 ± 0.2	Deduced from the activation energy for thermal electron attachment rate.
Nalley et al. (1973)[b]	$> -0.15 \pm 0.1$	Collisional ionization of Cs.
Tiernan and Clow (1975)[c]	0.6	Linear extrapolation of collision-induced dissociation cross section.
Present Work	0.23 ± 0.1	Levine model fit to collision-induced cross section, corrects for Doppler motion of target gas and for ion velocity spread.

[a]Reference 8

[b]Reference 9

[c]Reference 10

Table VI

Parameters for the parametric Morse functions of Eq (19) for $N_2O(X^1\Sigma^+)$ and $N_2O^-(X^1A')$

Parameter[a]	Units	Molecule N_2O	Reference	N_2O^-	Reference
D_{NN-O}	eV	3.9		0.5	Present work, SCF
β	$Å^{-1}$	3.0	21	4.9	Present work, SCF
R^e_{NO}	Å	1.184	21	1.38	Present work, SCF
k	10^{-3} eV/deg^2	1.24	27	2.03	Present work, SCF
θ^e_{NNO}	deg	180	21	124	Present work, SCF
a	-				
b	rad^{-1}				
c	rad^{-2}				

[a] D_{NN-O} is the adiabatic decomposition energy: $D_{NN-O} = D^e_{NN-O} + E_{N_2}(V = 0) - E_{N_2O}(0, 0, 0)$ where $E_{N_2}(V=0) = 0.146$ eV, $E_{N_2O}(0, 0, 0) = 0.4$ eV for $N_2O(X^1\Sigma^+)$ and 0.2 eV for $N_2O^-(X^2A')$. $N_2O(X^1\Sigma^+)$ dissociates adiabatically to $N_2(X^1\Sigma^+_g) + O(^1D)$ and $N_2O^-(X^1A')$, to $N_2(X^1\Sigma^+_g) + O^-(^2P)$. See Table XXVI of Reference 11.

Table VII

Summary of the quantities determined in the present study to characterize the potential energy surface of the ground state X^2A' ($^2\Pi$) of N_2O^-

Parameter[a]	Value	Method[b]
$D^o_{NN-O^-}$	0.43 ± 0.1	CID
$D^o_{N-NO^-}$	5.13 ± 0.1	CID
R^e_{NN}	1.20 Å	SCF
R^e_{NO}	1.38 Å	SCF
θ_{NNO}	124°	SCF
k_{NN}	11.5 md/Å	SCF
k_{NO}	3.9 md/Å	SCF
k_{NNO}	0.65 md/Å	SCF

[a] $k_{NNO} = \frac{\partial^2 V}{\partial \theta 2} / R^e_{NN} R^e_{NO}$

[b] CID - Collision Induced Dissociation Experiment;
SCF - Self Consistent Field Calculation

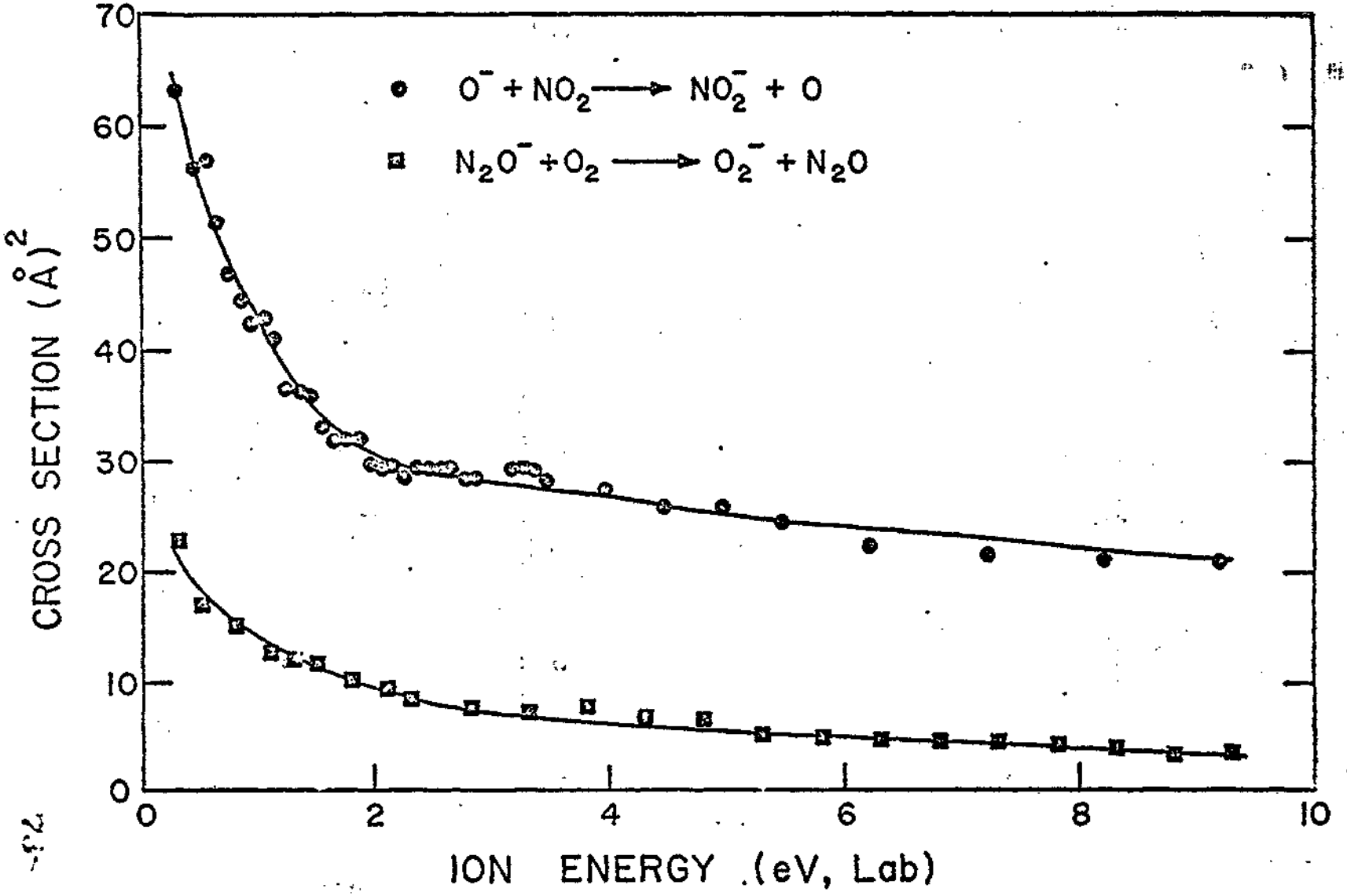
$O^- + NO_2 \longrightarrow NO_2^- + O$
$N_2O^- + O_2 \longrightarrow O_2^- + N_2O$
CROSS SECTION ($Å^2$)
ION ENERGY (eV, Lab)
0
10
20
30
40
50
60
70
0
2
4
6
8
10

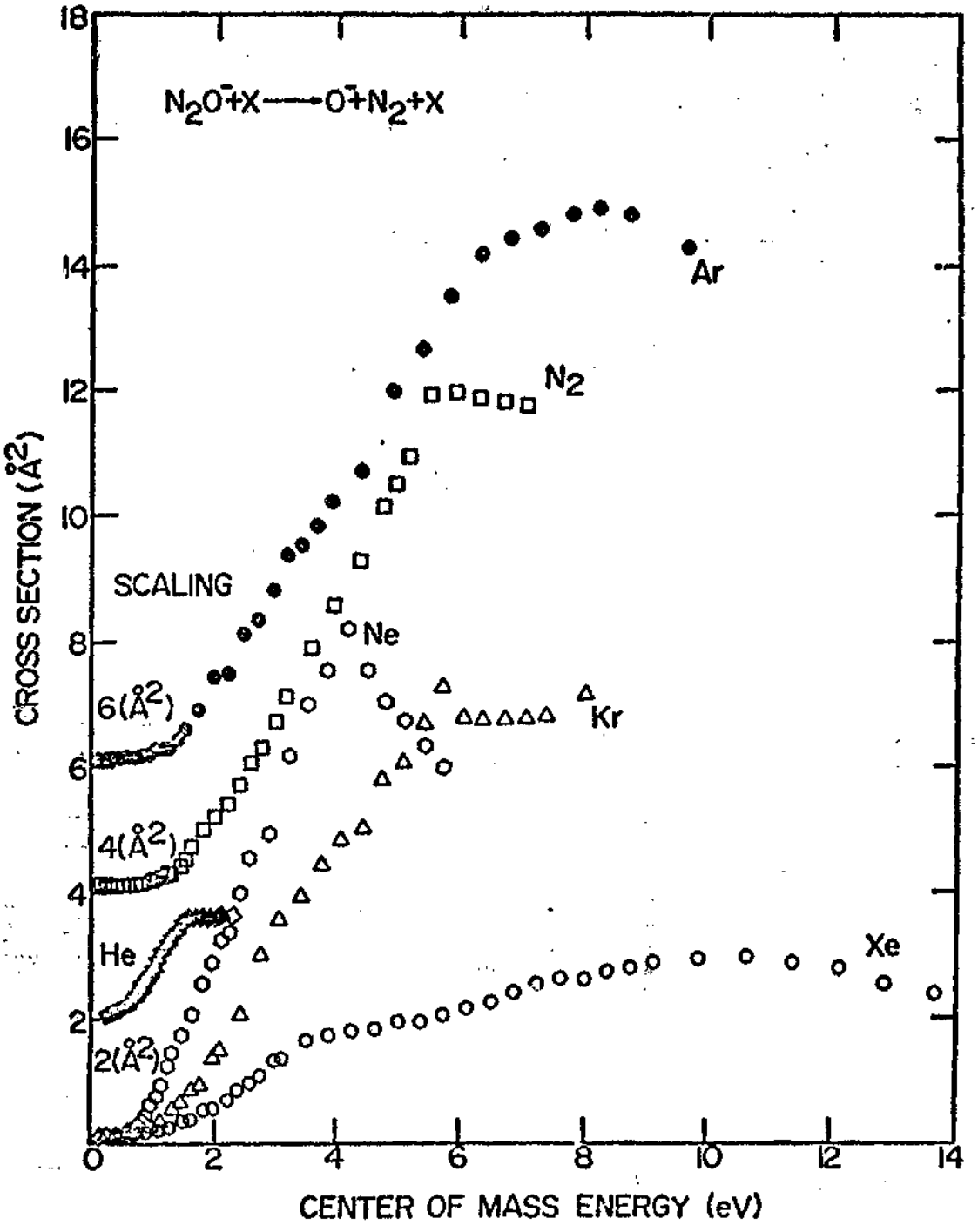
$N_2O^- + X \longrightarrow O^- + N_2 + X$
CROSS SECTION (Å²)
CENTER OF MASS ENERGY (eV)
SCALING
Ar
N_2
Ne
Kr
Xe
He
6(Å²)
4(Å²)
2(Å²)
0
2
4
6
8
10
12
14
16
18

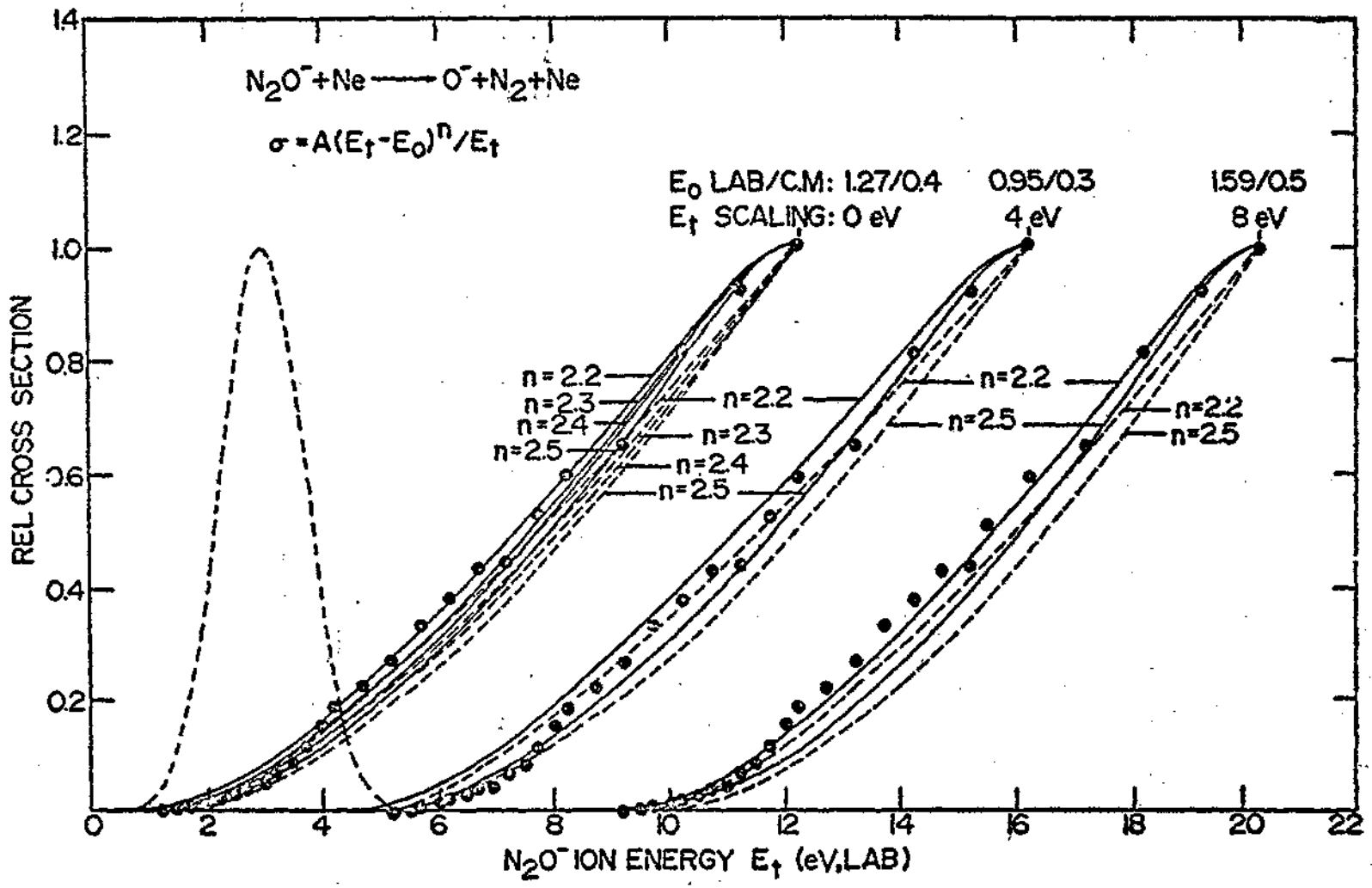
$N_2O^- + Ne \longrightarrow O^- + N_2 + Ne$
$\sigma = A(E_t - E_0)^n / E_t$
E_0 LAB/C.M: 1.27/0.4
0.95/0.3
1.59/0.5
E_t SCALING: 0 eV
4 eV
8 eV
n=2.2
n=2.3
n=2.4
n=2.5
REL CROSS SECTION
N_2O^- ION ENERGY E_t (eV,LAB)
0
2
4
6
8
10
12
14
16
18
20
22
0.2
0.4
0.6
0.8
1.0
1.2
1.4

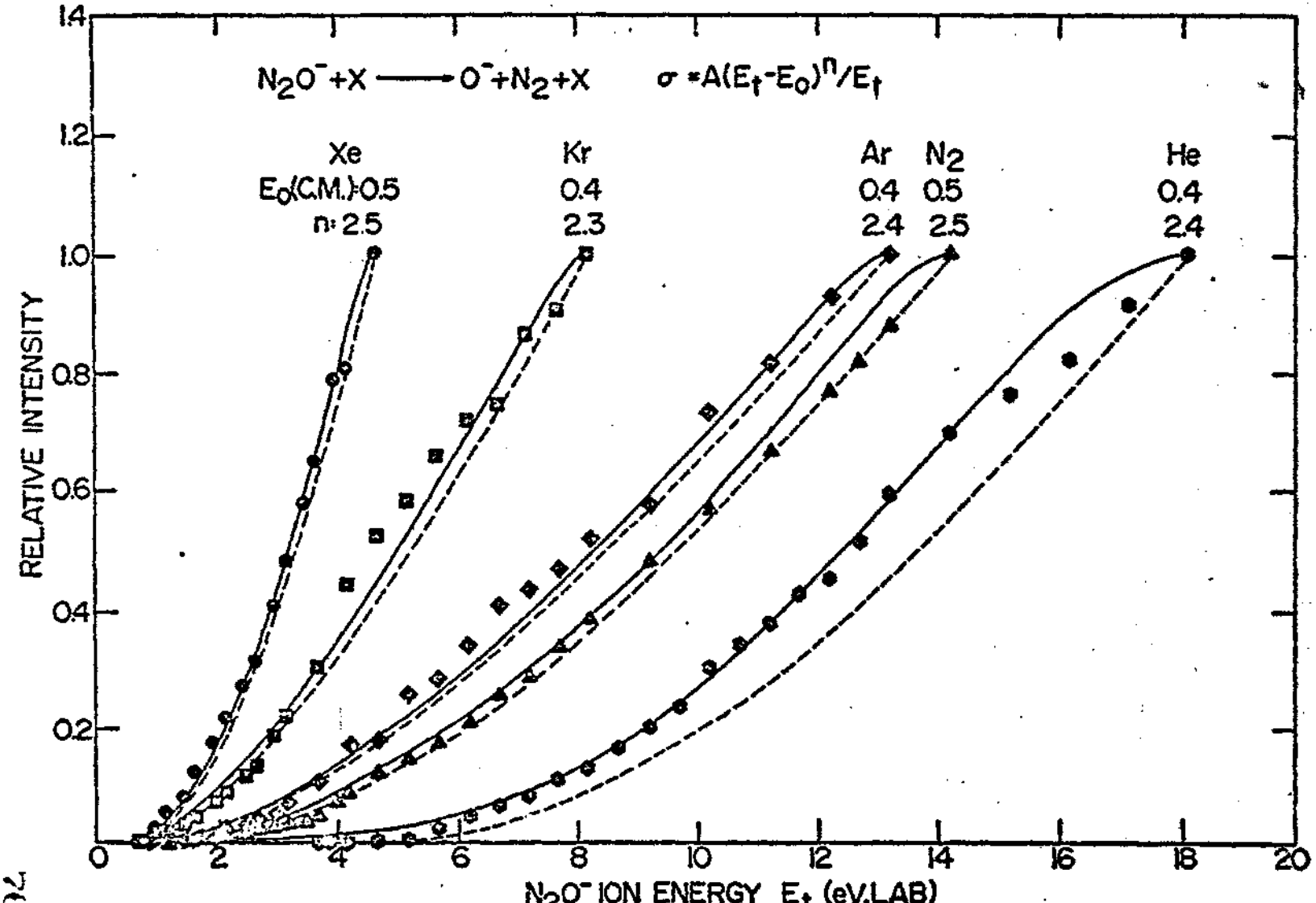
$N_2O^- + X \longrightarrow O^- + N_2 + X$
$\sigma = A(E_t - E_0)^n / E_t$
Xe
E_0(C.M.)-0.5
n: 2.5
Kr
0.4
2.3
Ar
0.4
2.4
N_2
0.5
2.5
He
0.4
2.4
RELATIVE INTENSITY
N_2O^- ION ENERGY E_t (eV,LAB)
0
2
4
6
8
10
12
14
16
18
20
0.2
0.4
0.6
0.8
1.0
1.2
1.4

-92-

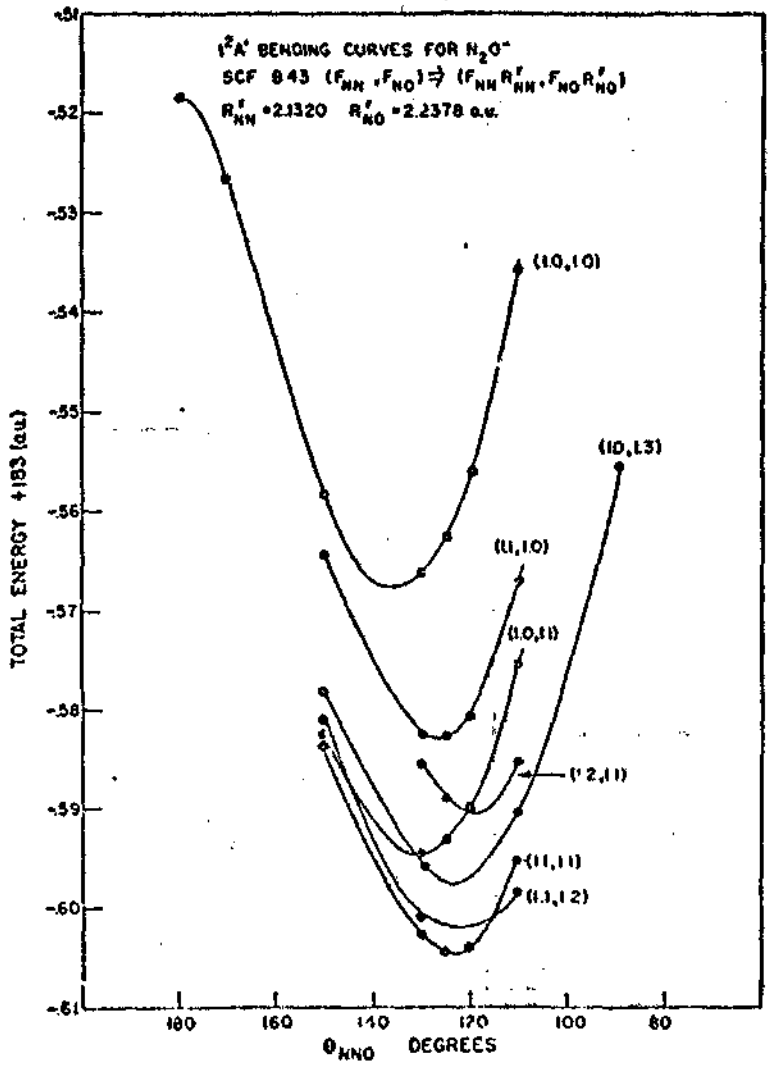
$^2A'$ BENDING CURVES FOR N_2O^-
SCF 843 $(F_{NN}, F_{NO}) \Rightarrow (F_{NN}R'_{NN}, F_{NO}R'_{NO})$
R'_{NN} =2.1320 R'_{NO} =2.2378 a.u.
(10,10)
(10,13)
(11,10)
(10,11)
(12,11)
(11,11)
(11,12)
TOTAL ENERGY +183 (a.u.)
-51
-52
-53
-54
-55
-56
-57
-58
-59
-60
-61
180
160
140
120
100
80
θ_{KNO} DEGREES

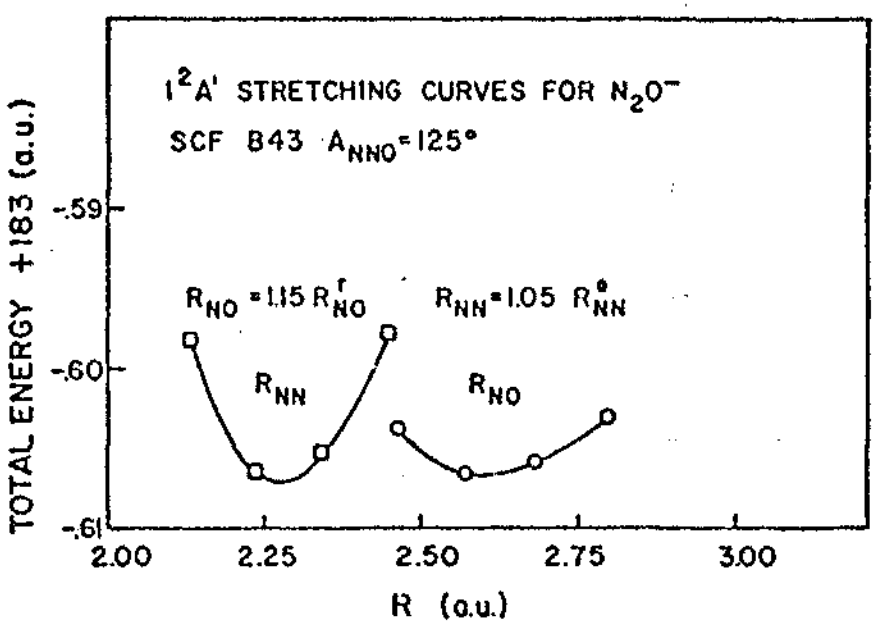
$1^2A'$ STRETCHING CURVES FOR N_2O^-
SCF B43 A_{NNO}=125°
R_{NO} = 1.15 R^r_{NO}
R_{NN}=1.05 R^e_{NN}
R_{NN}
R_{NO}
TOTAL ENERGY +183 (a.u.)
-.59
-.60
-.61
2.00
2.25
2.50
2.75
3.00
R (a.u.)

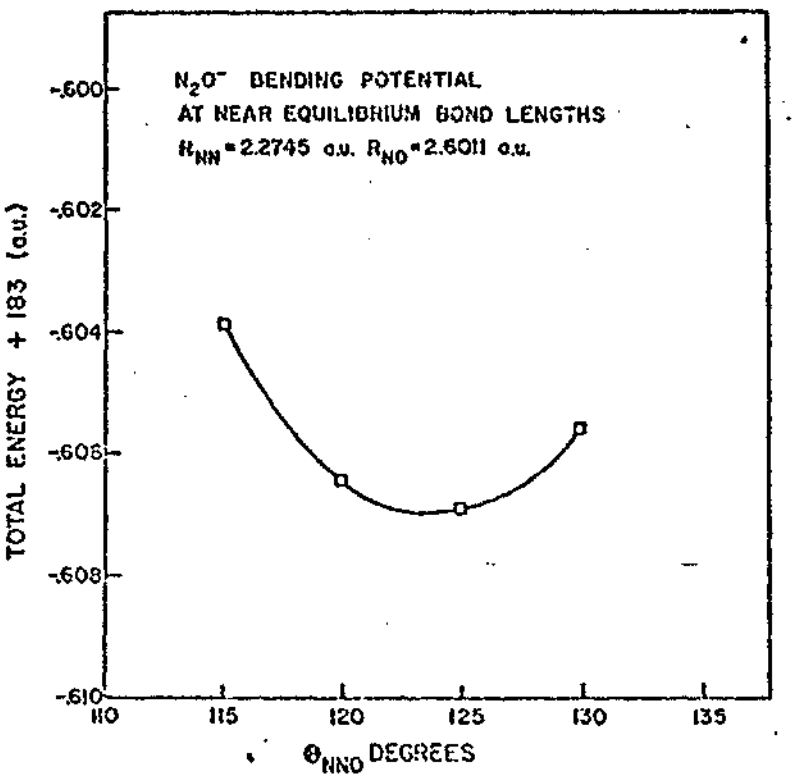
N_2O^- BENDING POTENTIAL
AT NEAR EQUILIBRIUM BOND LENGTHS
R_{NN}=2.2745 a.u. R_{NO}=2.6011 a.u.
-.600
-.602
-.604
-.606
-.608
-.610
TOTAL ENERGY + 183 (a.u.)
110
115
120
125
130
135
Θ_{NNO} DEGREES

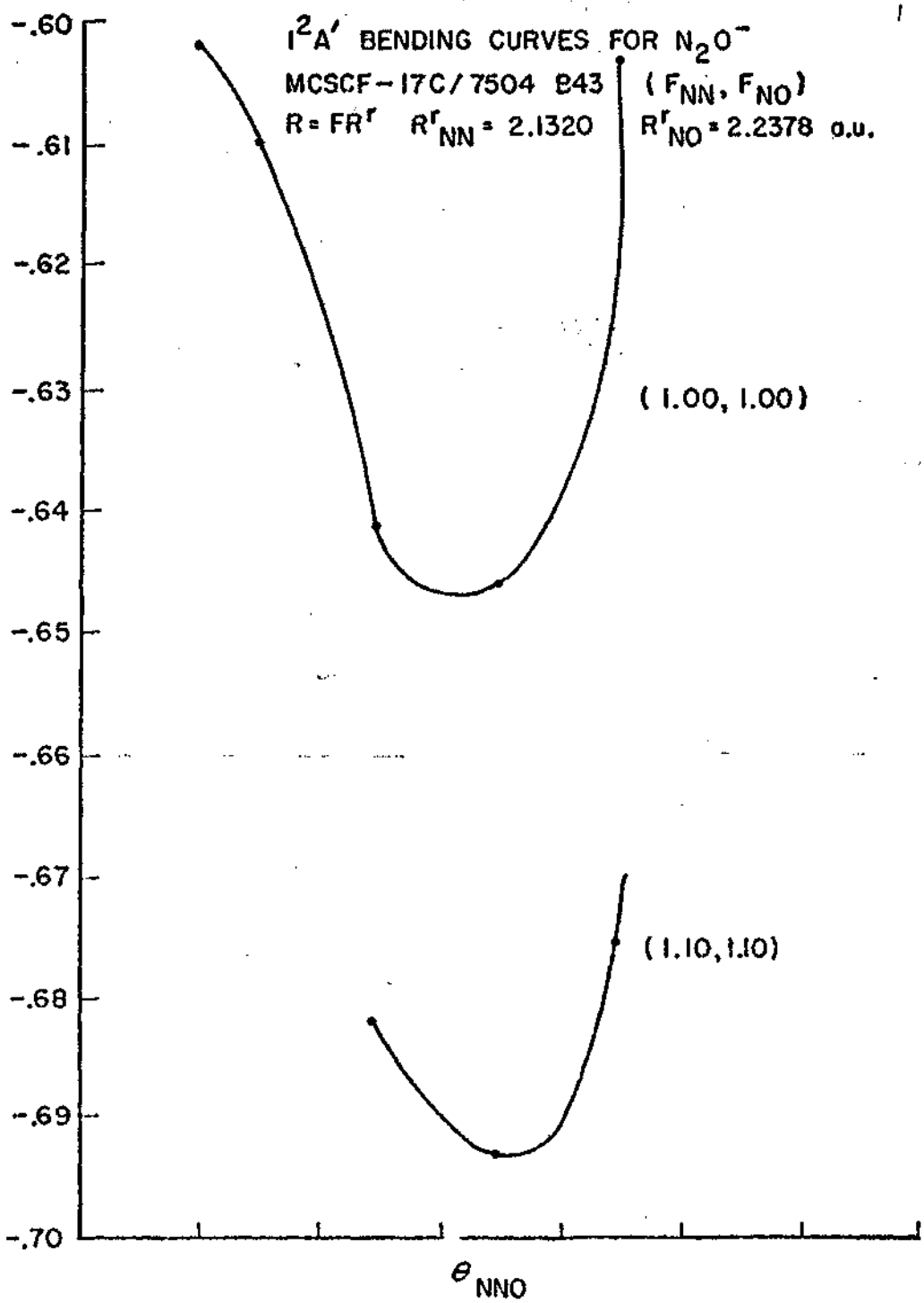
$1^2A'$ BENDING CURVES FOR N_2O^-
MCSCF – 17C / 7504 B43
R = FR^r R^r_{NN} = 2.1320
(F_{NN}, F_{NO})
R^r_{NO} = 2.2378 a.u.
(1.00, 1.00)
(1.10, 1.10)
-.60
-.61
-.62
-.63
-.64
-.65
-.66
-.67
-.68
-.69
-.70
θ_{NNO}

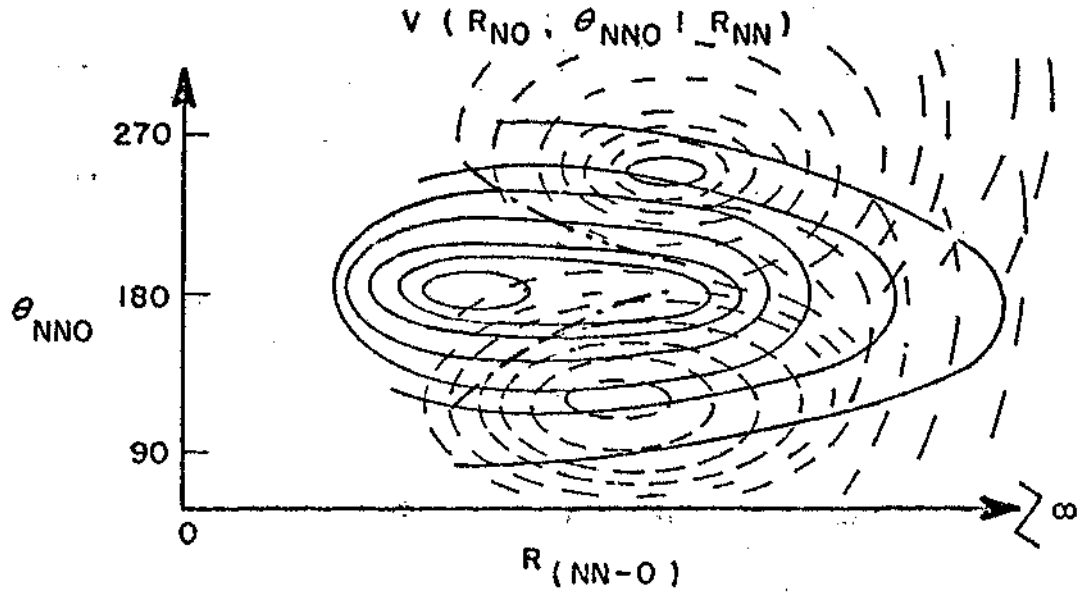
V (R_{NO} , θ_{NNO} , R_{NN})
270
180
90
θ_{NNO}
0
∞
$R_{(NN-O)}$

SECTION II

CROSSED-ION MOLECULAR-BEAM STUDIES

Over the course of this contract, a sophisticated crossed ion-molecular beam instrument has been developed. This instrument was designed to facilitate studies on the basic physic and chemistry of ionized gases, including identification of elementary positive and negative ion processes, and their kinetic parameters as well as determination of fundamental atomic and molecular properties which directly influence the ionized media. In addition to the applications of this instrument for investigating the dynamics and energy-transfer characteristics of ion-neutral collisions, this instrument can also be utilized in the study of the chemistry of high-temperature molecules.

The following is a brief outline of the instrument. Further details of the design and experiments are available in a series of SRI reports[1-4] and two technical presentations.[5,6]

ION SOURCE AND LENS SYSTEM

The ion beam is formed by electron impact on molecules introduced either from a resistance-heated Knudsen cell or from a conventional gas-inlet system. Temperatures as high as 2600°K are attainable. The ion beam leaving the source is double focused by a 90° electric sector and a 60° negative sector before entering the deceleration lens. Mass resolution of ~ 130 and ion currents of 0.1 to 1.0 nA are obtainable. Recently the energy spread of a primary beam of Ar^+ ions has been measured using the newly assembled parallel-plate energy analyzer. Figures 1 and 2 show the energy distribution at three different nominal ion energies The

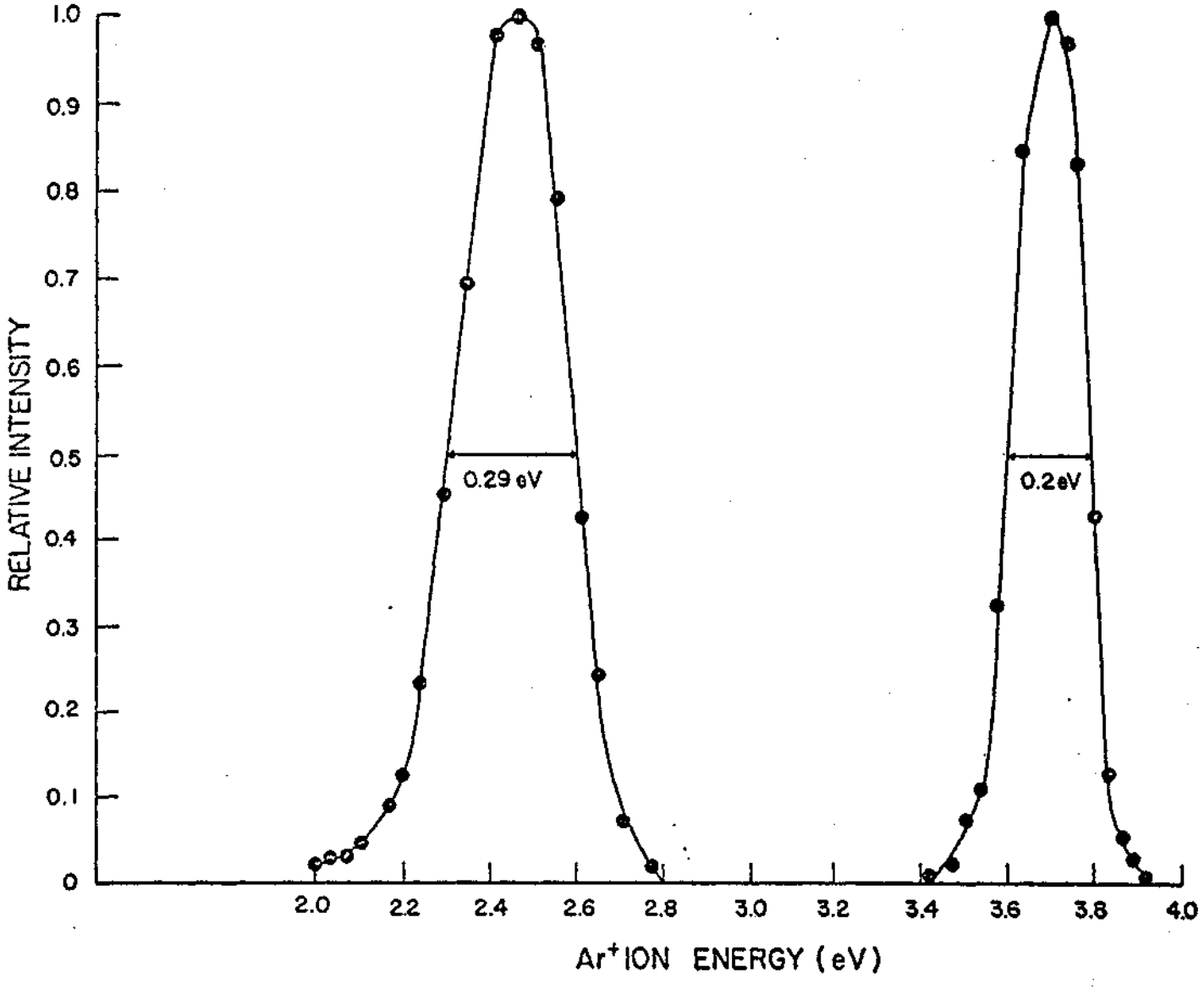

Figure 1. Ar^+ Kinetic Energy Distribution, Nominal Energy 2.4 and 3.7 eV

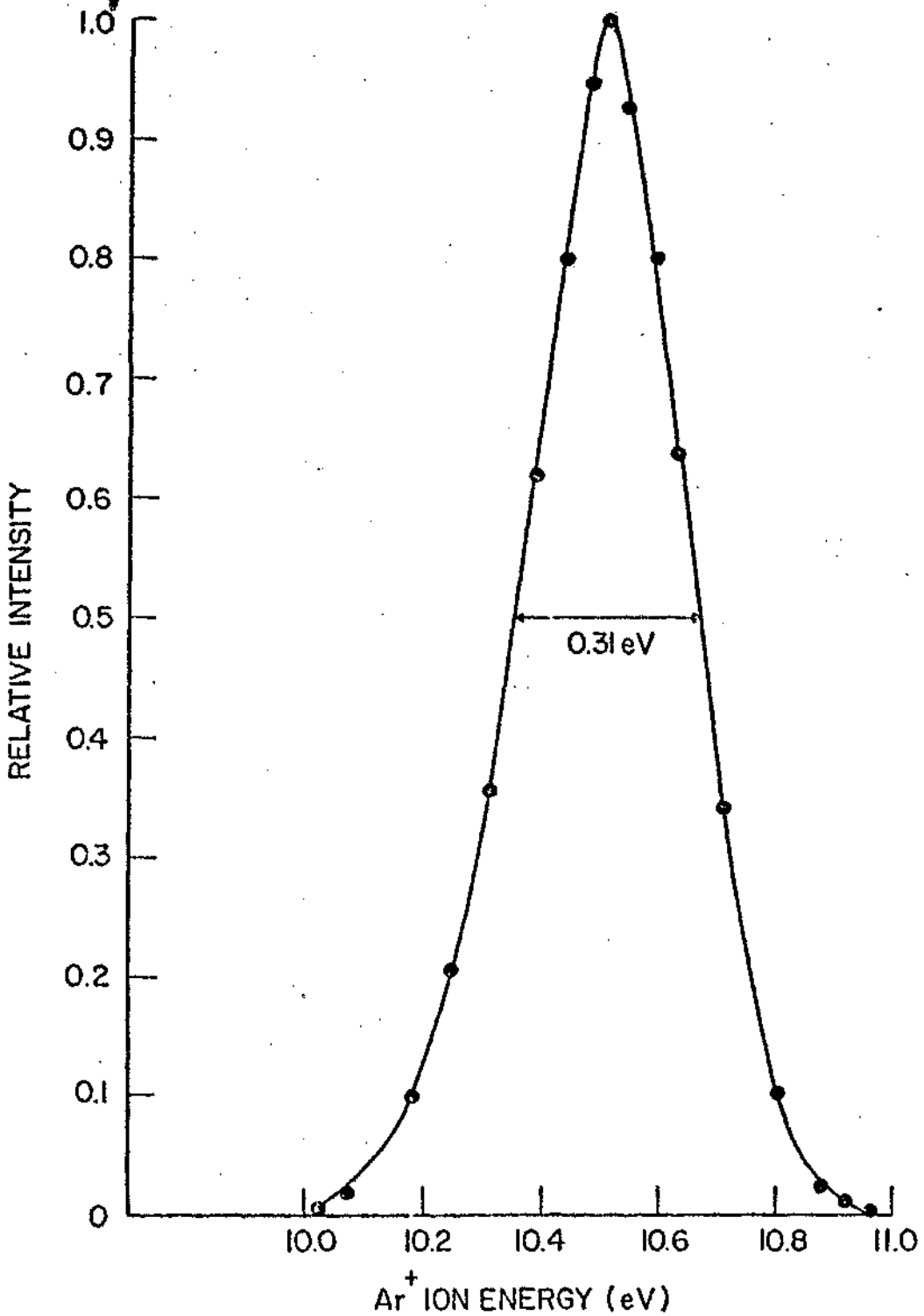

Figure 2. Ar^+ Kinetic Energy Distribution, Nominal Energy 10.5 eV

8-1-

distributions vary with energy; however, the full-width-half-maximum values do not exceed 0.3 eV at energies above 1 eV. A kinetic energy range of 1 to 170 eV is accessible with transmission-to-collision region above 90% down to 1 eV. Transmission to the second-stage detector is considerably less than this at low energies due to space-charge effects and angular divergence.

NEUTRAL-BEAM SOURCE

The mass and energy resolved beam is crossed at 90° by a molecular beam produced by a stainless steel multichannel capillary array. The beam is chopped for phase-sensitive detection.

PRODUCT-ION DETECTION SYSTEM

The main scattering chamber is stainless steel, 36 in. in diameter and 15 in. high, pumped by high-speed 10- and 6-in. oil diffusion pumps. The product ions from the scattering process enter a parallel-plate energy ananlzer, quadrupole mass spectrometer, and a Bendix Channeltron operated in the pulse-counting mode. The entire detection system rotates in the horizontal plane about the scattering center, and product ions are collected over the region -5° to +95° with respect to the incident-ion beam direction.

SECTION III

DEVELOPMENT AND APPLICATION OF ANALYTICAL METHODOLOGY FOR DETAILED CHARACTERIZATION OF AIR FORCE HERBICIDE ORANGE STOCKS

INTRODUCTION

In support of the U.S. Air Force for determining the feasibility of the soil-biodegradation method of disposal of excess Air Force herbicides in accordance with Environmental Protection Agency guidelines, personnel of Systems Research Laboratories, Inc., were requested to develop and apply analytical gas chromatograph-mass spectrometric (GC-MS) methods in the quantitative determination of Herbicide Orange and degradation products thereof in soil and milk and to establish the composition of representative samples of Herbicide Orange formulations.

This work under Contract No. F33615-73-C-4099 was undertaken in 1972 and continued through June 1975. The research was performed in conjunction with U.S. Air Force personnel at the Aerospace Research Laboratories, Wright-Patterson Air Force Base, Ohio, and in cooperation with personnel in the Department of Life and Behavioral Sciences, U.S. Air Force Academy, Colorado Springs, Colorado, who supplied samples of soil from various field-test plots.

Several analytical techniques were developed during the contract period for analyzing Air Force Herbicide Orange. As a result, each mission was accomplished within a different period of time and results reported to the Air Force Logistics Command. A brief description of each period follows:

A. 1972 - 1973: A detailed description of the results of this effort is available in SRL Semiannual Status Report 6776-1, Contract No. F33615-73-C-4099.[7] The work involved:

1. Extraction of the herbicides n-butyl 2,4-D and 2,4,5-T and related compounds by means of an organic solvent from soil samples.
2. Treatment of the extract to convert the 2,4-D and 2,4,5-T to a derivative (methyl esters) amenable to gas-chromatographic analysis.
3. Analysis of the extract using GC-MS.
4. Mass-spectral characterization of selected Herbicide Orange formulations.

B. 1973 - 1974: SRL Annual Status Report 6776-2, Contract No. F33615-73-C-4099.[8] Progress was made in the following areas:

1. Development of software for the data acquisition and control system used with the Loenco 160 gas chromatograph-DuPont 21-491 mass spectrometer system.
2. Development of improved gas-chromatographic methods for separation and identification of components of Herbicide Orange formulations.
3. Development and implementation of analytical methods for determining 2,3,7,8-Tetrachlorodibenzo-p-dioxin (2,3,7,8-TCDD).

C. 1974 - 1975: Progress during this period is described in detail in SRL Semiannual Status Report 6776-3, Contract No. F33615-73-C-4099.[9] Two progress reports have been submitted to the Air Force Logistics Command.[10,11] The work involved:

1. Completion of software for the data-acquisition and control system used with the ARL gas chromatograph-mass spectrometer (GC-MS).
2. Development and application of an analytical technique for quantitative determination of dichlorophenoxy and trichlorophenoxyacetic acids in Herbicide Orange.
3. Determination of tetrachlorodibenzo-p-dioxin in Herbicide Orange.

D. 1975 - present: Description of these results is available in SRL Annual Status Report 6776-4, Contract No. F33615-73-C-4099.[12] Two Aerospace Research Laboratories technical reports have been completed.[13,14] One manuscript[15] has been submitted for publication in Analytical Chemistry and is included as part of this section. The work included:

1. Complete construction of high-sensitivity gas chromatograph-quadrupole and AEI MS-30 double-beam mass-spectrometer systems.
2. Development of a successful liquid-chromatographic technique for extraction of 2,3,7,8-TCDD in Herbicide Orange.
3. Complete analysis of TCDD in 250 samples of Air Force Herbicide Orange.

The recent developments are application of GC-MS techniques for quantitative analysis of 2,3,7,8-TCDD in soil and milk and is described as follows.

DETERMINATION OF 2,3,7,8-TETRACHLORODIBENZO-p-DIOXIN IN MILK

A. Specificity and Selectivity

The gas chromatographic-mass spectrometric (GC-MS) technique is extremely sensitive and specific for the determination of TCDD. In order to assign a signal to 2,3,7,8-TCDD, two things must occur simultaneously: 1) the retention time must be correct and 2) it must respond at m/e 320 as tuned on the mass spectrometer.

B. Apparatus

1. Mini-aktor vials
2. 500-ml beaker
3. 8-ml (2-dram) vials (screw top)
4. Disposable transfer pipettes
5. 0.3-ml cone-shaped vials
6. AEI MS-30 mass spectrometer coupled to Varian 1400 gas chromatograph with all glass membrane separator

C. Reagents and Materials

1. Ethanol (MCB pesticide quality)
2. Hexane (MCB, HX 29, pesticide quality)
3. Benzene (Mallinckroldt, 1043, nanograde)
4. Silica Gel (MCB, SX 143-4, 100-120 mesh)
5. Alumina (Fisher, A-540, 80-100 mesh)
6. Potassium hydroxide

7. Sulfuric acid

8. (Column) 1/8-in. x 5 ft stainless steel tubing

9. (Packing) 1.5% OV-101 on Gas Chrom G (HP)

10. TCDD (available for Dow Chemical U.S.A., Midland, Michigan)

11. o-xylene (MCB)

D. Sample Preparation

1. Put 1 g milk and 1.0 ml 20% KOH in ethanol solution in a mini-acktor and drop in a 500-ml beaker of boiling H_2O for 5 min.

2. Remove and transfer contents to an 8-ml vial.

3. Rinse mini-acktor with 2-ml hexane and add this to the vial.

4. Shake well and allow the layers to separate.

5. With a transfer pipette, remove upper (hexane) layer and put this into another 8-ml vial.

6. To the vial containing the original reaction mixture, add another 2-ml mini-acktor rinse and again shake well.

7. Remove upper layer once again and add to original hexane extract.

8. Wash hexane extract with 2-ml (1N) KOH then with 2-ml concentrate H_2SO_4 and 2-ml 10% aqueous Na_2CO_3.

9. Evaporate extract to ~ 1 ml under a stream of air and add to alumina-silica gel combination column (see Fig. 3 for construction).

10. Discard first 5-ml of eluate ; collect next 6-ml and concentrate to ~ 0.3 ml in a Teflon beaker under a stream of air.

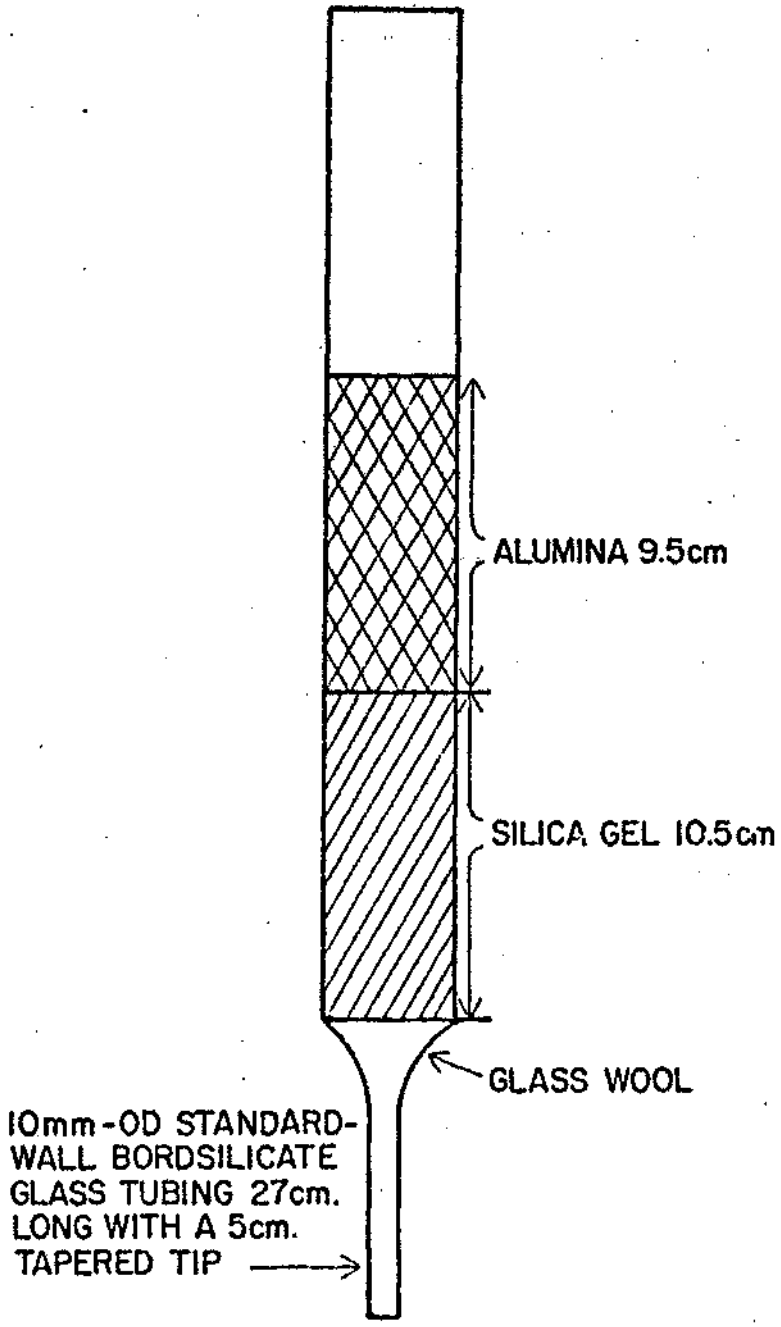

Figure 3. Alumina-Silica Gel Combination Column

11. Transfer extract to a 0.3-ml cone-shaped vial, evaporate just to dryness, and immediately cap with a rubber-lined cap.

12. Just before analysis, add 50 µl o-xylene to cone-shaped vial and analyze.

E. Instrument Conditions and Setup

An AEI MS-30 double-beam mass spectrometer coupled with a Varian 1400 series gas chromatograph was employed and set up according to the following conditions:

1. Column temperature - 230°C
2. Injector temperature - 280°C
3. Separator temperature - 200°C
4. Flow rate 55 cc/min helium at 60 psig
5. Filament current on number 3
6. Magnet tuned to monitor m/e 320
7. Strip chart recorder set 100 mv atten. at 1-in./min

Accelerating voltage - 4 kV
Ionizing voltage - 70 eV

F. Calibration

1. Inject 2 µl of TCDD standard into gas chromatograph; and as the TCDD elutes as displayed on the strip-chart recorder, fine tune the magnet to maximize the response at m/e 320.

2. Inject 2 µl of a dilute TCDD standard solution of known concentration in the gas chromatograph and record the response on the strip-chart recorder.

3. Repeat Step No. 2 until reproducibility of detector response is satisfactory.

G. Analytical Procedure

1. Inject 2 µl of the final extract into the gas chromatograph and record the response at proper TCDD retention time and m/e signal.

2. Repeat calibration at least after every two samples.

H. Calculation

1. Calculations are performed by comparing peak height of a standard of known concentration of TCDD to that of sample to obtain sample concentration in this case in 1.0 g of milk.

2/ Calculate percent recovery as determined by analysis of a doped sample.

I. Interferences

Interferences encountered utilizing this technique are somewhat greater than encountered in much more time consuming methods but with the use of a high-resolution instrument such as the AEI MS-30. These interferences could be eliminated at the expense of sensitivity.

J. Discussion

The method described here is at present still in the developmental stage. Interferences encountered near the TCDD retention time indicate the need for further extract cleanup modification. However, this method does display great promise as it can be performed in about half the time of previously developed methods (see Figs. 4 and 5).

DETERMINATION OF 2,3,7,8-TETRACHLORODIBENZO-p-DIOXIN IN SOIL

A. Apparatus

1. Ground glass stoppered Erlenmeyer flasks (50 ml)

2. 20-ml screw-capped tubes

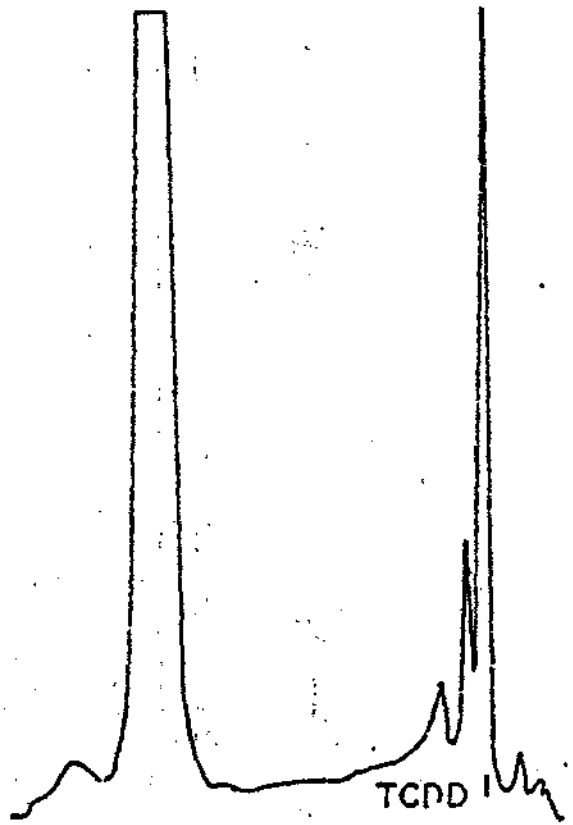

10μl INJECTION OF EXTRACT OBTAINED
WITH BAUGHMAN-MESELSON TREATMENT

(RECORDER ATTN = 100mv)

Figure 4. Extract - Dow Method Cleanup

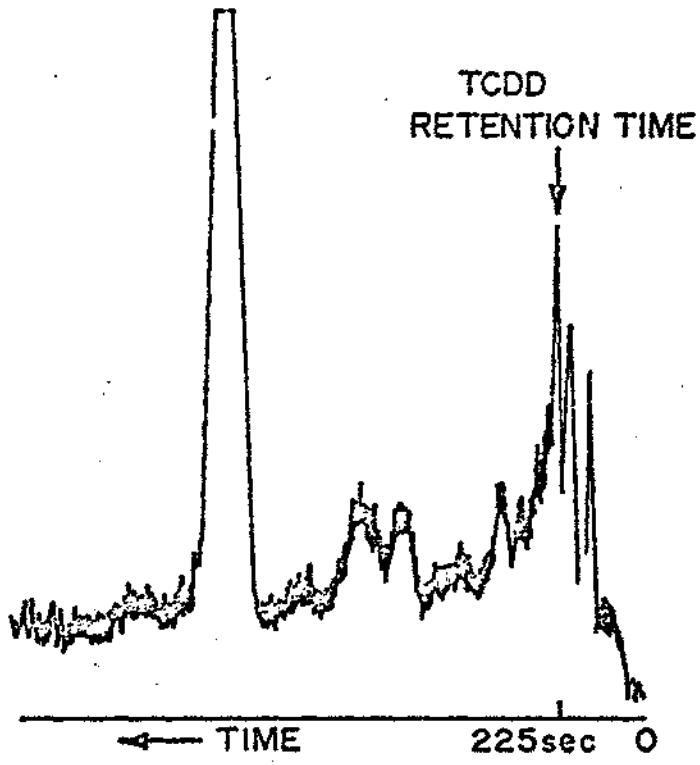

Figure 5. Extract - Milk Extraction Method Cleanup

3. Laboratory shaker

4. Disposable transfer pipettes

5. 0.3-ml cone-shaped vials

6. AEI MS-30 mass spectrometer coupled to Varian 1400 gas chromatograph and all-glass membrane separator

7. Aluminum foil

B. Reagents and Materials

1. Hexane (MCB, HX 297, pesticide quality)

2. Benzene (Mallincrodt, 1043, nanograde)

3. (G.C. Column) 1/8-in. x 5 ft stainless steel tubing

4. (Packing) 1.5% OV-101 on Gas Chrom G (HP) 100/120 mesh

5. TCDD (available Dow Chemical U.S.A., Midland, Michigan)

6. o-xylene (MCB)

C. Sample Preparation

Samples to be analyzed were packed in individual sample containers and kept frozen until time of analysis.

1. Remove sample containers from freezer compartment and allow to thaw (~2 hr).

2. Weigh out ~ 20 g of soil from each container and allow to air dry to a constant weight on aluminum foil (shiny side out).

3. Place 10 g of each sample in an ultra-clean Erlenmeyer flask.

4. Add 15 ml 20% benzene in hexane to each flask.

5. Put flasks on laboratory shaker and shake for 2 hr.

6. Decant the solvent into a 20-ml screw cap tube.

7. Rinse soil with 5 ml 20% benzene in hexane.

8. Add rinse to original extract and concentrate down to about 0.3 ml under a stream of air.

9. Transfer extract to a 0.3-ml cone-shaped vial and evaporate just to dryness and immediately cap with a rubber-lined cap.

10. Just before analysis add 50 µl o-xylene and then analyze.

D. Instrument Conditions and Setup

An AEI MS-30 double-beam mass spectrometer coupled with a Varian 1400 Series gas chromatograph and an all-glass membrane separator was utilized in the analyses and set up according to the following conditions.

1. Column temperature - 230°C
2. Injector temperature - 280°C
3. Separator temperature - 200°C
4. Flow rate 55 cc/min at 60 psig
5. Strip chart recorder set 100 mV attenuation at 1 in./min

   Ionizing voltage - 70 eV
   Accelerating voltage - 4 kV

6. Filament current on number 3
7. Magnet tuned to monitor m/e 320

E. Calibration

1. Inject 2 µl of TCDD standard into gas chromatograph; and as the TCDD elutes as displayed on the strip-chart recorder, fine tune the magnet to maximize the response at m/e 320.

2. Inject 2 µl of a dilute TCDD standard solution of known concentration in the gas chromatograph and record the response on the strip-chart recorder.

3. Repeat Step No. 2 until reproducibility of detector response is satisfactory.

F. Analytical Procedure

1. Inject 2 µl of the final extract into the gas chromatograph and record the response at proper TCDD retention time and m/e signal.

2. Repeat calibration at least after every two samples.

G. Calculations

1. Calculations are performed by comparing peak height of a standard of known concentration of TCDD to that of sample to obtain sample concentration in this case in 20 g of soil.

2. Calculate percent recovery as determined by analysis of a doped sample.

H. Interferences

1. Interferences resulting from materials having retention times similar to TCDD and response at m/e 320 may be encountered, especially if the particular sample contains large amounts of organic material.

2. Glassware and syringes used in the analysis of samples containing parts-per-billion levels of TCDD may retain sufficient TCDD to give high results at parts-per-trillion levels.

I. Discussion

The shake-extraction method described here has been found to be the least complicated and time-consuming method of all researched. Under ideal conditions (i.e., limited organic materials present in the soil), interferences were minimal and recoveries were on the order of about 90% at the parts-per-trillion level. The following report illustrates the usefulness of this shake-extraction method in the recent analysis of 2,3,7,8- Tetrachlorodibenzo-p-dioxin (TCDD) in soil samples from Eglin Air Force Base Test Range.

ANALYSIS OF 2,3,7,8 TETRACHLORODIBENZO-p-DIOXIN (TCDD) IN SOIL SAMPLES FROM EGLIN AIR FORCE BASE TEST RANGE

M. L. Taylor and T. O. Tiernan

Aerospace Research Laboratories (LJ)
Wright Patterson Air Force Base, Ohio 45433

R. O. Yelton

Systems Research Laboratories, Inc.
2800 Indian Ripple Road
Dayton, Ohio 45440

INTRODUCTION

Soil samples containing trace quantities of 2,3,7,8 tetrachlorodibenzo-p-dioxin were received from Eglin Air Force Base, Florida, packed in dry ice and were immediately transferred to the freezer compartment of the laboratory refrigeration units. It should be noted that samples designated as numbers 89 and 90 had been broken in shipment. This breakage may have resulted from the unusually high moisture content of these samples which, upon freezing, resulted in expansion and sample container rupture.

ANALYTICAL PROCEDURE

Soil samples were prepared for extraction and analysis by removing the sample containers from the freezer compartment and allowing them to thaw. Approximately 20 g of soil were removed from each container and allowed to air-dry on aluminum foil to a constant weight. After drying, 10 g of each sample were accurately weighed out and placed in an ultra-clean vessel for extraction.

A 4-hr extraction procedure was carried out on each sample utilizing 20% benzene in hexane (both pesticide quality), as the extracting solvent. The extracts obtained as a result of this operation were concentrated by a factor of 1000 and subjected to a column chromatography clean-up procedure using silica gel-alumina columns. Aliquots were then analyzed on Varian 144010 GL chromatograph, coupled to an AEI scientific apparatus MS-30 double beam mass spectrometer through an all-glass membrane separator. This instrument is capable of detecting low levels of 2,3,7,8 tetrachlorodibenzo-p-dioxin at a mass resolution as high as 10,000. The m/e 320 peak was monitored continuously and the response was integrated as the TCDD eluted from the chromatograph. The integrated TCDD response from unknowns was compared with the response for accurately known amounts of TCDD standard introduced into the instrument. Multiple analyses were accomplished for several samples at different mass resolutions to ensure that interferences were not a complication.

RESULTS

The results of these analyses are presented in Table I. Duplicate analyses for Sample 108 were in rather poor agreement. This may be due to the fact that this sample apparently contained a large amount of organic material in the soil which affects the extraction of TCDD from the matrix. In general, the analyses reflect a standard deviation of $\pm$ 30%. A total of about 300 manhours were spent in the extraction, preparation, and evaluation of the Eglin soil sample data.

TABLE I

TETRACHLORODIBENZO-p-DIOXIN LEVELS IN SOIL SAMPLES FROM EGLIN AIR FORCE BASE, FLORIDA

Sample Number	Mass Spectrometer Resolution	TCDD Concentration
85	1000	1549 ppt
85	10000	1241 ±424 ppt
86	1000	1237 ppt
86	10000	1261 ±431 ppt
87	1000	262 ppt
88	1000	293 ppt
89	Broken in Shipment	
90	Broken in Shipment	
91	1000	121 ppt
91	1000	106 ppt
92		
106	1000	173 ppt
106	1000	138 ppt
107	1000	231 ppt
107	1000	175 ppt
107	1000	247 ppt
108	1000	261 ppt
108	1000	418 ppt
109	1000	300 ppt
109	1000	309 ppt
119	1000	611 ppt
119	3000	514 ppt
120	1000	414 ppt
120	3000	353 ppt

Rapid Technique for Quantifying Tetrachlorodibenzo-p-Dioxin Present in Chlorophenoxy Herbicide Formulations

by

B. M. Hughes, C. D. Miller, M. L. Taylor, R. L. C. Wu[1]
C. E. Hill, Jr.[1] and T. O. Tiernan[2]

Chemistry Research Laboratory
Aerospace Research Laboratories (AFSC)
Wright Patterson Air Force Base
Ohio 45433

---

[1]Systems Research Laboratories, Dayton, Ohio 45440

[2]Author to whom reprint requests and correspondence should be addressed.

BRIEF

An improved column-chromatography procedure has been developed for use with a unique, automated gas chromatograph-quadrupole mass spectrometer system to determine 2,3,7,8-tetrachlorodibenzo-p-dioxin concentrations as low as 10^{-8} g/g sample, with a relative standard deviation of about 6%.

ABSTRACT

An improved column-chromatography procedure is described for efficient extraction of 2,3,7,8-tetrachlorodibenzo-p-dioxin (TCDD) from chlorophenoxy herbicide matrices. This procedure is rapid, does not require concentration of eluate prior to analysis, and minimizes sample and glassware handling, thus reducing toxicity hazards. A highly stable, automated gas chromatograph-quadrupole mass spectrometer (GC-QMS) system has been developed for quantifying TCDD in the column-chromatography eluate at levels as low as 10^{-8} g/g sample. The relative standard deviation is 6.3% for the overall procedure. The GC-QMS system permits direct introduction of the GC effluent at flow rates of up to 30 ml/min into the MS ion source and is equipped with pneumatically operated valves for automated venting of components which are not of interest. The GC-QMS is equipped with an automatic sample injector and a data acquisition and control system which allows continuous unattended operation for periods up to 24 hours.

The chemistry and toxicology of chlorinated derivatives of dibenzo-p-dioxin (I) are summarized in two recent publications.[1,2]

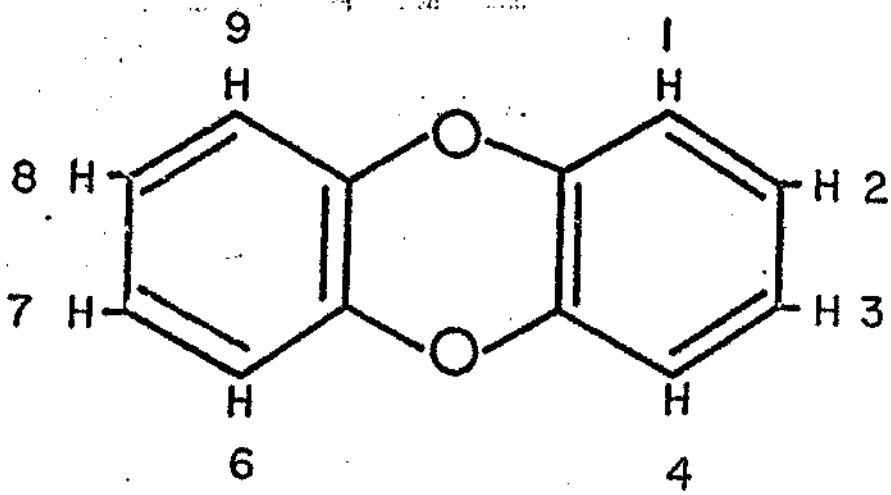

Blair[1] indicates that theoretically there are 75 possible chlorodioxins; after having investigated the toxicology of several chlorodioxins, Schwetz[3,4] concludes that 2,3,7,8-tetrachlorodibenzo-p-dioxin (2,3,7,8-TCDD) has "an unusually high toxicity." Based on laboratory animal studies, 2,3,7,8-TCDD has been found by Schwetz[3,4] and others[5,6] to be embryotoxic, acnegenic, and lethal (in guinea pigs) after a single oral dose amounting to 0.6 µg of 2,3,7,8-TCDD per kilogram of body weight. Kimbrough[7] in a review of the toxicology of 2,3,7,8-TCDD and related materials indicates that the physiological effects of this material in both animals and humans are quite detrimental; instances of illness among industrial workers in plants manufacturing trichlorphenol have been reported.[7] It has been established[8,9,10,11] that during the synthesis of trichlorophenol, involving alkaline hydrolysis of tetrachlorobenzene, 2,3,7,8-TCDD is formed. Subsequent use of contaminated trichlorophenol for synthesis of more complex

organochlorine compounds may lead to final products contaminated with 2,3,7,8-TCDD. Indeed, Moore[12] indicates that chlorinated dibenzodioxins or dibenzofurans have now been found as contaminants in fungicides (pentachlorophenol), herbicides (2,4,5-trichlorophenoxyacetic acid), and polychlorinated biphenyls. Interest concerning the possible effects of dioxin-contaminated 2,4,5-T was aroused by the work of Courtney[6,9] which precipitated Congressional hearings[10] and, subsequently, action by the U.S. Environmental Protection Agency.[13]

Continuing concern about 2,3,7,8-TCDD[14,15] has prompted attempts to determine its prevalance in a wide variety of substances including soil,[16,17,18] animal and plant tissue,[18,19,20,21,22] and various chemical matrices -- especially pesticides and herbicides.[16,19,23-30] Certain of the techniques reported for assaying environmental and biological samples for 2,3,7,8-TCDD content are purported to be quite sensitive, permitting quantitative analysis of concentrations as low as 10^{-12} g of 2,3,7,8-TCDD per gram of sample. However, methods for analyzing chemical products such as herbicide formulations need not be ultra sensitive, because herbicides are greatly diluted prior to application. Thus, analytical methods which are less sensitive (10^{-8} g of 2,3,7,8-TCDD per gram of sample) are sufficient for analysis of undiluted herbicides. In addition to the sensitivity of the analytical method, however, there is the need for specificity to permit unequivocal identification of the 2,3,7,8-TCDD. Many chlorinated herbicides and pesticides have chemical and physical properties which are similar to those of 2,3,7,8-TCDD, and these compounds may interfere with the quantitative determination of the latter. For example, polychlorinated

biphenyls and DDE (arising from dehydrohalogenation of DDT) have been implicated as interferences in certain methods.[20,21] Of those analytical methods currently available, coupled gas chromatography-mass spectrometry (GC-MS) affords the most powerful combination of specificity and sensitivity, and several of the methods cited previously[19,23-31] make use of GC-MS instrumentation.

In this laboratory a method for determining 2,3,7,8-TCDD in a large number of chlorophenoxy-type herbicide samples was sought. Implementation of methods reported in the literature[16,19,23-30] proved impractical because these methods either lacked specificity or required time-consuming, inherently irreproducible procedures which rendered them useless for large numbers of determinations. The aim of the present study was to develop a method which would eliminate these procedures -- particularly concentration steps, sample transfers, and rigorous glassware cleaning. A greatly improved method for determining 2,3,7,8-TCDD in chlorophenoxy herbicides is reported here; a simple and rapid sample-preparation sequence accomplished with completely disposable glassware and small volumes of herbicide and solvents minimizes handling -- thereby reducing toxicity hazards -- and eliminates the concentration of sample extracts. The sample preparation is followed by direct analysis of the extract using GC-MS. The instrument described here is a fully automated gas chromatograph-quadrupole mass spectrometer (GC-QMS) system developed in this laboratory; the quadrupole mass filter is capable of sequential monitoring of as many as six masses and unattended operation for periods up to 24 hours. With this procedure, TCDD detection sensitivities of 2×10^{-8} g of 2,3,7,8-TCDD per gram of sample are achievable routinely, and large numbers of samples can be analyzed rapidly.

EXPERIMENTAL

Stardards and Reagents. The benzene (Nanograde) used in this study was obtained from Mallinckrodt, and the hexane (Pesticidequality) was obtained from Matheson, Coleman, and Bell. Alumina (Fisher Scientific, A 540, 80-200 mesh) was conditioned at 120°C for at least 12 hr and maintained at that temperature until immediately prior to use. Silica gel (Matheson, Coleman and Bell, GC grade, 100-200 mesh) was used as received. The 2,3,7,8-tetrachlorodibenzo-p-dioxin used to prepare calibration standards was obtained from Dow Chemical Co., Midland, Michigan, and was certified to be 98.6% pure, based on mass-spectral analysis. The mass spectrum of the Dow 2,3,7,8-TCDD sample was also determined in this laboratory and compared with that of a sample of 1,2,3,4-TCDD obtained from Analabs, Inc. The results support the Dow purity estimates.

Column-Chromatography Procedure. The following sample pretreatment or clean-up procedure was developed for removing compounds which interfere with the GC-MS determination of 2,3,7,8-TCDD:

1. Prepare a 30-cm glass column using 10 mm o.d., standard-wall Pyrex tubing (one end of glass tube is pulled down to 2 mm o.d.).
2. Insert a plug of silanized glass wool into the column; add 4 g of silica gel followed by 4 g of alumina.
3. Moisten column with 20% benzene in hexane.
4. Dilute 1 g of herbicide with 0.5 ml of 20% benzene in hexane, and transfer this solution to the moistened column. Wash the vessel with an additional 0.3 ml of solvent, and add the wash to the top of the column.

5. Allow the herbicide solution to percolate into the alumina at the top of the column and then elute with 20% benzene in hexane.

6. Collect and discard the first 5 ml of column eluate.

7. Retain the next 6 ml of eluate for analysis. An aliquot of this eluate is injected directly into the GC-QMS apparatus.

The time required for this procedure is about 30 min; however, in practice, one analyst can operate up to four columns simultaneously. Automation of this procedure is possible.

Automated GC-QMS System. In order to perform quantitative determinations of TCDD at sub-parts-per-million concentrations in herbicide formulations, a unique, automated, multiple-ion-monitoring gas chromatograph-mass spectrometer system was designed and fabricated in this laboratory. The system, shown schematically in Figure 1, includes a gas chromatograph (Model 2740, Varian Instrument Division, Palo Alto, California) equipped with a Varian Model 8000 automatic sample injector and flame ionization detector. The chromatograph was modified to include a switching manifold (shown in detail in Figure 2) which consists of three high-temperature, two-way switching valves (Valco Instrument Co., Houston, Texas) and two variable leak valves (Granville Phillips Co., Boulder, Colorado). This manifold is mounted inside the oven of the gas chromatograph. The drivers on the variable leak valves were removed 4 in. from the hot zone -- although the valves can operate at temperatures in the region of 250°C,

the drivers can operate only to 75°C (engineering drawings for modifying these valves were supplied by the Granville-Phillips Co.). The tubing used in the manifold and throughout the heated portions of the system is 1/8-in.-o.d. stainless steel lined with glass (available from Alltech Associates, Arlington Heights, Illinois). Switching Valve No. 1 (see Figure 2) is equipped with a solenoid-actuated pneumatic operator which permits automated venting of the solvent (or other components which are not of interest). When the helium effluent from the chromatographic column is being vented, helium from an auxiliary line continues to enter the mass-spectrometer ion source. The needle valve in the vent line and the pressure regulator in the make-up helium line permit appropriate adjustment of flows and pressures; therefore, when Switching Valve No. 1 is in either "solvent vent" or "normal flow" position, identical pneumatic conditions prevail and mass-spectrometer ion-source conditions are unperturbed which prevents large shifts in the base-line signal output from the mass spectrometer and permits smooth instrument operation even during repetitive switching of Valve No. 1. Switching Valves Nos. 2 and 3 are interconnected by means of a loop which includes a Matheson Model ALL-100 linear mass flowmeter (Matheson Gas Products, East Rutherford, N.J.) and a pressure gauge (Matheson Model P/N 63-3103). The gas flow and pressure in the line to the mass spectrometer or to the flame-ionization detector (FID) can be measured during actual operation of the instrument, with only slight perturbation in signal output from either the FID or the mass spectrometer.

The quadrupole mass filter employed is manufactured by Extranuclear Laboratories (Pittsburgh, Pennsylvania). The mass filter and source are housed in a 6-in. stainless steel "T," and the source and mass-filter regions

are separated by means of a Teflon collar which permits differential pumping of the two regions. The analyzer region is pumped by a 4-in, Varian-NRC Model 161-2 oil-diffusion pump, and the source envelope is pumped by a 6-in. Bendix Model PVM-100 diffusion pump. Both pumps are equipped with gate valves and cryogenic traps. Pumping in the source region is adequate to permit direct introduction of the gas-chromatograph effluent at flow rates up to 30 cc/min without the use of a helium separator. Typical pressures in the source envelope during operation are on the order of 1×10^{-4} torr, and a pressure of 2×10^{-6} torr is maintained in the analyzer region.

The mass spectrometer in the configuration described has a maximum mass resolution of 1000; for the studies described herein, however, the mass resolution was adjusted to about 200 at m/e 320, and a single mass fragment (m/e 320 or m/e 322) was monitored as a function of time to obtain quantitative data.

To permit automatic data acquisition and control, the GC-QMS system was equipped with an Autolab System IV Computing Integrator (Spectra-Physics, Inc., Mountain View, California), to display the data in digital form and also to record the data on punched paper tape using an ASR-33 Teletype. Mass chromatograms were acquired on a strip-chart recorder. A HP 2116-C computer was programmed to reduce the data from the punched paper tape and to compute the dioxin concentration and the percent standard deviation for each sample injection.

In the fully automated mode, the GC-QMS functions sequentially as follows:

1. Automatic sample injector purges syringe, loads sample syringe, makes injection, and activates integrator.

2. Integrator begins data acquisition and, after a programmable time delay, activates solenoid vent valve. This valve automatically switches the GC effluent into the QMS after the solvent has eluted, allowing all effluent to enter the ion source.

3. After another programmable time delay, the integrator closes the solvent vent valve, computes areas, and yields printed and punched paper tape records of data.

4. After a preselected time interval corresponding to the duration of the above process, the automatic sampler reactivates the above cycle.

The time required for a complete instrument cycle under the operating conditions outlined is about 15 min. The instrument was calibrated using a 2,3,7,8-TCDD standard as noted previously. In practice, the automatic sample-injector carrousel was loaded in such a way that one standard was injected after each three unknown samples. Duplicate injections of samples and standards were also made. The procedure markedly improved the precision and accuracy of the data obtained.

Specific operating parameters for the gas chromatograph and mass spectrometer are as follows:

Gas Chromatograph;

Column:	6-ft x 1/8-in. o.d. glass coiled column packed with 10% OV-17 on Chromosorb W/HP
Carrier Gas:	Helium at 30 cc/min
Temperatures:	Injection Port - 240°C
	Column - 230°C
	FID detector - 240°C
	Transfer line into mass spectrometer - 310°C

Mass Spectrometer:

Ionizing Voltage:	23 eV
Multiplier Voltage:	3500 V
Envelope Pressure:	2.3×10^{-4} torr
Analyzer Pressure:	3.5×10^{-6} torr

To corroborate data obtained with the GC-QMS, a double beam MS-30 mass spectrometer AEI Scientific Apparatus, Ltd. (Manchester, England) coupled through a silicone membrane separator (AEI Model WF029) to a Varian 1440 gas chromatograph was employed. The operating parameters for this system are as follows:

Gas Chromatograph:

Column:	5-ft x 1/8-in. o.d. stainless steel packed with 1.5% OV-101 on Chromosorb G/HP (100/120 mesh)
Carrier Gas:	Helium at 55 cc/min
Temperatures:	Injection Port - 260°C
	Column - 262°C

Mass Spectrometer:

Resolution:	2000
Ionizing Voltage:	70 eV
Source Temperature:	250°C
Separator Temperature:	183°C

RESULTS AND DISCUSSION

Preliminary experiments with typical herbicide formulations demonstrated that successful implementation of a specific-ion-monitoring GC-QMS technique for determination of 2,3,7,8-TCDD would require a sample pretreatment or clean-up procedure. Nominal separation of the primary ester components of the herbicide matrix from the 2,3,7,8-TCDD can be accomplished by gas chromatography; however, since the ester components elute from the column prior to TCDD and are present in much larger quantities (by a factor of 10^6), they do in fact, interfere with the TCDD analysis due to tailing of the main component peaks. It is therefore desirable to remove the bulk of the esters prior to injection of the sample into the GC-QMS. Moreover, many of the herbicide samples were observed to contain other high-molecular-weight compounds which elute from the gas-chromatographic column long after the TCDD. If sample analysis time is to be minimized, these components must also be removed prior to injection into the GC-QMS. Otherwise, the peaks arising from these compounds interfere with the TCDD peaks originating from subsequent sample injections. Attempts to measure the TCDD by direct injection of herbicide samples into the mass-spectrometer ion source were also unsuccessful; in an attempt to detect the very low levels of TCDD present, a very large

volume of herbicide was introduced -- too large for the available pumping capacity of the system -- and the resulting ion-source pressures were excessive.

In initial efforts to isolate 2,3,7,8-TCDD from chlorophenoxy herbicide matrices a previously reported liquid chromatography method was used.[19] This procedure involves dissolving 5 g of sample in 25 ml of solvent (20% benzene in hexane) and introducing this solution onto a column containing 50 g of silica gel equilibrated with the solvent. This procedure requires about 2 hr and yields the TCDD in 100 ml of solvent. A concentration step must be performed before the sample is injected into the GC-QMS. A simple solvent evaporation step used in the procedure described earlier[19] is difficult to accomplish in a reproducible manner and can lead to TCDD losses. Also, all glassware and vessels used for a given sample must be cleaned with extreme rigor to avoid carryover of TCDD in subsequent analyses. Since these steps are time consuming, a shorter and more efficient procedure was sought which would minimize the volume of solvent needed in the liquid-chromatographic sequence and would permit the use of disposable columns and containers.

Since alumina has been mentioned in the literature[22,23] as a useful medium for isolation of TCDD from certain samples, its utility in separating TCDD from the chlorophenoxy matrix was examined. Liquid-chromatography columns of varying dimensions were prepared using alumina and alumina-silica gel combinations, and the efficacy of these columns was determined. Standard solutions of TCDD, as well as chlorophenoxy herbicide samples doped with known amounts of TCDD, were chromatographed using the various columns, and aliquots of the eluate were collected and analyzed for TCDD

using the GC-QMS apparatus described earlier. Plotted in Figure 3 are typical data which illustrate the distribution of TCDD in the eluate from a column prepared using 10 g each of silica gel and alumina in a 10-mm-o.d. x 30-cm-long glass tube. The 2,3,7,8-TCDD is seen to elute entirely in 6 ml of the solvent. Attempts to collect only the "center fraction" of the 6-ml aliquot led to irreproducible results. Apparently, variations which occur in the preparation of the columns cause the elution pattern of 2,3,7,8-TCDD to vary somewhat from column to column; nevertheless, analyses based upon collection of the entire 6-ml aliquot of eluate are observed to be quite consistent. Mass chromatograms (instrument tuned to monitor m/e 320) of a chlorophenoxy herbicide extract obtained using the silica gel-alumina column are shown in Figure 4. Most of the interfering compounds have been effectively removed, and the TCDD peak is clearly resolved from those of the remaining compounds which also exhibit m/e 320.

Further studies were conducted to assess the precision and accuracy of the analytical data for TCDD obtained by means of the clean-up technique described above. In these experiments accurately doped chlorophenoxy herbicide samples were analyzed as well as samples of herbicides known to contain 2,3,7,8-TCDD as a contaminant. Table I shows the measured concentration of 2,3,7,8-TCDD in an extract of an actual field sample of a chlorophenoxy herbicide which was determined by making six sequential injections of the same extract into the GC-QMS. These results are indicative of the precision of the GC-MS measurement, and the relative standard deviation is seen to be 1.8%. In Table II the results for five different 1-g aliquots of another herbicide specimen are presented. Each of the samples was subjected to the clean-up procedure, and the resulting extracts

were analyzed using the GC-MS. These data indicate that the reproducibility of the overall analytical process is ±6.3%.

In Table III the levels of TCDD observed in respective sub-fractions of the 6 ml of liquid-chromatography column eluate are shown for a series of replicate herbicide samples (both doped and containing only "native" TCDD). While the level of TCDD in a given sub-fraction varied markedly within the set, it should be noted that the analyses of replicate samples based on the total TCDD in the entire 6 ml of eluate are in excellent agreement.

It is evident from the data shown in Figure 4 that even after application of the sample clean-up procedure described above, several herbicide components which exhibit a mass spectral peak at m/e 320 remain. These components are usually resolved by the gas-chromatographic column, and the peak corresponding to TCDD can be determined by comparing the retention times of the unknown peaks with that obtained for a TCDD standard. To verify that the peak identified as TCDD includes no other components (having identical gas-chromatographic retention times) several isotopic peaks in the mass spectrum may be monitored simultaneously and the ratios of these compared with the corresponding ratio for a TCDD standard and with the theoretically predicted ratios of chlorine isotopes. Such a comparison is shown in Table IV for the ratio of the m/e 320 to m/e 322 peaks [molecular ion and (molecular ion + 2) isotopic peaks]. The expected peak ratios are observed for the unknowns, confirming that the monitored component is indeed TCDD.

For further verification of the accuracy of the results obtained with the described procedure, the extracts from several samples were also analyzed using an MS-30 double-beam mass spectrometer coupled to a Varian 1400 gas chromatograph. Single-ion monitoring was again employed, and the experimental conditions were similar to those described for the automated GC-QMS apparatus described earlier. With the MS-30 instrument, however, a different gas-chromatographic column packing was utilized -- 1.5% OV-101 on Chromosorb G. With the MS-30 tuned to m/e 320 and the resolution adjusted to 2000, the data reported in Table V were obtained for a series of samples. For comparison, the corresponding results obtained using the quadrupole instrument are also presented in this table. The data are seen to be in reasonably good agreement.

Other herbicide formulations consisting of octyl and isooctyl esters of various chlorophenoxyacetic acids were randomly selected for analysis using the described methodology. No difficulties were encountered, and these results indicate that 2,3,7,8-TCDD can be quantified in a wide variety of commercial herbicide formulations using the analytical methodology described here.

CONCLUSIONS

An analytical method has been reported for rapid determination of 2,3,7,8-TCDD at concentrations as low as 10^{-8} g/g sample in a variety of sample matrices, including the butyl esters of dichloro and trichlorophenoxyacetic acids. Commercially available herbicides -- consisting of solutions of octyl esters of 2,4-D and/or 2,4,5-T in concentrations ranging

from 7 to 65% -- have also been assayed for 2,3,7,8-TCDD content without difficulty. The automated GC-QMS system developed for these applications is highly sensitive -- yet extremely stable -- and thereby lends itself to unattended, automated operation for long periods. Such instrumentation is undoubtedly the key to cost-effective quality-control programs in which statistically valid sampling techniques are implemented to monitor hazardous components.

These studies were supported in part by the U.S. Air Force Logistics Command.

REFERENCES

1. "Chlorodioxins -- Origin and Fate," E. H. Blair, Ed., Advances in Chemistry Series No. 120, American Chemical Society, Washington, D. C. 1973.
2. Environmental Health Perspectives, Experimental Issue No. 5, G. W. Lucier, Ed., DHEW Publication No. (NIH) 74-218, U.S. Department of Health, Education, and Welfare, Public Health Service, National Institutes of Health, September 1973.
3. B. A. Schwetz, J. M. Norris, G. L. Sparschu, V. K. Rowe, P. J. Gehrig, J. L. Emerson, and C. G. Gerbig, in "Chlorodioxins -- Origin and Fate," E. H. Blair, Ed., Advances in Chemistry Series No. 120, American Chemical Society, Washington, D. C. (1973), p. 55.
4. B. A. Schwetz, J. M. Norris, G. L. Sparschu, V. K. Rowe, P. J. Gehrig, J. L. Emerson, and C. G. Gerbig, Environmental Health Perspectives, Experimental Issue No. 5, G. W. Lucier, Ed., DHEW Publication No. (NIH) 74-218, U.S. Department of Health, Education, and Welfare, Public Health Service, National Institutes of Health, September 1973, p. 87.
5. G. L. Sparschu, F. L. Dunn, and V. K. Rowe, Fd. Cosmet. Toxicol., 9, 405 (1971).
6. K. D. Courtney and J. A. Moore, Toxicol. and Appl. Pharmacol., 20, 396 (1971).
7. R. D. Kimbrough, Arch. Path. 94, 125 (1972).
8. G. R. Higginbotham, A. Huang, D. Firestone, J. Verrett, J. Ress, and A. D. Campbell, Nature, 220, 703 (1968).
9. M. Tomita, Nature, 220, 702 (1968).

10. Report on 2,4,5-T. A Report of the Panel on Herbicides of the President's Science Advisory Committee, Government Printing Office, Washington, D. C., March 1971.

11. M. H. Milnes, Nature, 232, 395 (1971).

12. J. A. Moore, Environmental Health Perspectives, Experimental Issue No. 5, G. W. Lucier, Ed., DHEW Publication No. (NIH) 74-218, U.S. Department of Health, Education, and WElfare, Public Health Service, National Institutes of Health, September 1973.

13. P. H. Abelson, Science, 170 (1970).

14. D. Shapley, Science, 180, 285 (1973).

15. Anon., Time, September 2, 1974, p. 69.

16. E. A. Woolson, R. F. Thomas, and P. D. J. Ensor, J. Agr. Food Chem., 20, 351 (1972).

17. P. C. Kearney, E. A. Woolson, and C. P. Ellington, Jr., Environ. Sci. and Technol., 6, 1017 (1972).

18. W. D. Crummett and R. H. Stehl. Private communication.

19. W. D. Crummett and R. H. Stehl, Environmental Health Perspectives, Experimental Issue No. 5, G. W. Lucier, Ed., DHEW Publication No. (NIH) 74-218, U.S. Department of Health, Education, and Welfare, Public Health Service, National Institutes of Health, September 1973.

20. R. Baughman and M. Meselson, "Chlorodioxins -- Origin and Fate," E. H. Blair, Ed., Advances in Chemistry Series No. 120, American Chemical Society, Washington, D. C., 1973.

21. R. Baughman and M. Meselson, Environmental Health Perspectives, Experimental Issue No. 5, G. W. Lucier, Ed., DHEW Publication No. (NIH) 74-218, U.S. Department of Health, Education, and Welfare, Public Health Service, National Institutes of Health, September 1973.

22. D. Firestone, D. F. Flick, J. Ress, and G. R. Higgenbotham, J. Assoc. Offic. Anal. Chemists, 54, 1293 (1971).

23. M. L. Porter and J. A. Burke, J. Assoc. Offic. Anal. Chemists, 54, 1426 (1970).

24. D. T. Williams and B. J. Blanchfield, J. Assoc. Offic. Anal. Chemists, 54, 1429 (1971).

25. R. W. Storherr, R. R. Watts, A. M. Gardner, and T. Osgood, J. Assoc. Offic. Anal. Chemists, 54, 218 (1971).

26. K. S. Brenner, K. Muller and P. Sattel, J. Chromatog., 64, 39 (1972).

27. D. Firestone, D. Ress, N. L. Brown, R. P. Barron, and J. N. Danico, J. Assoc. Offic. Anal. Chemists, 55, 85 (1972).

28. D. T. Williams and B. J. Blanchfield, J. Assoc. Offic. Anal. Chemists, 55, 93 (1972).

29. D. T. Williams and B. J. Blanchfield, J. Assoc. Offic. Anal. Chemists, 55, 1358 (1972).

30. T. J. N. Webber and D. G. Box, Analyst, 98, 181 (1973).

FIGURE CAPTIONS

Figure 1. Schematic representation of automated GC-QMS system.

Figure 2. Diagram of switching-valve manifold for automated GC-QMS system.

Figure 3. Distribution of tetrachlorodibenzo-p-dioxin in the solvent eluted from an alumina-silica gel liquid-chromatography column.

Figure 4. Mass chromatograms (monitoring m/e 320) obtained with the GC-QMS for a TCDD standard (80 ppb in 20% benzene-hexane solvent) and for two herbicide extracts.

Table I. Replicate Analyses of a Single Extract From An Unknown Herbicide Sample

Analysis No.	µg/g Found (ppm)
1	0.135
2	0.134
3	0.133
4	0.131
5	0.138
6	0.148
	$\bar{X}$ = 0.137[a]
	s = 0.0025[b]
	%s = 1.8[c]

[a] $\bar{X}$ = Arithmetic mean

[b] s = Standard deviation of the mean

[c] %s = Relative standard deviation

Table II. Replicate Analyses (Separate Extractions) of An Unknown Herbicide Sample

Sample No.	µg/g Found (ppm)
1	0.22
2	0.18
3	0.20
4	0.25
5	0.25
	$\bar{X}$ = 0.22[a]
	s = 0.0138[b]
	%s = 6.3[c]

[a] $\bar{X}$ = Arithmetic mean

[b] s = Standard deviation of the mean

[c] %s = Relative standard deviation

Table III. TCDD Levels in Fractions of the Eluate from Liquid Chromatography Column (Alumina-Silica Gel)

	µg TCDD Found[a] (ppm)				
	275K[b]	275E	275F	275G	275J[b]
First 4 ml of eluate	N.D.	N.D.	N.D.	N.D.	N.D.
Next 1 ml of eluate	N.D.	N.D.	N.D.	N.D.	N.D.
Next 1 ml of eluate	0.034	0.013	0.007	0.004	0.20
Next 1 ml of eluate	0.240	0.058	0.065	0.048	0.32
Next 4 ml of eluate	0.32	0.148	0.116	0.138	0.04
Total Found	0.59	0.221	0.188	0.19	0.59

[a]Samples designated K, E, etc., are replicate samples from same herbicide specimen.

[b]Spiked with an additional 0.33-µg TCDD/g.

Table IV, Observed and Theoretically Predicted Ratios of TCDD Isotopic Peaks

Sample[a]	I_{320}/I_{322}
80 ppm Std.	0.84, 0.87
275 V	0.86
275 F	0.78, 0.74
275 G	0.74
275 L	0.80
Theoretical	0.77

[a]Samples designated as V, F, etc. are replicate samples from same herbicide specimen.

Table V. Comparison of High-Resolution and Low-Resolution GC-MS Results

Sample[a]	µg/g Found (ppm) ARL GC-QMS	GC-MS-30
436-1	0.07	0.07
436-2	0.07	0.05
414-1	0.53	0.31
414-2	—	0.38
413-1	0.14	0.11
413-2	—	0.11
17	< 0.02	0.01

[a]Samples designated -1 and -2 are duplicate injections of the same sample extract.

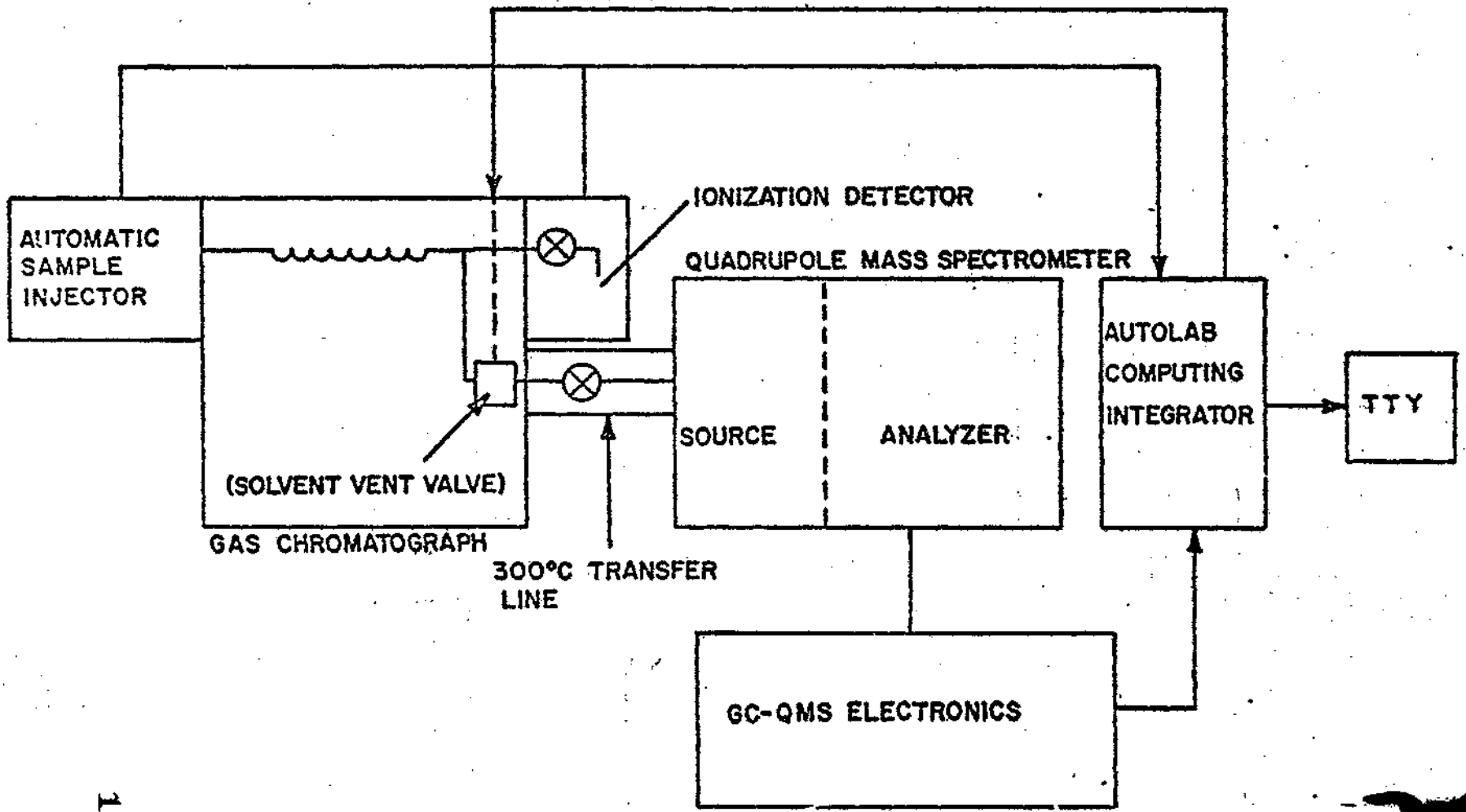
AUTOMATIC
SAMPLE
INJECTOR
IONIZATION DETECTOR
QUADRUPOLE MASS SPECTROMETER
AUTOLAB
COMPUTING
INTEGRATOR
TTY
SOURCE
ANALYZER
(SOLVENT VENT VALVE)
GAS CHROMATOGRAPH
300°C TRANSFER
LINE
GC-QMS ELECTRONICS

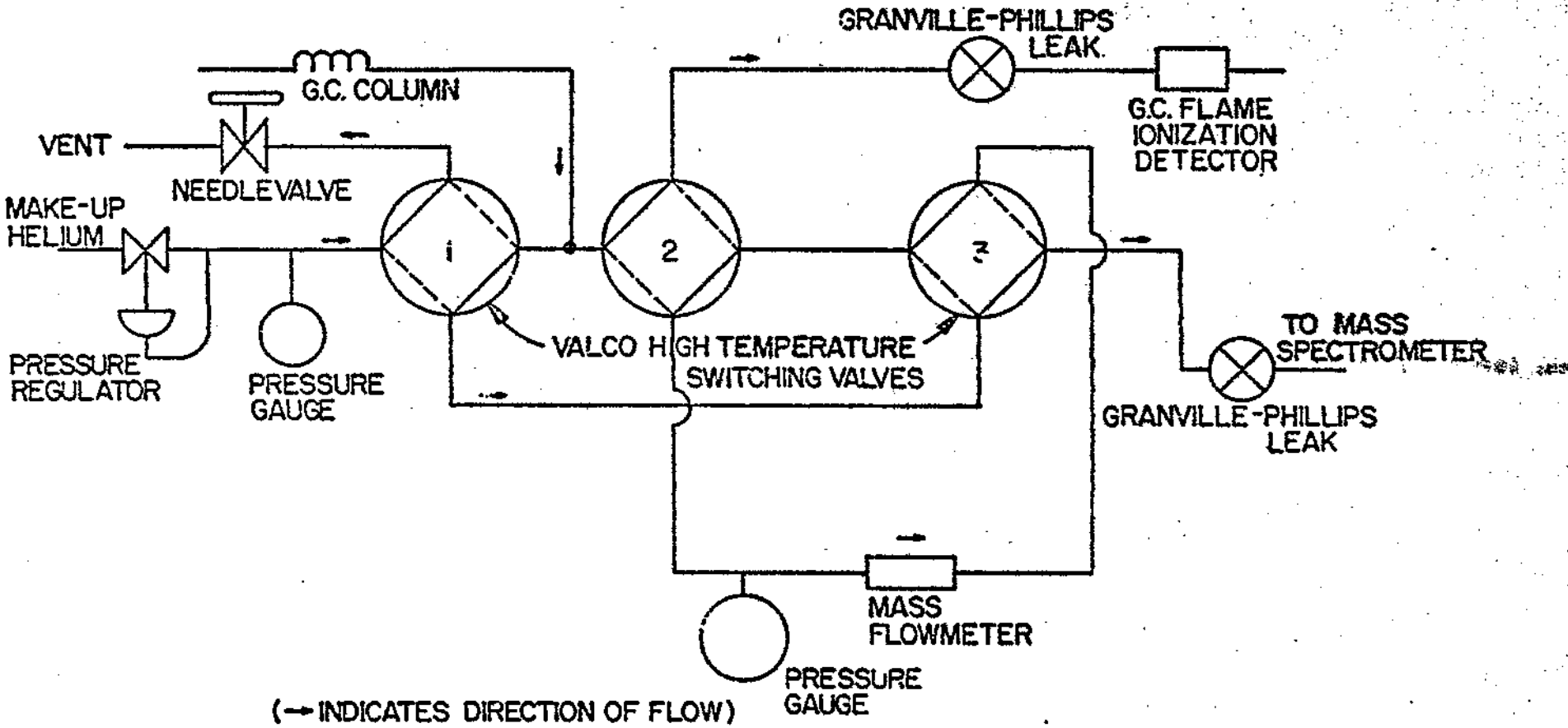
GRANVILLE-PHILLIPS LEAK
G.C. COLUMN
G.C. FLAME IONIZATION DETECTOR
VENT
NEEDLE VALVE
MAKE-UP HELIUM
1
2
3
TO MASS SPECTROMETER
PRESSURE REGULATOR
PRESSURE GAUGE
VALCO HIGH TEMPERATURE SWITCHING VALVES
GRANVILLE-PHILLIPS LEAK
MASS FLOWMETER
PRESSURE GAUGE
(→ INDICATES DIRECTION OF FLOW)

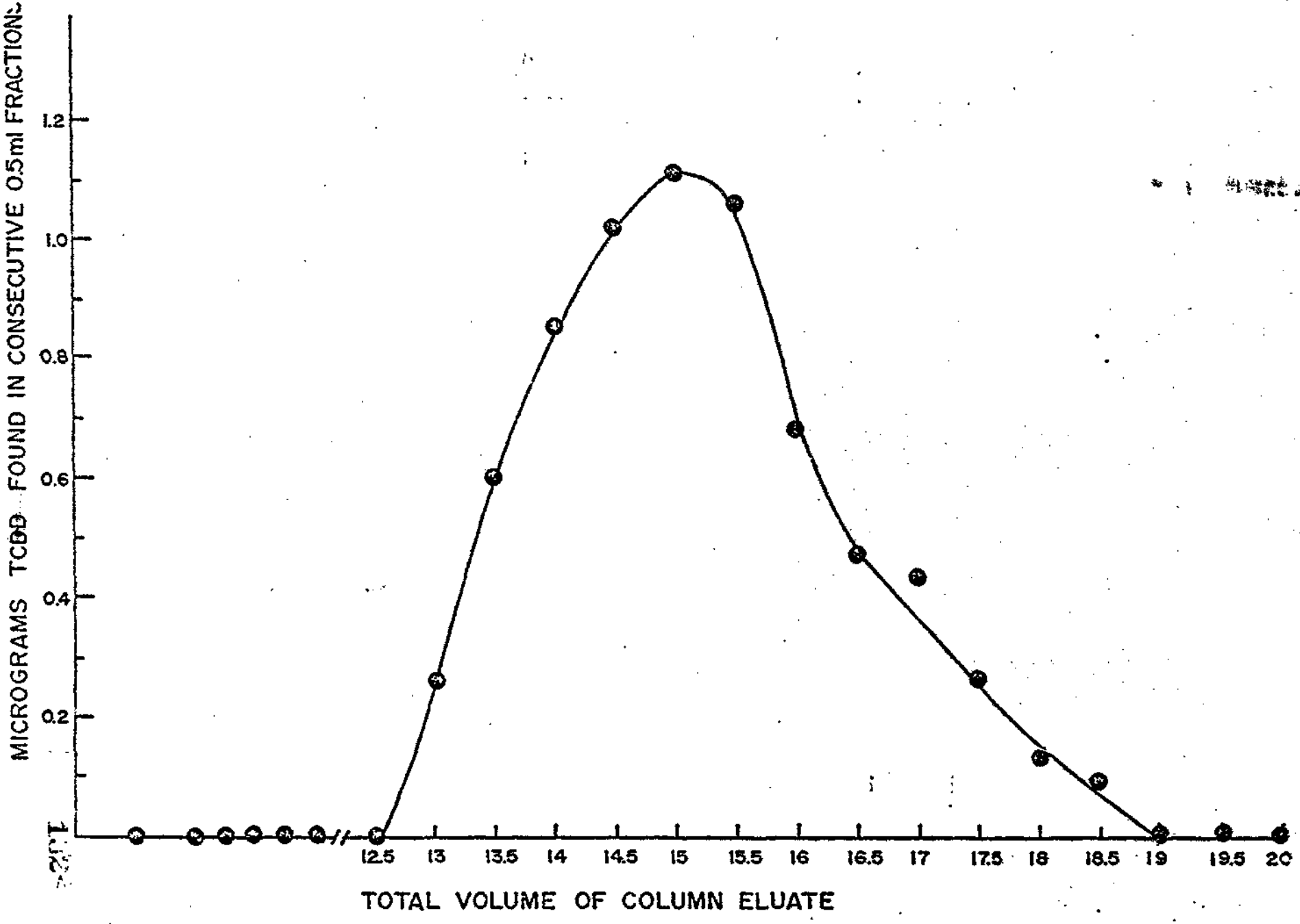
MICROGRAMS TCDD FOUND IN CONSECUTIVE 0.5ml FRACTIONS
1.2
1.0
0.8
0.6
0.4
0.2
12.5
13
13.5
14
14.5
15
15.5
16
16.5
17
17.5
18
18.5
19
19.5
20
TOTAL VOLUME OF COLUMN ELUATE

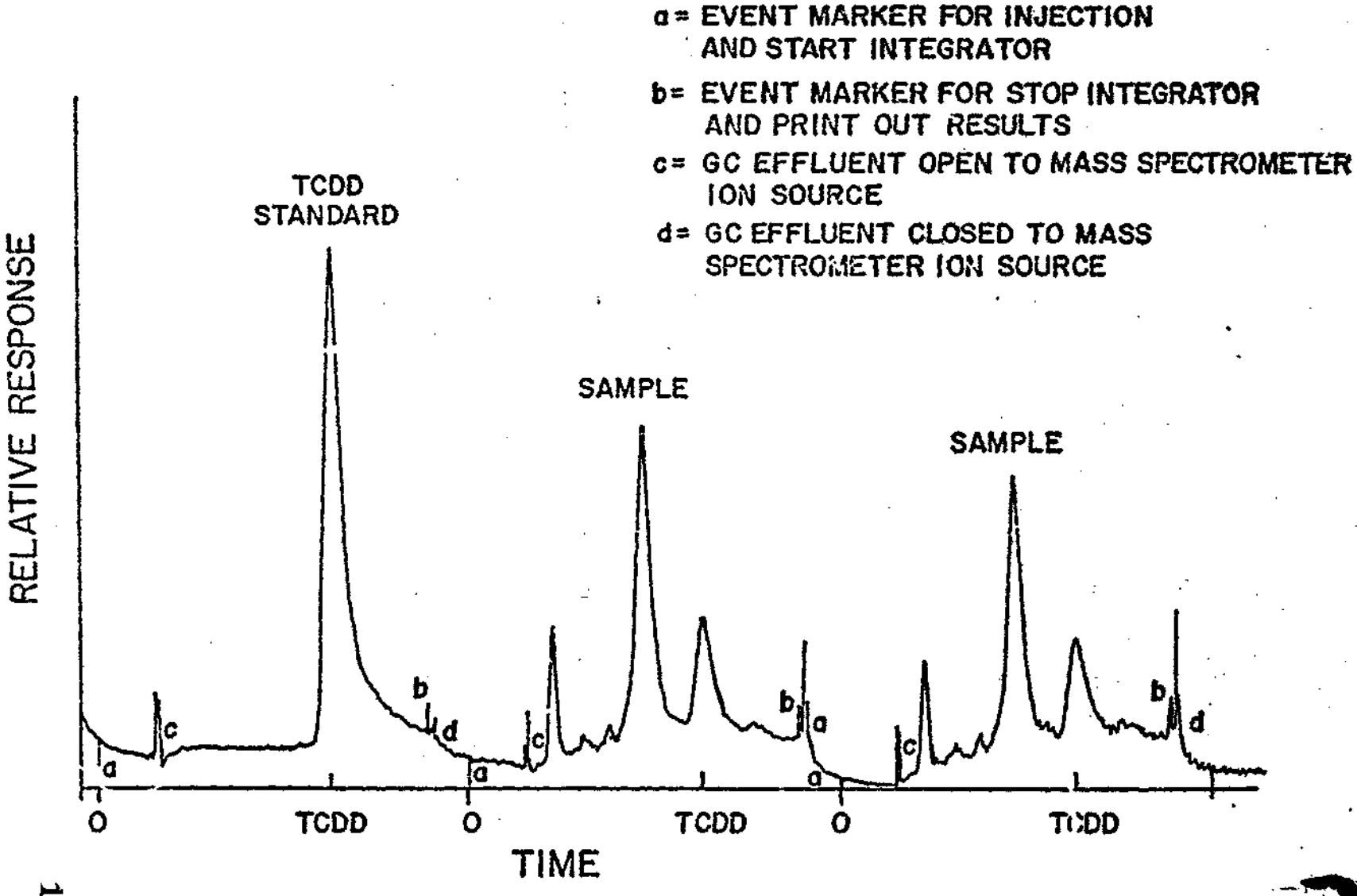
a = EVENT MARKER FOR INJECTION AND START INTEGRATOR
b = EVENT MARKER FOR STOP INTEGRATOR AND PRINT OUT RESULTS
c = GC EFFLUENT OPEN TO MASS SPECTROMETER ION SOURCE
d = GC EFFLUENT CLOSED TO MASS SPECTROMETER ION SOURCE
TCDD STANDARD
SAMPLE
SAMPLE
RELATIVE RESPONSE
TIME
O
TCDD
O
TCDD
O
TCDD

SECTION IV

SPARK-SOURCE AND ELECTRON-IMPACT MASS-SPECTROMETRIC STUDIES

During this final reporting period, spark-source and electron-impact mass-spectrometric methods were employed in Air Force Materials Laboratory (AFML) research programs. These analytical efforts and results are described herein. Spark-source mass-spectrographic (SSMS) studies performed earlier are detailed in previous reports.[16-18]

INTRODUCTION

Specific causes of failure of bearings in the Third Generation Gyro (TGG) to be used in Minute Man III were sought by various nondestructive analytical mass-spectrometric techniques. The amount and kind of inorganic contaminants on the surfaces of several "inner" bearing components as well as other specimens were determined using spark-source mass spectrography; the sample-handling procedures and results are given below. In addition, composition of seven gas samples and the outgassing products from a rejected motor stator were determined using conventional electron-impact mass spectrometry, and these results are also discussed here.

SPARK-SOURCE ANALYSIS

Spark-source mass-spectrographic analyses of beryllium bearings, sublimation products collected on glass slides, stators, and epoxy were carried out and the resulting elemental data are shown in Tables II, III, and IV. These analytical efforts were carried out with the aim of identifying surface contaminants causing bearing failure.

TABLE II

SSMS ANALYSIS OF BERYLLIUM-BEARING SURFACES[a]

Bearing Designation	Elemental Composition
No. 3[b]	Ca, Ti, Cl, Si, Al - High S, Fe, Zn, P, B, F, K - Medium
No. 17	Cl, Si - High Al, S, Ti, Ca, K, Fe, Zn, P, B, F - Medium
No. 32	Ca, Ti, Si - High Cl, Al, S, Fe - Medium F, Zn, Li - Low
No. 32 (after benzene, hexane ultrasonic rinse)	Ca, Si - High Cl, Al, S, Fe - Medium Ti, F, Zn, B, Li - Low
c	Cr, Fe - High

[a]Elements listed left to right in approximate order of decreasing abundance.

[b]Relative amounts of observed surface contamination: No.>3 No. 17>No. 32> No. 32 (cleaned).

[c]No sample designation - submitted for analysis in early March of 1975.

TABLE III

SSMS ANALYSIS OF DEPOSITS ON MICROSCOPE SLIDES

Slide Designation	Elemental Composition
8A[a]	B,S - High
	Ti,F - Medium
	Zn,Cl - Low
6	B - High
	S,F,Ti,Zn,Cl - Appear to be slightly above background
5	B - High
	Zn,Ti,S,F - Medium
	Cl - Low

[a] Slide 5>Slide 8A>Slide 6

TABLE IV

SSMS ANALYSIS OF STATORS AND EPOXY

Sample Designation	Elemental Composition
Stator 17 [a]	F,Cl,K,Ca,Si,Al,Zn,Cu,Fe - High Li - Medium Ti,Cr,P,B - Low
Stator 22	Si,Al,B,Cl,Ca,Ba - High Zn,P,Fe,Cr,Ti,Al,Si,Ca - Low
Epoxy	Si,Al,Cl,Li - High Cd,Fe,Co,S - Medium K,Ba,Cs,B,P - Low

[a] Stator 17>>Stator 32

The technique used for sample removal and analysis involved wiping areas of interest with one end of an indium wire (~ 3-mm diam) and subsequently analyzing the wire using an AEI MS-702R spark source mass spectrometer. Recorded spectra were compared with suitable "blanks." Surface contamination was not apparent (visual inspection) in any of the analyses, and the amount of surface contaminants removed by indium pressing is unknown. However, relative amounts of surface contamination are indicated in the tables.

Additional suggested analytical work to aid in diagnosis of the bearing problem includes:

(1) SSMS analysis of cleaning and polishing agents employed during bearing fabrication such as Freon, diamond paste, alumina, etc.

(2) Further SSMS analyses of surfaces of bearings having known failure characteristics.

ELECTRON-IMPACT MASS-SPECTRAL ANALYSIS OF GASES

The gas-sample vessels received from AFML were labeled as follows:

TW No. 11, 1-15-75
Float Sample Atm No. 220
Gas Sample from No. 11 Float, 1-16-75
TW No. 13, 1-13-75
Gas Sample from Float No. 20
Charge Gas - CSDL
Charge Gas - Northrup

The content of the seven vessels was determined using an AEI MS-30 mass spectrometer with 70-eV ionizing voltage and a resolution of 1000. All samples were admitted directly into the source region of the MS-30 via an all-glass inlet system which was maintained at a temperature of ~ 40°C.

The gas-sample vessels were heated to 65°C during introduction of the samples. Table V gives the results of these analyses; representative spectra are attached. The helium-Freon mixture listed in the table (prepared to contain 0.147 volume % Freon) was used to calibrate the system (the Freon was obtained through AFML from Northrup). The Freons determined in the gas samples consist primarily of Freon 113 ($ClF_2C\text{-}CFCl_2$) as indicated by the presence of intense peaks at m/e 101, 103, 151, and 153 in the mass spectrum, with m/e 101 as the base peak. The presence of some other similar fluorocarbons (such as $Cl_3\text{-}C\text{-}CF_3$) is indicated by the fact that the relative intensities of certain of the mass peaks in the spectra are somewhat greater than indicated in the available standard spectra;[19,20] however, the overall cracking pattern is most certainly that of a $C_2F_3Cl_3$ Freon. The levels of carbon dioxide indicated in Table V are corrected for background--which was quite substantial--and, thus, the accuracy of these results is not so high as for toluene and Freon.

MASS-SPECTRAL ANALYSES OF OUTGASSING PRODUCTS FROM TGG COMPONENTS

A. Rejected Motor Stator

A special inlet was fabricated which permitted the intact motor stator to be enclosed in a glass and Teflon chamber; after evacuation of the chamber, the outgassing products were admitted into the source of the mass spectrometer via the gas-sample introduction probe. Initial attempts to analyze the outgassing products from the rejected motor stator were halted when gross amounts of Freons and possibly other outgassing products were encountered. The all-glass inlet system used in the analysis of the gas samples (which provides a means for controlled admission of gas samples) can be implemented in future studies of the motor-stator outgassing products.

TABLE V

PERCENTAGE OF CO_2, TOLUENE, AND FREON FOUND IN GAS SAMPLES

Sample	Freon (total)	Toluene	CO_2
11 Float	0.0414	0.0130	0.0197
TW 11	2.92	--	0.0205
Helium Charge Gas (CSDL)	0.0007	--	0.0004
Float No. 220	0.0065	--	0.0263
Freon Calibration	0.1136	--	0.0001
Helium Charge Gas (Northrup)	--	0.0004	--
TW 13	0.0001	--	0.0189

NOTE: Sample No. 20F was depleted prior to completion of the quantitative analyses of these mixtures; however, based upon earlier qualitative studies conducted in this laboratory, Sample No. 20F was found to contain toluene and a lesser amount of Freon.

B. No. C-61 Inner

This bearing component was analyzed using another special chamber which was fabricated from stainless steel. The chamber was housed inside the gas-chromatograph oven (an integral part of the MS-30) and was connected to helium which constantly flowed through the chamber and into the inlet system of the mass spectrometer--in this case, the inlet is a silicone separator which is much more permeable to organic molecules than to helium gas. Thus, organic species are preferentially admitted into the source region of the mass spectrometer. The results obtained for C-61, under admittedly less than ideal conditions, did not indicate the presence of contaminants. This method of studying outgassing products is presently being refined, and subsequent studies will be made after system optimization.

FLAME-IONIZATION GAS-CHROMATOGRAPHIC ANALYSIS OF SOLVENTS

For preliminary characterization of the three solvent samples from Northrup, 1 μℓ of each of these solvents was injected into a Varian 1440-10 gas chromatograph equipped with a flame-ionization detector and a 6-ft 1/8-in.-OD glass column packed with 3% CV-3 on Chromosorb W H/P. The column temperature was maintained at 50°C. The chromatograms obtained are shown in Figs. 6 - 8. The relative % compositions of each of the solvents are as shown. The presence of several impurities is readily apparent from the data. Whether the liners of the caps on the sample vials contributed to these results is open to question. The liners appeared to have sorbed the solvents to some degree, particularly in the case of the isopropyl alcohol. The solvents were colorless, however.

TIME	AREA %
21	0.315
24	0.614
29	96.210
47	0.803
53	1.507
65	0.547

Quantity Injected: 1 µℓ

Attenuation: 4×10^{-11}

Chart Speed: 4 in./min.

Column Temp.: 50°C

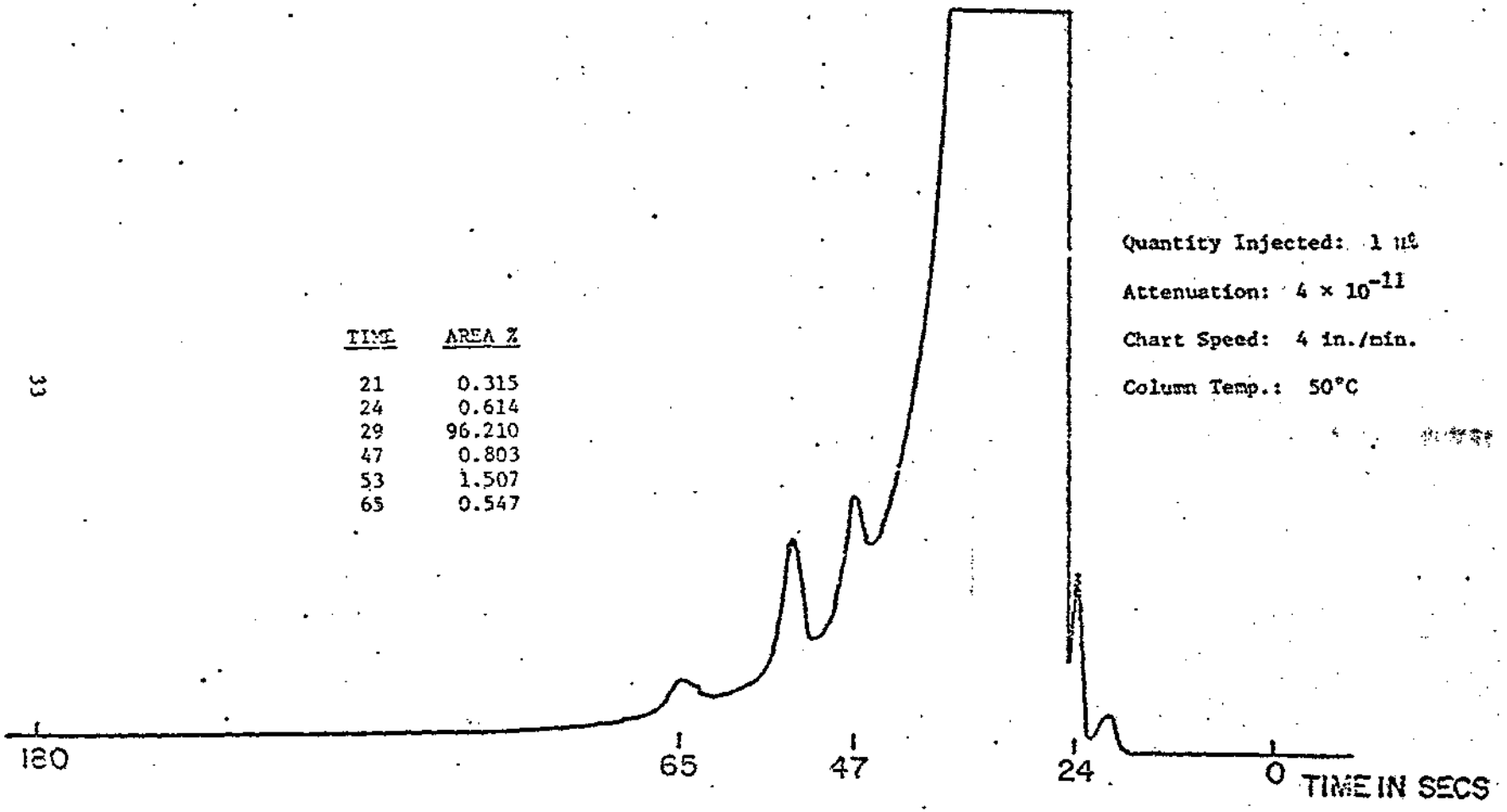

Figure 6. Freon.

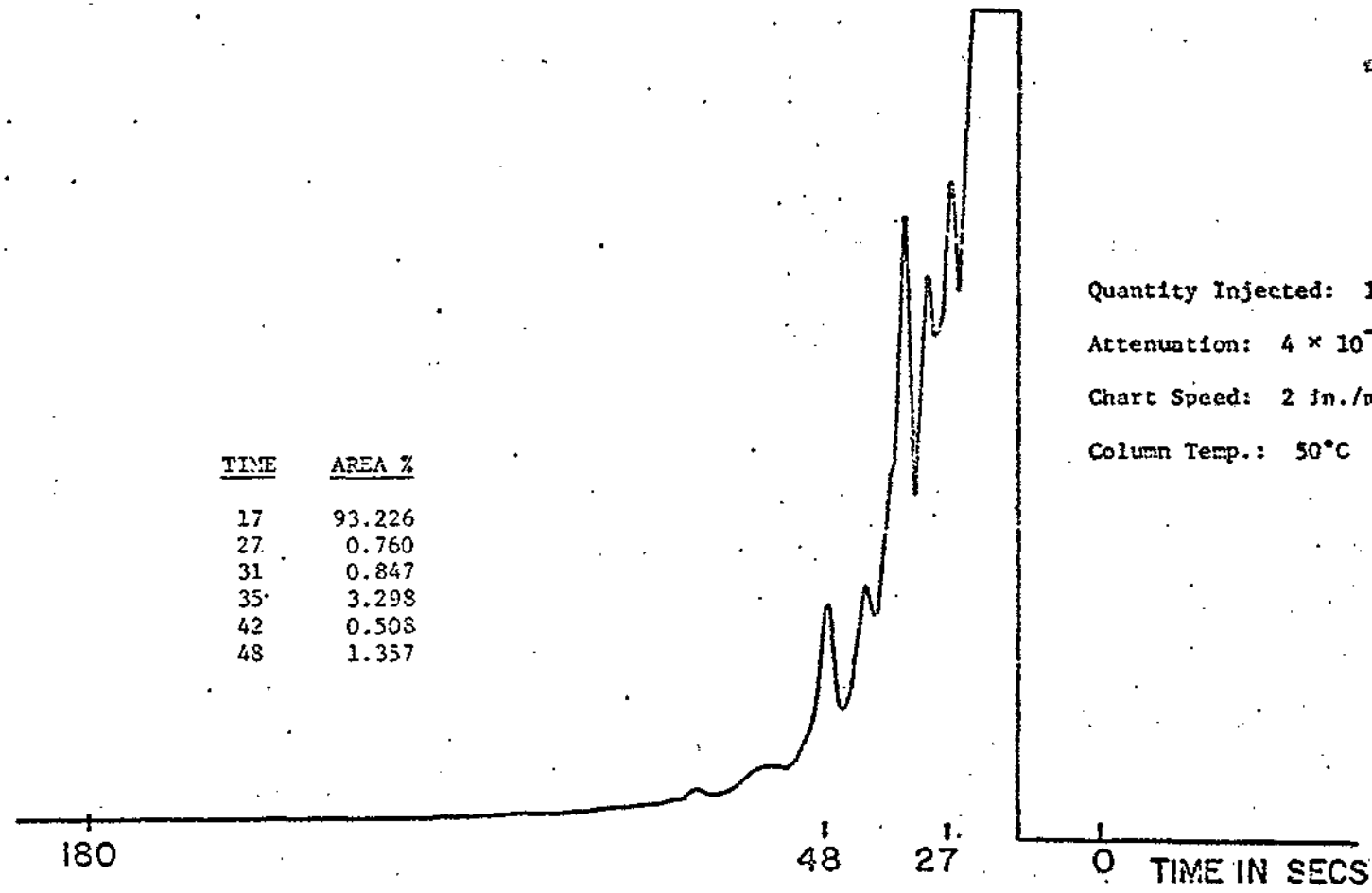

Figure 7. Isopropyl Alcohol from Drum

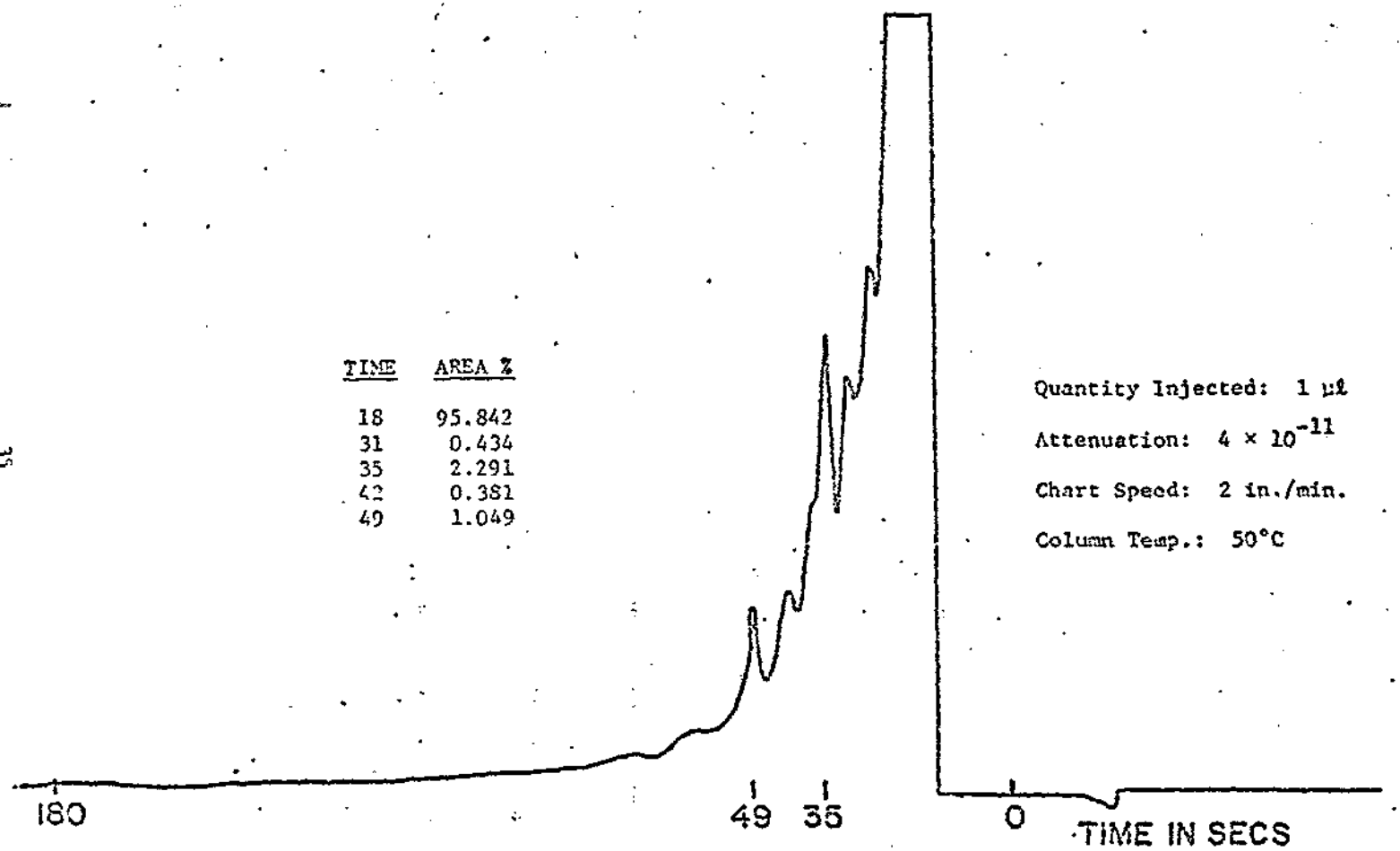

Figure 8. Isopropyl Alcohol from Vapor Booth

ANALYSES OF SURFACE CONTAMINATION ON HYDRAULIC PISTON FROM M-60 ARMY TANK IN CONNECTION WITH FLUID FAILURE PROBLEMS

The turret control system in certain versions of the Army's M-60 tank deployed at CONUS and overseas locations utilizes a new, flame-retardant hydraulic fluid developed under the aegis of AFML which has the following approximate composition:

Fluid: C_3O oligomer of 1-decene (Mwt is estimated ~ 4000)

Additives: 15-20% dihexyladipate or alternatively a trimethyl-O-propane ester

0.5-1.0% Ethyl 702 (a phenolic) (Mwt 425)

1.5-3% tricresylphosphate (Mwt 368)

?% Ba dinonylnaphthalene

In certain of the tanks the turret control system has malfunctioned because of sticking of hydraulic valves. The problem has been ameliorated in the field by simply disassembling the valve and wiping clean the control surfaces. At the request of Major L. Fehrenbacher and Mr. E. Snyder, AFML/MBT, a piston removed from a faulty valve was examined by personnel in the Gaseous Ionization and Excitation Processes Group and analyses of surface contaminants were accomplished.

The hydraulic valve component received from AFML is approximately 4-in. long and 1/2-in. diam. with 10 raised, polished metering surfaces which apparently are in close contact (< 0.001 in. clearance) with the valve body. Readily observable on the surface of the piston are minute, black, stringy particles and a rather uniform coating of hydraulic fluid. The piston was handled carefully (by grasping only the extreme end of the piston) during all sampling. Three separate procedures were employed to remove surface contaminants from the piston. First, several of the dark, stringy particles were removed from the surface using the indium

press technique. (Soft indium wire was pressed onto the surface which attaches surface contaminants.) Since the piston as received was coated with a film of hydraulic fluid, particles harvested in this first analysis necessarily included some hydraulic fluid. In a second analysis additional particles were collected from the surface and washed with hexane which readily dissolves the fluid. The washed particles were separated from the hexane, the hexane evaporated, and an indium press sample of the washed particles was obtained. In the third and final analysis one end of the metal piston, including two of the metering surfaces, was washed by submerging the piston in hexane. The cleaned metering surfaces were found to be coated, rather uniformly, with a grey, amorphous deposit, a sample of which was removed using the indium press method. All of the above samples were analyzed by D. Walters using the MS702R spark source mass spectrometer.

In all three analyses, the dominant elemental species observed were carbon, barium, silicon and sulfur. Some metals which were found in moderate amounts, such as iron and chromium, are presumed to be from the substrate. In addition, somewhat lower levels of phosphorus and aluminum, (amounting to only a few % of the major species) were also found. As expected the first of t' .nree analyses yielded large quantities of hydrocarbon fragments, resulting, of course, from the hydraulic fluid. In the second and third analyses which were performed subsequent to hexane washings, hydrocarbons were not detected above background.

In further studies performed by Drs. Terwilliger and Taylor, a few micrograms of the hexane-washed gum from the controlling surface were placed in a glass capillary and inserted into the source region of the MS-30 electron impact mass spectrometer. The direct insertion probe used in this case was not equipped for auxiliary heating of the sample and heating

could be accomplished only via transference from the source block. One can only roughly estimate the temperature attained by the sample in this instance, but certainly the sample temperature did not exceed 100°C. Source pressure during this analysis was on the order of 1×10^{-6} torr. Results from these studies are quite complex, but overall, the data suggest that some high molecular weight components are present in the sample which in part at least are hydrocarbon in nature. The presence of m/e 368 (along with other fragment ions which one would expect from TCP) in certain of the scans suggest that TCP (tricresylphosphate) may be present. Other masses in the spectra could be accounted for by the barium nonylnaphylene sulfonate. However, unequivocal identification of the atomic composition of the mass peaks will require additional work. The presence of TCP or some other phosphorus containing species is also suggested by the SSMS results which indicated the presence of phosphorus. The major constituents found by SSMS - C, Ba, Si, and S - suggests that either the Ba dinonylnaphthalene sulfonate or a derivative thereof is present on the surface. Other distinct possibilities are as follows:

a) The compound may be a physical mixture of the barium naphthylene sulfonate, TCP and other substances which could arise from the rubber components of the hydraulic system. Silicon rubber could be the source of the Si observed.

b) Since the manufacturer has indicated that in some cases the barium dinonylnaphthalene sulfonate is added to the fluid as a solution and the excess solvent is subsequently removed by heating, one wonders if decomposition of the components occur during this heating process and/or if it is conceivable that interactions of the individual components may

occur during heating. In this regard the presence of Si could be explained if the heating takes place in a glass vessel.

It should be noted that a more detailed and rigorous characterization of the chemical compounds on these surfaces is possible, but will require a mc. extensive program. A proper study, which could be conducted given sufficient time and support, would subject the various components volatilized from the surfaces by programmed or selective heating to a preliminary gas chromatographic separation. Each of the individual compounds would then be analyzed and identified by mass spectrometry. Simil analyses would be made of the various chemical compounds which constitute the fluid of interest (major components and all additives), and a direct comparison would then be made with the surface contaminants in order to determine the origin of the problem. Such an approach would have important applications to a wide variety of materials degradation/contamination problems in which our laboratory has an interest.

ANALYSIS OF M-60 TANK HYDRAULIC FLUID AND FLUID COMPONENTS

A. Gas-Chromatographic and Mass-Spectrometric Analyses of Fluids

Initial analysis of a sample of M-60 hydraulic fluid obtained from the field (labeled FRH Fluid April 2, 1975) was accomplished using a flame-ionization gas chromatograph equipped with bulk sample inlet. The procedure for analysis entailed placing ~ 2 mg of the fluid into an aluminum sample boat, inserting the loaded sample boat into the chamber of the bulk-sample inlet, and then--while flowing helium through the inlet at 20 cc/min and heating the chamber--shunting the helium effluent from the bulk-sample inlet at regular intervals into the gas chromatograph

(equipped with a 3-in. Porapak P column and flame-ionization detector). Thus, the outgassing products from the fluid sample can be monitored and plotted as function of sample temperature. Using the gas-chromatographic procedure, the FRH fluid sample was found to contain large quantities of a volatile component which was present in the gas phase at 35°C and which was increasingly apparent as the sample temperature approached 120° after which the component dissipated. Mass-spectral analysis of the outgassing product(s) indicated the presence of Freon 113 (see TableVI); in subsequent discussions with Mr. E. Snyder, it became apparent that the source of Freon 113 was--at least in part--the solvent used to clean the sample vessel. Nevertheless, it was decided to examine samples of unused fluid obtained from barrels received from the supplier of the M-60 fluid in order to ascertain whether any volatile impurities were present.

Samples of unused fluid were to be obtained in vessels which were not cleaned using Freon 113. Accordingly, the fluid samples CS206-175C and CS-206-176D were received from AFML/MBT on 5 May 1975 and were analyzed using the same procedure as that described for the FRH fluid sample. A volatile component was observed in both fluid samples which outgassed from the fluid over the temperature range of 50°C-180°C. The quantity of the outgassing product was rather small but, none the less, quite apparent. Mass-spectral analysis of the outgassing components from the fluid samples yielded the data also tabulated in Table VI. The results show that all mass peaks in the mass spectra of the outgassing components from the FRH sample, the 175C sample, and the 175D sample correspond to peaks observed in the mass spectrum of either Freon 113 or Inhibisol--a cleaning solvent used during assembly of the M-60 hydraulic system. These

TABLE VI

MASS-SPECTROMETRIC ANALYSIS OF M-60 FLUIDS

FRH Fluid	CS-206-175C	CS-206-176D	Inhibisol	Freon
April 2, 1975	May 5, 1975	May 5, 1975	May 5, 1975	April 28, 1975
m/e	m/e	m/e	m/e	m/e
170				170
172				172
174				174
151		151		151
153		153		153
155		155		155
132				
134				
136				
117	117	117	117	
119	119	119	119	
121	121	121	121	
123				
116		116		116
118		118		118
101	101	101		101
103	103	103		103
105	105	105		105
97	97	97	97	
99	99	99	99	
87		87		87
85		85		85
61	61	61	61	
47		47		47
38	38	38	38	38
36	36	36	36	36
31	31	31		31

results indicate that either the sample containers for samples 175C and 175D were cleaned with halocarbon-type solvents, contrary to the procedure recommended, or the M-60 fluid from which samples 175C and 175D were obtained is contaminated with traces of halocarbon solvents.

The possible significance of the presence of halocarbon solvents is quite readily appreciated if one is familiar with the chemistry of the halocarbon solvents. According to the literature[21] and product information[22] from the manufacturer of Freons (E. I. DuPont), Freon 113 readily dehalogenates according to the following reaction:

$$ClF_2C\text{-}CFCl_2 \xrightarrow[\substack{40 - 50^\circ \\ HOH}]{Zn} F_2C = CFCl + ZnCl_2$$

It is extremely significant that only mild conditions are required for the above reaction and that alkali metals--including barium--enter very readily into a reaction similar to that noted above. Whether or not the halocarbon components of Inhibisol can readily dehalogenate or dehydrohalogenate in an analogous fashion may be verified by consulting the literature and/or performing simple experiments in the laboratory. The presence of Cl^- or HCl in the M-60 hydraulic system could quite possibly lead to the following reaction involving the rust inhibitor in the fluid:

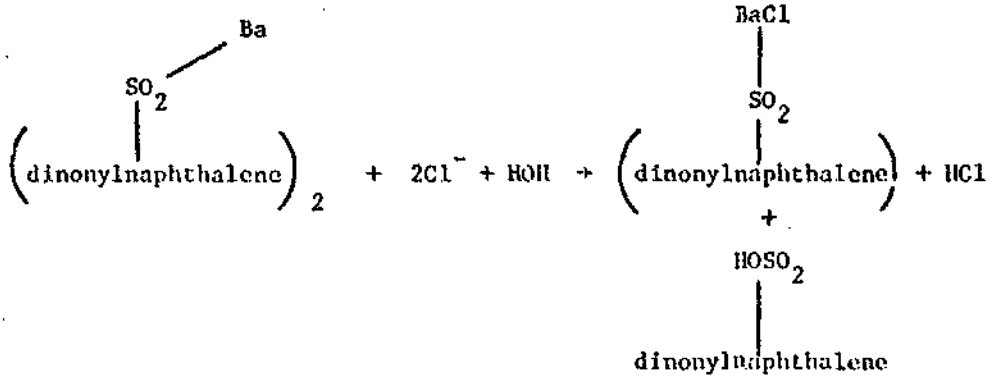

151

Whether such a reaction is a mechanism for the generation of particulate matter in the used M-60 fluid could be verified by simple laboratory experiments. The composition of the particulate from the fluid was determined by spark-source mass spectrography and is discussed in the next section.

B. Spark-Source Mass Spectrometry

Finely divided particles were microscopically observed to be suspended in the M-60 hydraulic fluid (ML 075-39). A sample of these particles was collected by filtration using a Millipore silver filter (1.2 μ) and 50 cc of fluid. After filtration, the sample filter was rinsed with heptane to remove residual hydraulic fluid. The silver filter and a blank filter were submitted to the Gaseous Ionization and Excitation Processes Group for compositional examination.

The subsequent spark-source mass-spectrometric analysis revealed the major impurities collected on the filter to consist of Ba and S. Certain elements of particular interest such as C, S, and P--previously observed by SSMS on a hydraulic valve piston--as well as Cl and F were obscured by extremely high blank levels. However, the observed SSMS spectra indicate the likeness of the fluid and piston contaminants. A likely explanation for the origin of this colloidal suspension would seem to involve undissolved barium additive or precipitation occurring during fluid preparation, with aggregation of these particles during valve operation forming surface contamination observed on the hydraulic valve piston. Finally, re-examination of SSMS spectra taken from piston particles indicates a

reasonably strong likelihood of Cl and F presence in moderate amounts. Confirmation of the presence of Cl and F would require analysis of additional sample material and, if accomplished, would lend additional evidence to the suspected reaction of residual Freon in the lubricated valving system.

SECTION V

DEVELOPMENT OF SOLID SORBENTS FOR MONITORING WORK-PLACE AIR POLLUTANTS: NITROGEN DIOXIDE (NO_2) AND NITRIC OXIDE (NO)

INTRODUCTION

As documented in previous reports,[1-4] a procedure employing activated molecular sieve 5A is suitable for monitoring nitrogen dioxide (NO_2) which is present in air at parts-per-million (ppm) concentration levels. In the present report, further work is described to examine the consistency of the sorbent in dealing with actual ambient air where several potential interferring components are known to exist. Extensive trials on the sample-storage experiments reveal that substantial loss of NO_2 recovery can be avoided only when the sorbent is completely shielded from contamination by air moisture over the entire period from adsorption-column preparation to the final desorption stage. Further modification of the sampling column was made by placing a P_2O_5 prelayer in front of the adsorbent. Positive sealing is required on both ends of the column. One version of this sealing is achieved by attaching the rear end of the column to a Teflon sealable valve and the front end to a rubber O-ring joint cap. The modified columns are found to be equally effective in sampling, using either dry air or ambient air as the mixing gas. The loss of NO_2 recovery is less than 5% after the column has been stored for two weeks after sampling.

After experiments on NO_2 had been largely completed, effort was shifted to the next air pollutant at the top of the NIOSH priority list--nitric oxide (NO). Molecular sieve 5A was first chosen for the screening test. It was found that NO with concentration as high as 40 ppm can be quantitatively and catalytically converted to NO_2 and adsorbed on the surface of molecular sieve 5A. The amount of molecular sieve 5A required

for complete conversion is compatible with the pocket-sized sampling device. The desorption of the converted NO_2 is thus achieved in the similar fashion as in the NO_2 analysis previously designed. The recovery is independent of NO concentration either with controlled dry air or ambient moist air as the carrier gas. The differentiation between NO and NO_2 is achieved by using a precolumn filled with molecular sieve 13X coated with a solution of triethylenediamine (TEA). Extensive tests show that this precolumn can quantitatively adsorb NO_2 and allow NO to pass through with negligible loss. A complete analysis of NO and NO_2 can be achieved by running parallel experiments, the first one using a single molecular sieve 5A column and the second one a molecular sieve 5A column attached with a TEA precolumn. After sample collection the analysis of the single column should yield the total amount of NO and NO_2 and the latter one the amount of NO alone. The difference between them is thus the amount of NO_2 adsorbed.

A desorption apparatus for the NIOSH 21-429 mass spectrometer has been completed and delivered according to the specification given in a previous report.[23] A duplicate was also constructed for routine use in this laboratory. Although this apparatus was originally designed for SO_2 experiments, it is also applicable to NO_2 and NO experiments after minor modifications. Tests show that results are essentially the same whether the desorption of the sampling column is carried out in this desorption apparatus or the apparatus shown in Fig. 9.

During this reporting period 50 prototype tubes for SO_2 collection (designed previously in this laboratory) were prepared and delivered for NIOSH use.

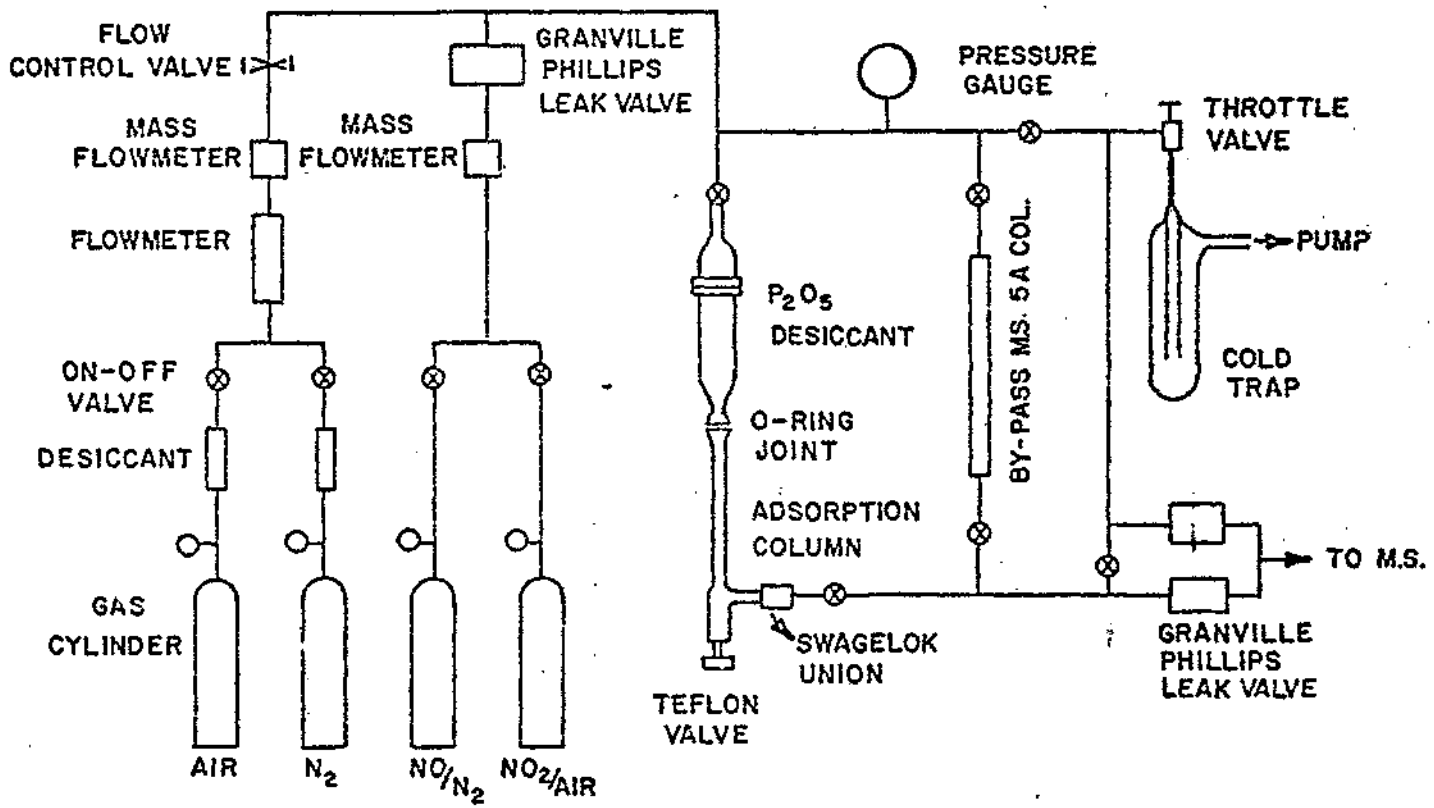

Figure 9. Schematic Diagram of the Adsorption-Desorption Apparatus

NITROGEN DIOXIDE (NO_2)

A. Experimental

1. Experimental Procedure

Figure 9 is a schematic diagram of the gas handling apparatus used in performing the adsorption-desorption studies. The details of this apparatus have been described in a previous report.[24] Briefly, a premeasured quantity of the sorbent is placed into a column which is attached to the sampling rig. After preconditioning of the column, a mixture of NO_2-air at various concentrations is allowed to flow through the column, with NO_2 adsorbed on the surface of the sorbent. The adsorbent NO_2 is then desorbed by simultaneous heating and purging with air or nitrogen flow and finally analyzed by detecting the NO^+ ion signal recorded in the ARL CEC 21-103C mass spectrometer.

The sampling column employed in the present work has been customarily in the form of a open-end tube, either of straight or U-shaped structure. A typical amount of 0.5 g of molecular sieve 5A (45/75 mesh, Hylar M. Supelco, Inc.) is placed inside the tube, with both ends being held by glass wool. Before sampling the column is preconditioned by heating with a heating tape to 300°C while at the same time purging it with dry air flow, typically at 100 cc/min. The preconditioning period is usually set at 30 min but should be higher if more than 0.5 g of molecular sieve 5A is used in the column.

In the storage experiment the aforementioned sampling column was conveniently sealed with recently procured polyethylene caps for the purpose of sample storage. However, it was later discovered that neither the sampling columns nor the caps were efficient in maintaining high NO_2

recovery. Extensive trials revealed that substantial loss of NO_2 recovery can be avoided only when the sorbent is completely shielded from contamination by air moisture over the entire period from sampling-column preparation to the final desorption stage.

In order to meet the stringent requirements of avoiding contamination of the sorbent molecular sieve 5A by air moisture, the adsorption apparatus was redesigned with the final version shown in Fig. 9 . The rear end of this column is rigidly attached to a sealable valve such as the Teflon valve (Fischer and Porter Company, Cincinnati, Ohio). The front end is also fitted by some positively sealable means such as the o-ring joint seen in the figure. The column is filled with a premeasured amount of molecular sieve 5A and held by a piece of glass wool on each side. A short layer (~ 0.5 cm) of P_2O_5 powder is also added in front of the 5A sieve to retain any trace amount of air moisture that may enter from the front side. It is desirable to place the P_2O_5 prelayer at least several cm away from the sorbent material in order that it will not be affected when the sorbent sieve is heated during precondition and desorption. It is also preferable that the column be made from glass for better heat insulation and good visibility. The sampling column should be discarded if the P_2O_5 prelayer is found to be completely soaked with moisture prior to desorption. It is strongly suggested that the Teflon valve be closed and the front end sealed with an o-ring joint cap until the moment just prior to sample collection. After collection both sides should also remain sealed until the final desorption analysis.

The above description is adequate only in the laboratory-controlled system when dry air is used in the sampling process. If the NO_2 gas is to be collected in an ambient wet-air environment, a P_2O_5 desiccant (see Fig. 9) should also be attached in series with the sampling column. The desiccant is prepared in a similar manner to that described in the SO_2 monitoring reported previously. However, one test showed that a commercially available P_2O_5 desiccant with indicator (Aquasorb, J. T. Baker Chemical Company, Hudson, Ohio) is also equally effective. The desiccant is simply attached to the sampling column with a short piece of Tygon tubing which can be sealed with a metal clamp. The desiccant can be used for more than one sample collection and discarded when completely consumed, as indicated by the built-in indicator of the desiccant. More extensive testing is required if this method is to be adopted since the effectiveness of the Tygon tubing sealing has not been tested on a long-term basis.

Although the cost involved in preparing this prototype column is moderate, it is economically unfeasible to dispose of the column after a single use since the column is rigid enough for multiuse and shows no signs of deterioration. After the Teflon stem of the valve is removed, the column is essentially a straight open-end tube which can be cleaned easily.

2. Sampling Column Preparation Within a Drying Box

In an effort to study the possible cause of the loss of recovery after sample storage, the sorbent column is occasionally preconditioned at relatively high temperature and for a prolonged time period up to 24 hr. Since a large number of sample columns is usually required for a given test, it is desirable to precondition a large amount of sorbent at one

time and transfer it into a group of sampling tubes for later use. For this purpose a preconditioning apparatus was built--essentially a quartz U-tube with a diameter of 25 cm and sealable valves attached on both ends. Each time ~ 80 g of sorbent can be preconditioned at any temperature up to 600°C either at vacuum or with a flow of flashing gas. The transfer of the sorbent from the apparatus into the sampling column was done in a drying box where the moisture level is always maintained at 2 ppm or lower, this was done in order to avoid the readsorption of the moisture by the preconditioned sorbent material.

3. Calibration of the Standard NO_2/Air Mixture

In a previous report[25] the calibration of the NO_2/air standard mixture procured from Minewld Co. was described briefly, the result being found in good agreement with the supplied specification of 2000 ppm. This calibration was done mass spectrometrically by comparing the I_{30}/I_{29} ratio of the standard mixture with that of the individually monitored NO_2 and air-flow mixture. The accuracy of this type of calibration depends largely upon detailed knowledge of the equilibrium of $NO_2 \rightleftarrows N_2O_4$ at operating conditions as well as on the heat capacity of the NO_2/N_2O_4 mixture which directly affects the reading of the linear mass flow meter. In view of the possible uncertainty of these parameters, a completely different calibration method is conducted here which has been widely used [26,27] in measuring the NO_2 concentration at levels higher than 100 ppm.

In the new calibration method, the standard NO_2/air mixture is introduced into a glass bottle of 1093 cc at known total pressure. Then

6 cc of 3% H_2O_2 solution was added to this mixture. The NO_2 gas is expected to be quantitatively oxidized by H_2O_2 into nitric acid according to the following reaction

$$2NO_2 + H_2O_2 \rightarrow 2HNO_3 \qquad (1)$$

The bottle was allowed to be settled for 2 hr with occasional shaking. At the end of this period the solution was withdrawn into a beaker and titrated with 0.009 N NaOH solution. The NO_2 concentration in ppm (x) is calculated according to the following equation

$$\text{(amount of NaOH in cc)} \times 0.009 = \frac{x \cdot 10^{-6} \cdot 1093 \cdot \text{(pressure of } NO_2\text{/air mixture in mm)}}{0.082 \cdot 300 \cdot 760} \qquad (2)$$

Three independent experiments show results of 1550, 1500, and 1529 ppm, with the average being 1543 ppm. Taking into account a 5% loss due to process treatment which was established in a later work of NO calibration (details to be described in a later section), the final value is thus set at 1,624 ppm with accuracy of $\pm$ 5%.

It is noted that the above accuracy has no direct bearing on the accuracy of the present NO_2 monitoring work since the analysis was done by measuring the mass-spectrometric peak area whose accuracy is better than 5%, as seen in the NO_2 desorption result. This area can be readily converted into the true amount of NO_2 if more accurate NO_2/air mixtures such as NBS NO_2 permeation devices are available for standardization.

4. Calibration of Integrated Peak Area

In order to arrive at the absolute amount of NO_2 desorbed from a typical desorption experiment, a calibration is required to correlate

the actual amount of NO_2 introduced under given flow conditions and the mass spectrometrically recorded peak integration area in mV-sec. Consider a typical case where the standard NO_2/air mixture (NO_2 1624 ppm) is introduced at a flow rate of 100 cc/min. A fraction of this flow is introduced into the ion source of the mass spectrometer through the precolumn Granville-Phillips leak valve (Fig. 9) at a controlled leak rate at which the I_{29} ($^{14}N^{15}N^+$) signal is registered at an intensity of 6.8 x 256 unit. At this leak rate the I_{30} (NO^+) signal is at 11.2 x 32 unit (i.e., $I_{30}/I_{29} = 0.206$). For an integration of 10 min, the signal integrator recorded a total value of 2,082,304 mV-sec. The amount of NO_2 introduced (i.e., detected by mass spectrometer) for this 10-min period is also known according to the following equation

Amount of NO_2 detected

$$= \frac{10 \times 100 \times 10^{-3} \times 1624 \times 10^{-6}}{0.082 \times 300} = 66.02 \times 10^{-6} \text{ moles} \qquad (3)$$

Thus, the integrated peak area per μmole of NO_2 detected is 2,082,304/66.02 = 31,540 mV-sec/μmole NO_2 detected.

In the case where desorption was done with air as the carrier gas at flow rate of 100 cc/min, the desorption peak area in mV-sec can be readily converted to μmole of NO_2 as detected by the mass spectrometer if the desorbent was confirmed to be in the form of NO_2. Of course, during desorption the leak rate should also be controlled in such a way that the I_{29} signal will have an intensity of 6.8 x 256 unit. If, instead, nitrogen is used as the carrier gas during desorption, in order to maintain the same leak rate the I_{29} signal should be at 6.8 x 256 x 100/78 = 8.72 x 256 unit where 78% is the fraction of N_2 in an air stream. In this case the same converting factor of 31,540 mV-sec/μmole NO_2 detected is still applicable.

B. Results

1. Reproducibility of NO_2 Desorption with Dry-Air Sampling

The reproducibility of NO_2 adsorption-desorption data obtained with the molecular-sieve-5A column has been shown to be good,[2,5] provided that each column material is used only once. In Table VII this reproducibility is demonstrated again using the newly designed sampling column in which the 5A sieve is protected by a P_2O_5 presection in the front end and a sealable valve in the rear end. For each experiment a NO_2/dry air mixture with NO_2 at 18.17 ppm flows through the column at a total flow rate of 545 cc/min for a period of 30 min. Upon completion of adsorption, the column is removed from the rig and immediately attached to the desorption apparatus and desorbed in the usual manner. Averaging the integrated peak areas for the five test runs yields an average area of 11.619 mV-sec/μmole NO_2 sampled, with standard deviation of 2.1%. Reproducibility is, therefore, seen to be quite acceptable.

2. NO_2 Recovery as a Function of NO_2 Concentration with Dry-Air SAmpling

It has been reported previously[23] that the recovery of NO_2 is independent of the NO_2 concentration within the range of NIOSH interest. This conclusion is confirmed through the use of the newly designed P_2O_5-5A column as shown in Fig. 10. In these experiments the standard NO_2/dry air mixture (with NO_2 at 1624 ppm) is mixed with dry air to yield a total flow of 545 cc/min for a sampling time of 30 min at various concentrations as indicated. One additional test was done where the standard NO_2/air mixture (with NO_2 concentration at 1624 ppm and flow rate of 100 cc/min) was directly sampled by the column for a period of 15 min. The desorption

TABLE VII

REPRODUCIBILITY OF NO_2 SORPTION WITH MOLECULAR SIEVE 5A COLUMN[a]

Column No.[b]	Desorption I_{30} Peak[c,d] Area (mV-sec)	Desorption Peak Area per μmole NO_2 Sampled (mV-sec/μmole)
1	137,079	11,329
2	136,221	11,258
3	139,936	11,565
4	145,786	12,048
5	143,916	11,894
	Average	11,619
	Standard Deviation	242

[a]Column: 0.5 g of molecular sieve 5A with P_2O_5 presection in a 5/16-in.-OD glass tube with its rear end attached to a Teflon valve. Each column is preconditioned by heating to 300°C while being purged with dry air at flow rate of 100 cc/min for 50 min.

[b]Sampling Condition: NO_2/dry air mixture (NO_2 18.17 ppm) flows through the column at a total flow rate of 545 cc/min for a period of 30 min. Amount of NO_2 sampled = 12.1 μmole.

[c]Desorption Condition: Each column is heated to 240°C with pure N_2 carrier gas at a flow rate of 100 cc/min.

[d]All mass-spectrometrically recorded areas in this work were obtained in reference to a constant I_{29} ($^{14}N^{15}N^+$) peak height at 6.8 x 256.

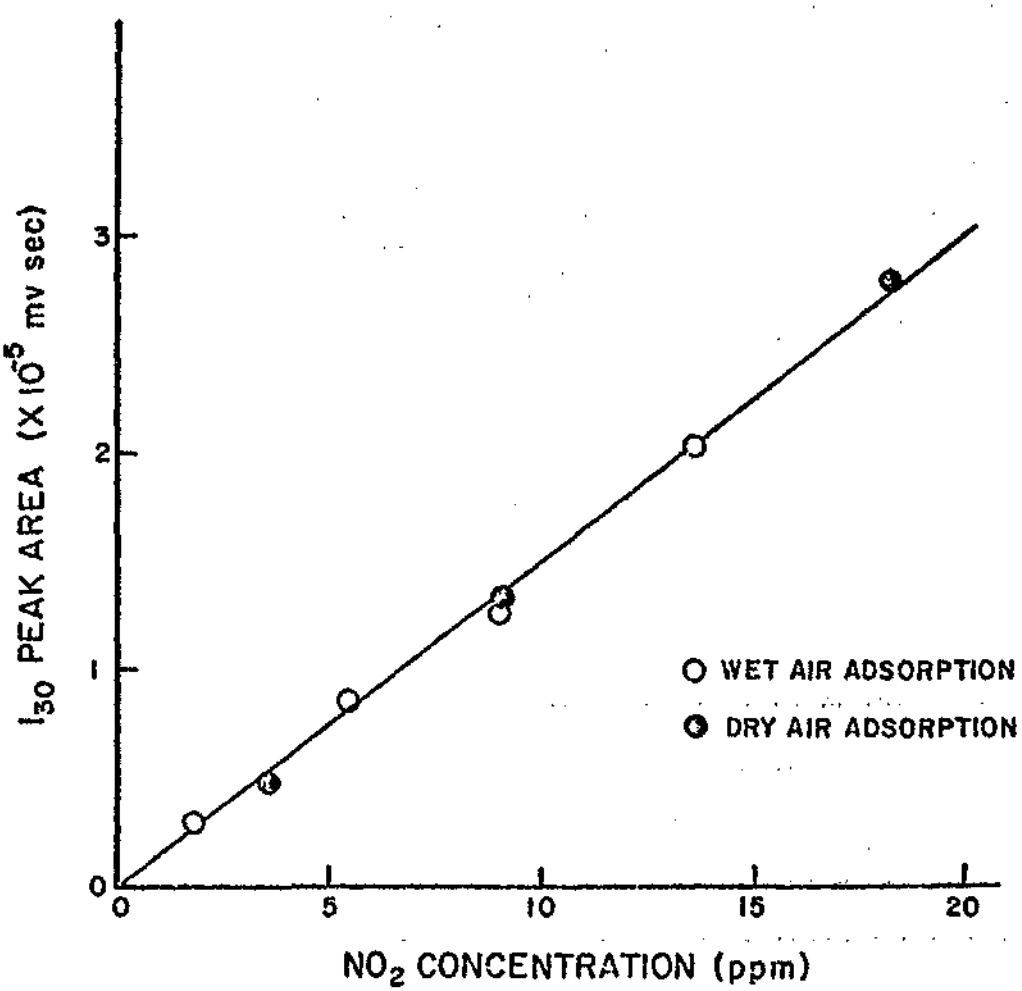

Figure 10. Desorption of NO_2 as a Function of NO_2 Concentration.

Column: As described in Table VII
Sampling Condition (for open-circle data):
o - Standard NO_2/dry air (NO_2, 1624 ppm) is mixed with ambient air (75°F; rel. hum. 60%) to provide a total flow of 1090 cc/min; sampling time = 30 min.

result showed a recovery of 11,900 mV/sec-μmole NO_2) also in excellent agreement with the established value of 11,619 mV-sec/μmole NO_2. These results indicate that the NO_2 recovery is workable not only over a wide concentration range but also under various sampling conditions. Thus, the present technique is potentially applicable to the extreme cases where sub-part-per-million levels of NO_2 can be sampled at a higher flow rate and for a longer period; while on the other hand for a higher NO_2 level environment, sample collection can be achieved with a lower flow rate and shorter collection time.

3. Effect of Moisture on NO_2 Recovery

The existence of moisture is believed to reduce the recovery of NO_2 through the following reactions

$$2NO_2 + H_2O \rightarrow HNO_3 + HNO_2 \quad (4)$$

$$3HNO_2 \rightarrow HNO_3 + 2NO + H_2O \quad (5)$$

The first evidence of this moisture effect was seen during experiments when an earlier model of the sampling column was used in sampling the NO_2/dry air mixture. The dry air used in these experiments customarily comes from a commercial air cylinder dried with a drying tube but may still contain some trace amount of moisture. As a result some loss of NO_2 actually occurred during the sampling process as evidenced by the results in Columns 1-4 of Table VIII.

In an actual field test, the adsorption columns are expected to be exposed to ambient atmosphere momentarily during the transfer period. This brief contact between the adsorbent and moist air has the potential

TABLE VIII

EFFECT OF MOISTURE ON NO_2 RECOVERY

Column No.[a]	Column Description: P_2O_5 Layer	Column Description: Column Exposed to Ambient Air Before Desorption	Desorption Peak Area Per mole of NO_2 Sampled (mV-sec/ mole)	Deviation From the Estab. Value (%)
1[c]	No	No	8,082	-30.5
2[c]	No	No	8,240	-29.1
3[c]	No	No	8,306	-29.1
4[c]	No	No	7,975	-31.4
5	No	Yes	4,414	-62.0
6	No	Yes	3,893	-67.5
7	No	Yes	4,227	-63.6
8	Yes	Yes	7,540	-35.1
9	Yes	Yes	7,518	-35.3
10	Yes	Yes	7,795	-33.0
11	Yes	Yes	7,412	-36.2
12	Yes	Yes	8,165	-29.8
13	Yes	Yes	8,682	-25.3
14	Yes	Yes	8,264	-28.9

[a]Sampling Condition: NO_2/dry air mixture with NO_2 concentration of 18.2 ppm at a flow rate of 540 cc/min for 30 min.

[b]The established value is 11,619 mV-sec/ mole NO_2 sampled (Table VII).

[c]Data of previous report[25] (Cols. 2 to 5 of Table IX).

to cause a severe loss of recovery of NO_2 during analysis (due to their premature interaction). In order to gauge this effect, a laboratory-simulated test was carried out by momentarily removing the adsorption column from the rig upon the completion of sample collection. The subsequent desorption was done either in the same rig or the desorption apparatus. As evidenced by the results of Cols. 5-7 of Table VIII, this has consistently caused a more than 50% loss of NO_2 recovery. This loss of NO_2 recovery clearly demonstrates the inadequacy of the design of the sampling column used in the early stage of the present work.

The first modification of the sampling column was accomplished by placing a thin layer (0.5 cm) of P_2O_5 powder in front of the molecular-sieve-5A column, with each end of the P_2O_5 layer being supported by glass wool. The P_2O_5 layer is at a distance of ~ 2 cm from the 5A section in order to avoid excessive heating during preconditioning and desorption. As seen in Cols. 8-14 of Table VIII, this has greatly improved the recovery of NO_2, although the results are still about 30% lower than the established value.

One obvious approach to further improve the NO_2 recovery is to use an after-column layer of P_2O_5. However, some experimental difficulties have been encountered. First, during preconditioning large quantities of hot moisture released from the 5A sieve almost completely soaked the after-column P_2O_5-layer, making it useless for sieve protection. Two experiments were actually conducted with this after-column layer. The NO_2 recovery (3821 mV-sec/μmole NO_2) was found to be too low to be acceptable. The

recent development of the technique of sorbent preparation inside the drying box could eliminate the problem of preconditioning, but the result may still be undesirable since the after-column P_2O_5 would be heated during desorption. P_2O_5 is known to melt or sublimate at temperatures as low as 200°C. It is not clear what would happen to this P_2O_5 layer during desorption when the hot carrier gas flows through this P_2O_5 layer as well as to the ion source under extensive use under this condition. Other candidates for the after-column desiccant--such as magnesium perchlorate, drierite, and calcium chloride--are not suitable either due to their known interference with NO_2.[28]

The result of the above experimental findings led to the further modification of the sampling column by placing a sealable valve at its rear end as described in the previous section. Figure 10 shows the result of the use of this column in sampling the mixture of NO_2 and ambient air (75°F; relative humidity 60%) at various NO_2 concentrations. In this experiment a P_2O_5 desiccant is also attached to the front end of the adsorption column and removed at the completion of sample collection. The amount of P_2O_5 in the desiccant is not critical but should be adequate to prevent the breakthrough of the moist air during sample collection. In order to reduce the resistance of flow, a granule P_2O_5 is preferable to P_2O_5 powder.

The results of Fig. 10 clearly demonstrate the capability of the P_2O_5-5A-sealable valve column in dealing with NO_2 adsorption where ambient air is used as the carrier gas. The P_2O_5 desiccant is shown to completely eliminate moisture from the airstream and let NO_2 pass unaffected or with negligible loss.

4. NO_2 Storage Experiment

It is a NIOSH requirement that an acceptable solid sorbent must be capable of retaining the sorbed pollutant of interest for periods up to two weeks without substantial loss of the sorbed gas or deterioration of the recovery capability. The storage experiment of NO_2 was carried out using the newly developed sampling column. The NO_2 sampling condition is essentially the same as that described in the previous section, i.e., NO_2/dry air mixture with NO_2 concentration of 18 ppm is drawn through the column at a total flow rate of 545 cc/min for a period of 30 min.

Upon the completion of the sample collection, the Teflon valve of the column is closed, and the front end of the column is sealed with an o-ring cap. It is important that the stored sorbent be protected from the contamination of atmospheric moisture. This is achieved by the positive sealing on both sides of the column. The failure of this sealing is indicated by the gradual soaking of the P_2O_5 precolumn over the prolonged period of storage. While partial soaking of the P_2O_5 prelayer is generally acceptable, the complete soaking of this layer probably indicates that the air moisture has penetrated through this protection layer and caused some interaction with the stored NO_2.

Table IX gives the results of an NO_2 storage experiment which covers the sample storage period range from 1 day to 29 days. The NO_2 recovery is essentially unchanged during the first day of sample storage but gradually decreases as the storage time is increased. The cause of this deterioration is not clear. It is conceivable that in spite of the fact that every precaution was taken to avoid contact of the sorbent with moisture, still

TABLE IX

NO_2 STORAGE EXPERIMENT DATA

Column No.[a]	Storage Time[b] (day)	Desorption I_{30} Peak Area (mV-sec)	Peak Area per μmole of NO_2 Sampled (mV-sec/μmole)	Ratio[c] (%)
1	1	144,112	11,910	102.5
2	1	142,286	11,759	101.2
3	2	133,815	11,059	95.2
4	4	134,519	11,117	95.7
5	5	133,996	11,074	95.3
6	12	136,436	11,276	97.0
7	13	132,794	10,975	94.5
8	13	133,597	11,041	95.0
9	15	125,273	10,353	89.1
10	19	126,636	10,466	90.1
11	23	129,246	10,681	91.9
12	23	116,740	9,648	83.0
13	23	110,111	9,100	78.3
14	28	120,180	9,932	85.5
15	29	116,528	9,630	82.6
16[d]	1	133,203	11,008	94.7
17[e]	1	130,163	10,757	92.6
18[e]	1	135,839	11,226	96.6

[a]Column and Sampling Condition: as described in Table VII.

[b]During storage the Teflon valve of the column is closed and the front end of the column is sealed with an o-ring cap.

[c]Ratio is expressed as the ratio of the value in Column 4 and the average value (11,619 mV-sec/μmole) obtained from Table VII.

[d]Column is stored at 110°F.

[e]Columns are stored at a pressure of 550 mm Hg.

some trace amount of moisture existed within the sample column. The source of this moisture could be either insufficient pretreatment of the sorbent sieve or the air moisture that penetrated through the P_2O_5 prelayer. It has been reported[28] that P_2O_5 itself can also adsorb about 10% NO_2 when when sampled at 1 ppm NO_2 concentration. This is not fully established in the present work due to the lack of an ideal system where the interference of trace moisture can be eliminated without the use of a P_2O_5 prelayer. Thus, it is possible that in addition to an initial loss of NO_2 during sampling the process, more loss of NO_2 may actually occur during the storage period due to the slow adsorption of NO_2 gas on the P_2O_5 prelayer. Ultimate resolution can be achieved by placing a sealable valve between the P_2O_5 prelayer and the sorbent sieve if the deterioration is truly caused by the existence of this P_2O_5 layer.

Nevertheless, the deterioration seen in Table IX is mild. The recovery of NO_2 after a storage time of two weeks is only decreased by 5% compared with a freshly desorbed sample. After three weeks of storage, the recovery is still as high as 90% of the established value. It is suggested that a scaling correction factor may be used for samples stored up to three weeks, with accuracy better than 5%, i.e., a correction of 5% is applied for samples stored for less than two weeks and 10% for those stored for three weeks. Better correction procedures can be established which would require more extensive experimental data.

Column No. 16 of Table IX is the result of the recovery of the NO_2 sample stored at 110°F for a period of 24 hr. This is a test to detect the deterioration of NO_2 recovery when samples must be stored at some extremely high ambient temperature. It is found that a further deterioration of NO_2 recovery of about 5% occurs as a result of such an extreme storage

condition. Column Nos. 17 and 18 of the same table also reveal an average loss of 6% of NO_2 when stored at a pressure of 550 mm Hg for a period of 24 hr. It is concluded that additional loss of NO_2 may occur at either high-ambient-temperature or low-pressure storage conditions. However, this loss is compatible with experimental error and perhaps negligible, especially when the duration of this exposure is less than 24 hr.

C. Discussion

1. NO_2 Adsorption-Desorption Mechanism

The adsorption of NO_2 on molecular sieve 5A is believed to be a simple physical process as discussed previously.[24] Adsorption efficiency of 100% is generally observed in the present work, which is also anticipated in view of the high adsorption capacity of molecular sieve 5A.[24,25] However, the mechanism of NO_2 desorption from the sorbent is found to be far more complicated. The understanding of this mechanism is not only of interest by itself but also important in determining the absolute recovery, as will be described in a later section.

The use of the mass spectrometer is of no aid in resolving this mechanism since the only observable information is the NO^+ ion which can be formed from either NO_2 or NO as well as many other compounds such as nitric acid. The NO_2^+ (m/e = 46) ion--which would have been a positive indication of NO_2--is not detectable at low NO_2 concentration as previously reported.[24,25] The identification of NO_2 is possible through visual observation since NO_2 gas is dark brown in color which is easily visible at moderate concentration. A desorption test was done on a 5A sieve column

which had adsorbed 99 mole of NO_2. (The standard NO_2/air mixture with NO_2 concentration of 1624 ppm was sampled at a flow rate of 100 cc/min for 15 min.) During desorption using N_2 as the carrier gas at a flow rate of 50 cc/min, the effluent was collected in a 1-liter glass bottle which had been evacuated prior to collection. The collection starts 30 sec after the onset of heating and ends 10 min thereafter. This period covers the entire desorption NO^+ peak as recorded by the mass spectrometer from a separate experiment under identical desorption conditions. It is thus believed that all desorbed NO_2 should be collected in this bottle. The desorbed effluent exerts no brown color which would have been clearly seen if the same amount of NO_2 (i.e., 99 μmole) had been collected in the bottle prior to adsorption. When the collected effluent was cooled to liquid-nitrogen temperature, a small amount of white solid was found which quickly turned to colorless liquid as soon as the liquid nitrogen cold trap was removed. There was no trace of blue condensate which would indicate the existence of NO_2. Although the above visual observation does not constitute unequivocal evidence of the absence of NO_2 at any trace level, it is clear that the majority of the desorbed material from the column does not exist in the form of NO_2. It is more likely that the desorbed material is NO, in accordance with the above observation. More positive identification through other independent means would be desirable.

It was discovered through later work that the present method of using molecular sieve 5A sorbent can also be used to monitor NO at parts-per-million levels. During sampling NO gas was found to be quantitatively oxidized with NO_2 on the catalytic surface of the 5A sieve in the air

oxygen environment. The oxidized NO_2 is subsequently adsorbed by the 5A sorbent. This technique can also be adopted here to verify the identity of the NO_2 sample-column desorption product to see whether it is indeed in the form of NO. A long glass U-shaped column is prepared with both its front and rear legs each filled with ~ 0.5 g of molecular sieve 5A. The bottom U-shaped portion is filled with glass beads. The preconditioning of both 5A sections is done in the manner described previously. During sampling a typical flow of the NO_2/air mixture with NO_2 concentration of 18 ppm is introduced through the front leg of the U column at a flow rate of 1 liter/min for 30 min. After sample collection the rear 5A section alone is desorbed first in the usual manner with no NO^+ peak found which indicates that all the NO_2 sample has been collected in the front 5A section. After desorption the rear 5A section is allowed to cool to room temperature. Thereafter, the front 5A section is desorbed with pure N_2 as the carrier gas entering through the front inlet at a flow rate of 100 cc/min. In the meantime, the glass-bead filled U-shaped portion is immersed into a dry ice bath. The desorption of the front 5A section yields the same NO^+ peak area as the normal single-column experiment. Upon completion of the front 5A section desorption the dry ice bath is removed and the entire column is allowed to return to room temperature. Now the rear 5A section is desorbed again to ensure that nothing desorbed from the front 5A leg has been trapped either in the rear 5A section or the U trap as a result of the cooling of the effluent by the dry-ice bath. No NO^+ peak was found during this time, as expected.

The above procedure is repeated with a newly prepared 5A double column in the same manner until the stage of front 5A section desorption. Instead of using pure N_2 as the carrier gas, air is chosen for the desorption of the front 5A section. Contrary to the result when N_2 gas was used as the carrier gas, no NO^+ ion peak resulted from the desorption of the front 5A section with air flow acting as the carrier gas. Apparently during desorption it is NO, not NO_2, that actually comes out of the 5A column. As this desorbed NO is flushed out with air flow and subsequently cooled by passing through the dry-ice cold trap, it is oxidized back to NO_2 on the surface of the rear 5A section and adsorbed thereon.

On desorption of this rear 5A column, the NO^+ ion peak reappears, which further confirms the above mechanism. It is interesting to note that the existence of the dry-ice cold trap is crucial to this experiment. In a similar test the U-shaped portion of the column is immersed in a water bath at room temperature instead of the dry-ice bath chosen in the previous work. As a result of the insufficient cooling, the rear 5A column failed to hold the NO desorbed from the front 5A section. This failure could either reflect the inefficient oxidation condition at higher temperature or simply the breakthrough of the oxidized product--NO_2--at such a high temperature. No further investigation was conducted on this interesting subject.

It seems clear from both visual observation and the double-column experiment that the major desorbed component under the present experimental condition is NO, as a result of certain chemical reactions. One likely mechanism, as discussed in the previous report,[24,25] for converting NO_2 to NO is through the NO_2-water reaction [Reactions (4) and (5)]. During desorption the carrier gas is dried with both a commercial dryer and a

P_2O_5 prelayer; it is unlikely that a substantial amount of water moisture could enter the column and participate in the reaction. If said reaction does occur on the molecular sieve during desorption, then some water must be retained by the sieve crystal that survives the preconditioning treatment. It is found that NO_2 recovery is linear with respect to the NO_2 sampling dose up to the breakthrough region. A substantial amount of water would be required to account for the conversion.

One other possible mechanism to account for the formation of NO is through thermal decomposition of NO_2.

$$2NO_2 \rightarrow 2NO + O_2 \qquad (6)$$

In the gas phase this reaction begins at 150°C, and the extent of conversion is 5% at 184°C, 13% at 279°C, 17% at 494°C, and 100% at 620°C.[29] Under the present desorption conditions, the temperature of the sorbent generally only reaches 240°C at the end of desorption. This corresponds to only ~ 10% decomposition according to the above decomposition scheme. The much higher NO_2-recovery-rate data of the present experiment, which is to be discussed in a later section, either indicates that the decomposition of NO_2 on the molecular sieve follows a much higher rate than that suggested by the gas phase decomposition or that the thermal decomposition constitutes at most a minor contribution to the formation of NO.

2. Percent Recovery of NO_2 from the Molecular Sieve 5A Column

It is noted in this report that all recoveries for NO_2 experiments are expressed in terms of the NO^+ ion integrated peak area as recorded by the mass spectrometer. The calculation of absolute percent recovery

of NO_2 from the molecular sieve requires the detail knowledge of the adsorption and desorption mechanism of NO_2 under present experimental conditions. Since it has been established--based on the tests described in the previous section--that the major component desorbed from the molecular sieve 5A is in the form of NO, it is logical to express the percent recovery (PR) in the form of

$$PR = \left(\frac{\mu\text{mole of } NO_2 \text{ adsorbed}}{\mu\text{mole of } NO_2 \text{ sampled}}\right) \left(\frac{\mu\text{mole of NO desorbed}}{\mu\text{mole of } NO_2 \text{ adsorbed}}\right) \times 100\% \quad (7)$$

The first term of the product is commonly referred to as "adsorption efficiency," while the second is referred to as the "stroichiometric factor." In the present case the value of PR is equivalent to the stoichiometric factor since the adsorption efficiency of 100% is readily achievable under the present experimental conditions. The amount of NO_2 sampled is known for a given sampling condition. The μmole amount of NO desorbed is obtained by measuring the desorption NO^+ ion-peak area recorded by the mass spectrometer. The calibration of the NO^+ peak area, which is described in detail in a later section, reveals a peak area of 48,905 mV-sec for each μmole of NO detected during desorption using air as the carrier gas with a preset ion source pressure which corresponds to a I_{29} ion intensity of 6.8×256 unit.

$$PR = \left(\frac{\mu\text{mole of NO desorbed}}{\mu\text{mole of } NO_2 \text{ sampled}}\right) \times 100\% \quad (8)$$

$$= \left(\frac{1}{\mu\text{mole of } NO_2 \text{ sampled}}\right) \left(\frac{NO^+ \text{ peak area (mV-sec)}}{48{,}905 \text{ mV-sec}/\mu\text{mole NO detected}}\right) \times 100\%$$

The above equation can also be written in a more common form, i.e.,

$$PR = \left(\frac{1}{\text{mole of } NO_2 \text{ sampled}}\right)\left(\frac{NO^+ \text{ peak area}}{48{,}905} \times \frac{6.8 \times 256}{I_{29}}\right) \times 100\%$$

$$= \left(\frac{1}{\text{mole of } NO_2 \text{ sampled}}\right)\left(\frac{NO^+ \text{ peak area}}{I_{29}} \times 0.0356\right) \times 100\% \quad (9)$$

where I_{29} is the ion intensity of m/e = 29 whose value can be set higher than 6.8 x 256 unit in the event a larger ion-source pressure is desired for a more accurate measurement.

Table VII shows an average desorbed NO^+ ion peak area of 11,619 mV-sec/μmole of NO_2 sampled. The average percent recovery of NO_2 is readily obtained from Eq (9)

$$PR = \frac{11{,}619 \text{ mV-sec}/\mu\text{mole of } NO_2 \text{ sampled}}{48{,}905 \text{ mV-sec}/\mu\text{mole of NO detected}} \times 100\%$$

$$= 23.8\%$$

The above result indicates that for each μmole of NO_2 sampled, only 0.23 μmole of NO is desorbed under the present desorption condition, assuming that all desorbed components exist in the form of NO which is subsequently measured by the mass spectrometer. Apparently during desorption a substantial portion of the adsorbed NO_2 gas is either not desorbed under the present desorption conditions or desorbed in a form other than NO [such as HNO_2 from Reaction (4)] and fails to reach the ion source for detection. One obvious approach to improving the percent

recovery of NO_2 is to further increase the temperature of the sampling column during desorption. However, the recovery was found to be insensitive to desorption temperature up to 300°C. No experiment was done for desorption with temperatures higher than 300°C since a portion of the column materials (Teflon valve) cannot withstand much higher temperature.

It is interesting to point out that the current result is also in accordance with the previous observation which shows the adsorption capacity of the molecular sieve to decrease with repetitive use of the same sieve material. This could indicate either that part of the sites with adsorbed NO_2 are not reversible upon desorption and thus decrease the NO_2 adsorption during a subsequent adsorption or simply the collapse of some sieve site after such a desorption heating.

The measurement of NO_2 recovery was also carried out by the titration method, the details of which are described in the previous section. During desorption the effluent is collected in the 1-liter glass bottle and subsequently added with 6 cc of 3% H_2O_2 solution. The desorbed NO gas is allowed to react with H_2O_2 according to the following equation

$$2NO + 3H_2O_2 \rightarrow 2HNO_3 + 2H_2O \qquad (10)$$

Any trace amount of NO_2 existing in the effluent is also converted to nitric acid by Eq (1). The formed HNO_3, as well as any possible nitric acid directly desorbed from the sieve, is then titrated with the NaOH solution. The results of NO_2 recovery expressed as the ratio of μmole of HNO_3 detected to μmole of NO_2 sampled are 0.29 and 0.31 from two experiments with an average of 0.30. This value is slightly higher than

the percent recovery obtained from the mass-spectrometric method. This is probably an indication of some chemicals other than NO that are also desorbed but are not detected by the mass spectrometer or yield a relatively lower NO^+ ion signal than that of NO gas.

NITRIC OXIDE (NO)

A. State-of-Art Review

Nitric oxide (NO) has long been recognized as a significant air pollutant. Although it is toxic in high concentration, the major concern is due to its quick conversion into the more dangerous nitrogen dioxide (NO_2) in atmosphere. Many techniques now are available commercially for monitoring nitric oxide in ambient air. However, most of them such as chemiluminescent, photometric, coulometric, and electrochemical-cell techniques require some rather elaborate instrumentation and are not suitable for personal sampling as dictated by NIOSH specifications.

Perhaps the method of largest interest is to oxidize NO into NO_2 and determine the latter by the colorimetric analysis either in the continuous mode[28] or by integrated processes.[30] Many extensive studies[31] have been devoted to the oxidation of NO. These studies propose the systems using such compounds as a mixture of $KMnO_4$ and H_2SO_4, ozone, heated I_2O_5, acidified MnO_2, periodate, persulfate, N_2O_5, ClO_2, oxygen, and CrO_3 as oxidizing agents. Each method, however, either suffers the problem of quantitative conversion of NO into NO_2 or requires the strictly controlled conditions that leave something to be desired for the personal sampling of present purposes.

Most commonly used solid adsorbers such as molecular sieve, alumina, silica gel, and active carbon are not capable of absorbing NO physically under the ambient condition. However, one acid-resistant molecular sieve, namely AW-500, manufactured by Union Carbide has been reported[26] successful in converting high concentrations of NO from waste gas streams in a nitric acid plant into NO_2 which is subsequently adsorbed on the surface of the molecular sieve surface. No work has been reported using the technique in monitoring NO in the lower concentration commonly existing in the ambient air. Since it is closely associated with the type of work currently underway in this laboratory, this technique will be further explored here in our first-stage effort.

One other technique which is also of high interest to this study is a method recently developed by D. A. Levagii and coworkers[32] using a triethanolamine (TEA) solution or a TEA-impregnated molecular sieve to differentiate NO_2 and NO existing in ambient air at sub parts-per-million levels. With a flow of air stream containing NO/NO_2 passing through the reagents, it can quantitatively retain NO_2 while letting NO escape unaffected or with negligible loss.

One ideal solution which would meet the goal of the present work of monitoring NO/NO_2 at concentrations of NIOSH concern involves the successful adoption of the two above-mentioned techniques. First, a solid sorbent will be chosen that not only can adsorb and desorb NO_2 quantitatively but also is capable of convering NO completely into NO_2 within the sorbent and adsorbing it subsequently. The recovered NO_2 from the sorbent should yield the total amount of NO and NO_2 initially collected from the air stream. Second, a parallel adsorption process will be conducted using the

chosen sorbent column attached with a TEA-impregnated molecular-sieve precolumn that allows the measurement of NO alone. The difference between the two measurements will represent the initial NO_2 concentration. As shown by the preliminary test results presented in a later section, the originally chosen molecular sieve 5A has largely fulfilled the requirements of the present tasks.

B. Experimental

1. Experimental Procedure

The molecular sieve 5A is first chosen for evaluation in view of its success in the work of NO_2 adsorption. The detailed experimental procedures largely follow the previous work on NO_2 unless otherwise stated.

The amount of molecular sieve 5A used in each sampling column was originally set at 0.5 g which is the same as in the work on NO_2. However, it was found that this amount of 5A sieve is not adequate for the quantitative oxidation and adsorption of NO samples under typical sampling conditions. A greater amount of 5A sieve ranging from 1 to 4 g was used in later work. The longer preconditioning time was required for each column for the greater amount of sorbent sieve used.

2. Calibration of the Standard NO/N_2 Mixture

A 2000-ppm NO/N_2 standard mixture with a reported accuracy of $\pm$ 20 ppm was procured from Union Carbide. The NO concentration of this standard mixture was calibrated with the titration method in a manner similar to that described in the work on NO_2/air mixture calibration. Briefly, the gas mixture was introduced into a glass bottle of 1093 cc with known total pressure. To this mixture 6 cc of 3% H_2O_2 solution was

added. The bottle was then allowed to be settled for 2 hr with occasional shaking. The NO gas was expected to be oxidized by H_2O_2 into nitric acid according to Reaction (10). At the end of this period the solution was withdrawn into a beaker and titrated with 0.009 N NaOH solution. The NO concentration of the standard mixture in ppm can be calculated by an equation similar to Eq (2). Two experiments yield results of 1840 and 1908 ppm with an average of 1874 ppm.

The above calibration technique was also standardized by calibrating a pure NO gas through an identical experimental procedure. It was found that the above calibration method generally yielded a result - 5% lower than the actual value. This loss of 5% is probably due to the incomplete conversion and sample treatment of the present experiment. By taking into account this 5% loss, the acceptable value of the NO concentration should be 1973 ppm, with accuracy of $\pm$ 5%.

3. Calibration of Integrated Peak Area

The correlation between the actual amount of NO introduced under a given flow condition and the mass-spectrometrically recorded peak area in mV-sec is obtained in a manner similar to that in the NO_2 work. The standard NO/N_2 mixture with NO concentration of 1973 ppm is used as the calibration gas. During calibration this mixture is introduced at a flow rate of 100 cc/min for a period of 10 min. The amount of NO_2 introduced is found to be

$$\frac{10 \times 100 \times 10^{-3} \times 1973 \times 10^{-6}}{0.082 \times 300} = 80.2 \times 10^{-6} \text{ moles}$$

During the same period a fraction of this flow is also introduced into the ion source of the mass spectrometer. The ratio of I_{30} ion (NO^+) to I_{29} ion ($^{18}N^{15}N^+$) was found to be 0.3025. An integration of the I_{30} ion signal for a period of 10 min with the I_{29} ion set at 6.8 x 256 yield a total value of 3,059,320 mV-sec. Thus, the integrated peak area per μmole of NO detected is

3,059,320/80.2 = 38,146 mV-sec/μmole NO detected

Note that the above calibration was obtained using pure N_2 as the mixing gas. In the case of desorption where air is used as the carrier gas, a correction factor of (1/0.78) should be applied to obtain the actual amount of NO detected by the mass spectrometer.

4. Preparation of Triethanoamine Precolumn

A triethanoamine (TEA) impregnated molecular sieve precolumn was used in the present work for the differentiation of NO and NO_2 gases. The preparation of this agent follows the same procedure as that described by Levaggi.[32] In brief, add 25 g of triethoalamine to a 250-ml beaker; add 4.0 g of glycerol, 50 cc of acetone, and sufficient distilled water to dissolve. To the mixture add about 50 cc of 45/60 mesh molecular sieve 13X. Stir and let stand in the covered beaker for about 30 min. Decant the excess liquid and transfer the molecular sieve to a flat glass pan. Place under a heating lamp until the bulk of moisture has evaporated and then in an oven at 110°C for 1 hr until dry. Store in a closed glass container.

C. Results

1. Oxidation Capacity Test

The first logical investigation on molecular sieve 5A is to test whether it is capable of catalytically converting incoming NO into NO_2 in the environment of air oxygen, and what is the minimum quantity of sieve material required for a complete conversion. After the oxidation stage, the adsorption and desorption processes are expected to follow the same pattern as in the case of NO_2 experiments since exactly the same chemical identity--NO_2--is under consideration as soon as it is formed. However, it is clear from later discussions that the adsorption of the oxidized NO_2 appears to follow a somewhat different mechanism.

In the first test, an arbitrary amount of 0.43 g of molecular sieve 5A with a thin layer of P_2O_5 was packed into a 1/4-in. O.D. U-tube column. After preconditioning in the usual manner, a 40-ppm NO/air mixture was allowed to flow through the column at a rate of 500 cc/min for 15 min. During the same period a portion of the after-column effluent was introduced into the ion source of the mass spectrometer for monitoring NO gas escaping from the P_2O_5-5A column. A clear sharp increase of the NO^+ ion level was observed at the beginning of NO/air flow. This ion signal remained at an elevated level over the entire span of 15 min and gradually came back to base line after said period when the NO flow was closed. This certainly indicates that some portion of the NO initially introduced had escaped from the sorbent column, although the quantitative amount was not established in this experiment.

In the second test, two columns each with 0.5 g 5A were attached in tandem. When the same NO/air mixture as in the first test was allowed to flow through the columns, the escape of NO was no longer observable in the mass spectrometer. The desorption as done in the usual manner shows the ratio of the integrated NO^+ ion intensity of the front column to that of the rear one to be greater than 1000:1. It is concluded that the molecular sieve 5A is indeed effective in catalyzing the NO oxidation reaction under typical sampling conditions.

2. Recovery as a Function of NO Concentration Level and the Amount of Molecular Sieve 5A

One other crucial test in the present evaluation was to check the completion of oxidation over the whole range of NO concentration of NIOSH interest, namely from 2 ppm to 40 ppm. At low concentration the oxidation rate is expected to be slower if the rate is proportional to the NO concentration to the second order as shown in gas-phase kinetics. This will be reflected in the abnormally lower unit recovery for the low NO concentration adsorption. On the other hand, the oxidation will not be completed at the high NO concentration end if the amount of sorbent employed is lower than that required for a complete conversion.

In the test the recovery of NO is measured as a function of NO concentration using columns that contain 0.5 g, 1.0 g, or 2.0 g of molecular sieve 5A. For a constant adsorption time of 15 min and dry-air flow rate of 500 cc/min, each type column was adsorbed with five different NO/air mixtures, with concentration ranging from 2 to 40 ppm. These columns were preconditioned and desorbed in the same manner as that described in the NO_2 work.

The results of the above experiment are shown in Fig. 11. It is seen from this figure that, except for NO concentrations higher than 40 ppm, all recoveries are linear with respect to NO concentration for all cases where three different amounts of 5A sieve were used. However, the recoveries increase progressively as the amount of 5A sieve is increased. This is expected if a lower amount of 5A sieve is inadequate for the quantitative oxidation of the sampled NO gas.

The effect of the amount of 5A sieve was further investigated by varying the amount of molecular sieve 5A in each column ranging from 0.5 g to 4.0 g. Each column was adsorbed by a NO/dry air mixture (NO 22.1 ppm) with total sampling rate of 540 cc/min and a time period of 15 min. The desorption results are shown in Table X. Within experimental error, the recovery increases with increase in the amount of molecular sieve but levels off as more than 2.0 g of 5A sieve is used. This clearly indicates that the quantitative oxidation and adsorption of NO has been achieved with 2.0 g of 5A column under the present sampling conditions. It is anticipated that more than 2.0 g of molecular sieve 5A should be used for sampling the NO/air mixture at higher concentrations or longer periods if a quantitative oxidation and adsorption of NO is desired. It is suggested that a lesser amount of 5A column is still acceptable for monitoring NO since the recovery of NO during desorption is linear with the actual NO concentration level as demonstrated in Fig. 11. This is especially true where a lesser amount of 5A sieve is desirable in order to reduce the flow resistance during air sampling.

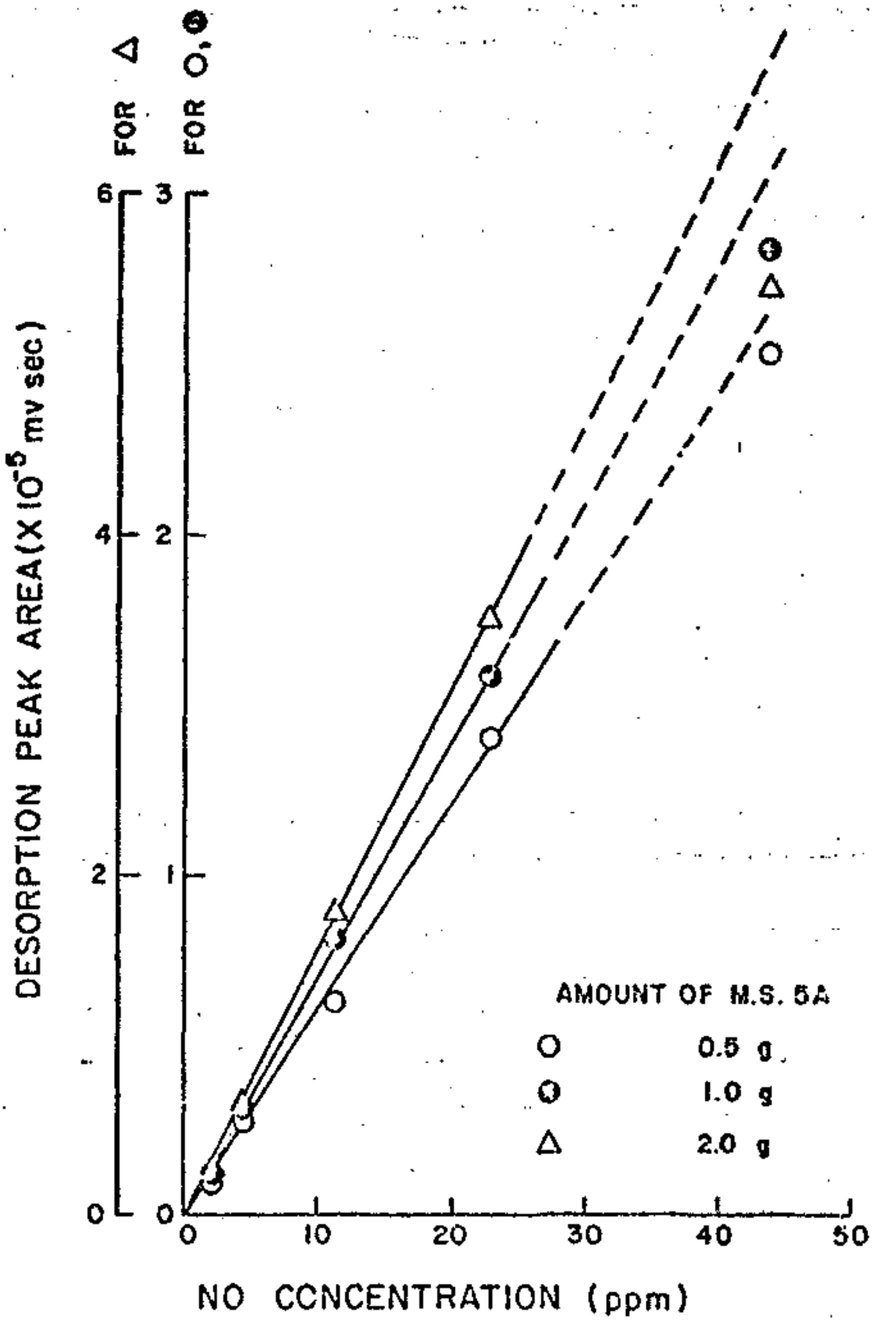

Figure 11. Recovery of NO as a Function of [illegible] Concentration and Amount of Molecular Sieve 5A

[illegible]

TABLE X

RECOVERY OF NO AS A FUNCTION OF THE AMOUNT OF MOLECULAR SIEVE 5A

Column No.[a]	Amount of Molecular Sieve 5A (g)	Desorption Peak Area[b] per pmole of NO Sampled (mV-sec / μ mole)
1	0.5	19,249
2	1.0	21,618
3	1.5	23,923
4	2.0	24,340
5	2.5	23,646
6	4.0	24,458

[a]Column: as described in Table VII.

[b]Sampling Condition: Standard NO/N_2 mixture (NO 1973 ppm) is mixed with dry air to yield a final mixture having a total flow rate of 540 cc/min and NO concentration 22.1 ppm.
Sampling time = 15 min
Amount of NO sampled = 7.34 μmole

One other noted phenomenon in Fig. 11 is that the recovery of NO for 44 ppm NO data is consistently lower than the expected value by - 10%. The possibility of experimental error is reasonably ruled out since the loss of recovery appears on all three experimental data. The explanation based on the insufficient oxidation of NO sample on the 5A sieve is unlikely since one would expect a remarkable improvement of the NO recovery when the amount of molecular sieve 5A is increased from 0.5 g to 2.0 g. This improvement is not seen in the 44 ppm NO data.

It is clear from later discussions that the adsorption and desorption of the surface catalytically oxidized NO_2 seem to follow a different mechanism from that which accounts for the adsorption and desorption of natural NO_2. As a result the desorption NO^+ ion-peak area per μmole of NO sampled is more than two times greater than the desorption NO^+ ion-peak area per μmole of NO_2 sampled. One plausible explanation for the discrepancy of the 44 ppm NO data is the possible premature oxidation of NO in the NO/air sampling stream before it enters the 5A sieve column. The prematurely oxidized NO_2, after being adsorbed on the 5A sieve sorbent, will yield a much smaller NO^+ peak area upon desorption. The premature oxidation of NO is prominant only at high NO concentration since it is known that the oxidation follows a second-order mechanism in the gas phase. This appears to be in agreement with the observation. To further test the possibility of this theory, two adsorption experiments were conducted with the 2.0 g 5A sieve columns in sampling a NO/air mixture with NO concentration of 110 ppm at a flow rate of 113 cc/min for a period of 30 min. The desorption of these two columns yields a recovery

of 13,849 and 13,880 mV-sec/ mole NO--more than 40% lower than the established value. This clearly demonstrates that the premature oxidation of NO is the real cause of the apparent decrease of the NO recovery in sampling NO/air sample with higher NO concentration. It also reflects the fact that there is no need to monitor NO in ambient air with concentration much higher than 40 ppm since the NO will convert into NO_2 in a matter of seconds.

3. Reproducibility of NO Sorption with Molecular Sieve 5A Column

The reproducibility test of NO recovery was done with a modified column containing 2.0 g molecular sieve 5A. Each column was preconditioned by heating to 300°C while purging with dry air at a flow rate of 100 cc/min for 2 hr. During sampling a NO/air mixture with an NO concentration of 111 ppm was introduced into the sampling column at a total flow rate of 540 cc/min for a period of 30 min. Table XI shows the results of four identical experiments with an average recovery of 24,240 mV-sec/μmole NO and standard deviation of $\pm$ 1.1%. Reproducibility is, therefore, seen to be very satisfactory.

4. Adsorption of NO with Ambient Air as the Carrier Gas

To test the effect of moisture on the NO oxidation and adsorption, ambient air with temperature of 80°F and relative humidity of 40% was used as a carrier gas in the NO adsorption. Adequate amounts of P_2O_5 were placed in front of each 1-g 5A sieve column. The experimental procedures are identical to the description given in the previous section.

TABLE XI

REPRODUCIBILITY OF NO SORPTION WITH MOLECULAR SIEVE 5A COLUMN[a]

Column No.[b]	Desorption I_{30} Peak[c,d] Area (mV-sec)	Desorption Peak Area per μmole of NO Sampled (mV-sec/μmole)
1	182,226	24,826
2	178,[illegible]	24,289
3	177,238	24,169
4	176,724	24,077
	Average	24,340
	Standard Deviation	277

[a]Column: 2.0 g of molecular sieve 5A with P_2O_5 presection in a 8 mm OD glass tube with its rear end attached to a Teflon valve. Each column is preconditioned by heating to 300°C while purging with dry air at a flow rate of 100 cc/min for 2 hr.

[b]Sampling Condition: Standard NO/N_2 mixture (NO 1973 ppm) is mixed with dry air to yield a final mixture with NO at 11.1 ppm and a total flow rate of 541 cc/min. Sampling time = 30 min; Amount of NO sampled = 7.34 μmole.

[c]Desorption Condition: The column is heated to 240°C with pure N_2 carrier gas at a flow rate of 100 cc/min.

[d]All mass-spectrometrically recorded peak areas in this work were obtained in reference to a constant I_{29} ($^{14}N^{15}N^+$) peak height at 6.8 x 256.

It is seen from the results presented in Fig. 12 that the agreement with the dry-air experiment is good within experimental error. It should be noted that a P_2O_5 precolumn layer is always provided even for the dry-air experiments to avoid any accidental contact of the sieve material with moisture.

5. No Storage Experiment

In order to assess the capability of the molecular sieve 5A column in retaining the collected sample for extended periods, a series of NO storage experiments was conducted with the sample column stored for a period ranging from 1 day to more than one month after sample collection. The column and sampling conditions adopted in this experiment are essentially identical to those described in Table XI for the reproducibility test. During storage the Teflon valve of the column is closed and the front end of the column is sealed with an o-ring joint cap.

The results are shown in Table XII. The loss of NO recovery is seen to be much larger than that in the case of NO_2. There is ~ 8% loss of NO recovery after the first week of storage, and this loss jumps to ~ 15% at the end of the second week. The enormous fluctuation seen in the recovery data suggests that--in addition to the storage time effect--the loss of NO recovery is also somehow influenced by the condition of each individual sampling column. The cause for this deterioration is not clear, although the possible contamination of water moisture is again considered as the prime reason for the loss of NO recovery. The inclusion of correction factors to account for the loss of NO after storage should also be feasible, although the detailed correction procedure may require some further experimental work.

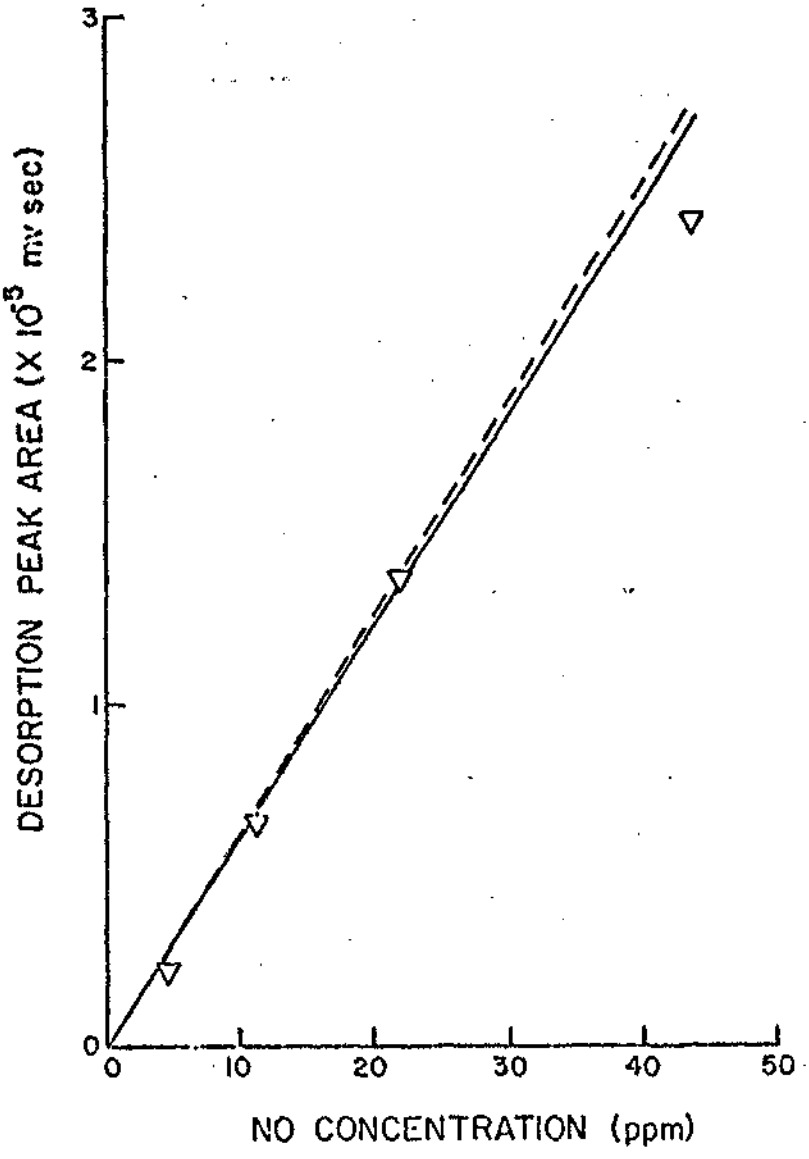

Figure 12. NO Recovery as a Function of NO Concentration Using Ambient Air as Sampling Mixture Gas

Ambient air temperature of 80°F; relative humidity of 40%
Column: 1.0 g of molecular sieve 5A in the modified sampling column (see Table VII)
Adsorption: NO/ambient air gas mixture with flow rate of 500 cc/min and adsorption period of 15 min.
Dashed line is reproduced from the 1.0-g 5A sieve column line of Fig. 11.

TABLE XII

NO STORAGE EXPERIMENT DATA

Column No.[a]	Storage Time[b] (day)	Desorption I_{30} Peak[c] Area (mV-sec)	Peak Area per μmole of NO_2 Sampled (mV-sec/μmole)	Ratio[d] (%)
1	1	168,085	22,900	94.1
2	2	172,055	23,522	96.6
3	3	160,866	21,916	90.0
4	7	163,565	22,284	91.6
5	7	166,513	22,686	93.2
6	14	150,793	20,544	84.4
7	14	155,649	21,206	87.1
8	21	146,891	20,012	82.2
9	34	142,572	19,424	79.8

[a]Column and Sampling Condition: As described in Table XI.

[b]During storage the Teflon valve of the column is closed and the front end of the column is sealed with an o-ring cap.

[c]Desorption Condition: As described in Table XI.

[d]Ratio is expressed as the ratio of the value in Col. 4 and the average value (24,340 mV-sec/μmole NO) obtained from Table XI.

Experiments were also conducted to examine the NO recovery for samples that have been stored under abnormal conditions such as extremely high ambient temperature or low pressure. Columns 1 and 2 of Table XIII reveal the recovery of NO for sample columns that had been stored at a temperature of 130°F for a period of 21 hr. Unfortunately, the loss of NO is too large to be acceptable. As shown in Cols. 3 and 4 of the same table, the experiments were repeated in a similar manner except that the column was stored at a lower temperature (120°F) and for a shorter period of time (6 hr). The results were found to be very satisfactory. Apparently there is no complication caused by the lower ambient pressure. As shown by Cols. 5 and 6, the recovery of NO is practically unchanged after the sample column has been stored at 500 torr for a period of 22 hr.

6. Passage of NO Through TEA-Impregnated Molecular Sieve Precolumn

The test of passage of NO through a TEA-impregnated molecular sieve precolumn has been conducted extensively by the group of D. A. Levaggi[32] at the sub parts-per-million NO concentration level. The purpose of the present work was to examine the same passage over a range of NO concentration of NIOSH interest; namely, 2 ppm to 40 ppm of NO. A glass tube of 1/4 mm O.D. containing 1.37 g of the TEA-impregnated molecular sieve was placed in series with each P_2O_5-5A (1.0 g) U-tube column tested. The experimental conditions are the same as those described in section 2 above.

The results are given in Fig. 13. It is seen from these data that the unit recoveries of the present data are essentially the same as those of Fig. 11 within experimental error. It is, therefore, established that

TABLE XIII

STORAGE OF NO SAMPLE UNDER ABNORMAL CONDITION

Column No.[a]	Storage Condition[b] Pressure (torr)	Temperature (°F)	Time (hr)	Desorption Peak Area[c] per mole NO Sampled (mV-sec/ mole)	Ratio[d] (%)
1	760	130	21	18,986	78.0
2	760	130	21	19,819	81.4
3	760	120	6	24,182	99.4
4	760	120	6	24,258	99.7
5	500	80	22	25,099	103.1
6	500	80	27	24,800	101.9

[a]Column: P_2O_5 - 5A sieve (2.0 g) column; column preconditioned in the same manner as in Table XII.

Sampling Condition: NO/dry air mixture (NO 11.1 ppm) sampled at a flow rate of 540 cc/min for 30 min.

[b]During storage the Teflon valve of the column is closed and the front end of the column is sealed with an o-ring joint cap.

[c]Desorption Condition: Same as described in Table XI.

[d]Ratio is expressed as the ratio of the value in Col. 5 and the average value (24,340 mV-sec/μmole NO) obtained from Table XI.

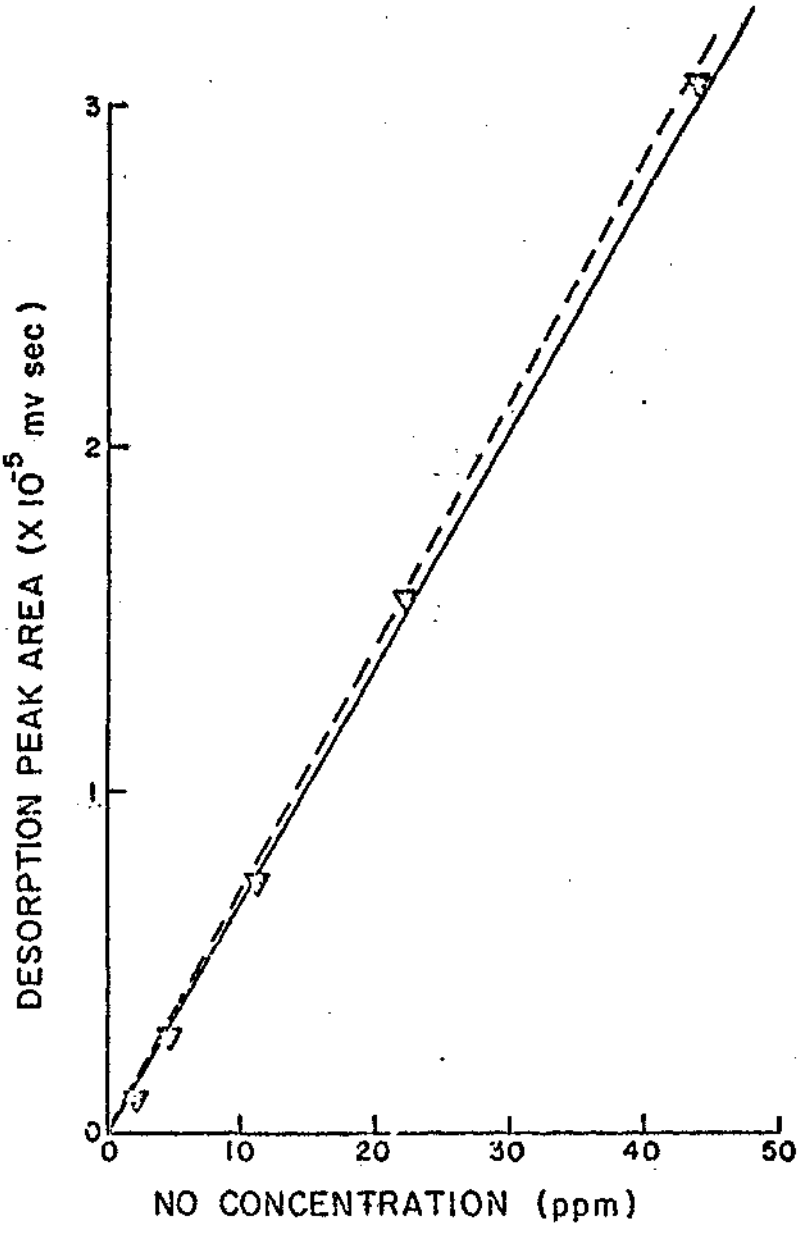

Figure 13. Recovery of NO as a Function of NO Concentration Using TEA-P_2O_5-Molecular Sieve 5A Column

Sampling Condition: NO/dry air mixture is sampled at a total flow rate of 500 cc/min for 15 min.
Dashed line is reproduced from the 1.0-g 5A sieve column line of Fig. 11.

NO at concentrations below 40 ppm in air can pass the TEA agent completely unaffected or with only negligible loss.

D. Discussion

1. Desorption-Peak Analysis

As discussed in the previous report on NO_2 work, the molecular sieve 5A desorption-peak shape was found to be highly dependent on sieve preconditioning, although the total peak area remains unchanged. With higher preconditioning temperature (> 250°C), it is clearly seen during desorption that there is actually a second, small broad peak riding on the tail of the first large sharp peak. Further resolution of these two peaks was recently attempted in a column containing as much as 13 g of molecular sieve 5A which was preconditioned by heating to 300°C for a period of 5 hr. Two desorption peaks were largely resolved under normal desorption conditions. There were reasons to believe that this second peak might be caused by a partial breakthrough of the nitric acid formed during column desorption. However, from the mass spectra recorded at various positions of these two desorption peaks, it was discovered that the NO_2^+ (m/e = 46) ion--which is an intense peak ion in the HNO_3 spectrum--was not observed along with the NO^+ ion corresponding to the second broad peak. It thus appears that this second peak is also an ion formed from NO, although its origin is still not clearly understood.

The double-peak phenomenon was also observed in the desorption of columns adsorbed with NO. The ratio of the first-peak area to that of the second peak is larger than 5:1 for the adsorption of high NO concentration

(40 ppm) but gradually decreases to ~ 1:1 for the NO concentration of 2 ppm. Therefore, it is the total desorption peak area rather than the area of any individual peak that should be counted in order to ensure a uniform unit recovery over the entire range of NO concentration.

2. NO Adsorption-Desorption Mechanism

It is reasonably well established that during the sampling of NO gas in the air stream with the molecular sieve 5A column, NO can be oxidized on the catalytic surface of the 5A sieve into NO_2 according to the reaction

$$2NO + O_2 \rightarrow 2NO_2 \qquad (12)$$

The oxidized NO_2 is then adsorbed by the molecular sieve 5A sorbent. Quantitative oxidation-adsorption can be achieved provided the amount of 5A sieve is adequate--the value being dictated by the actual sampling condition such as NO concentration, total reaction time, etc.

In the previous section dealing with NO_2 work a double 5A sieve tandem column was used to examine the desorption mechanism of the NO_2-adsorbed column. It was concluded that the major identity of the desorption product exists in the form of NO. It is of equal interest in the present work to determine whether the same mechanism is followed during desorption of the 5A sieve column that has sampled the NO/air mixture. The same long glass U-shaped column with each leg being filled with 0.5 g molecular sieve 5A was used in the present test. After sampling the NO/air mixture (NO 22.1 ppm) at a flow rate of 540 cc/min

for a period of 15 min, the front 5A sieve section was desorbed using N_2 as the carrier gas while the rear section as well as the U-trap section was immersed in a dry-ice bath. To our surprise only a small NO^+ peak was recovered having an area of 429 mV-sec. The rear 5A sieve section was subsequently desorbed with an NO^+ peak area of 76,064 mV-sec recorded by the mass spectrometer. The only plausible explanation for this finding is that the major component desorbed from the front 5A sieve column is not in the form of NO. The most likely candidate which fits the observation is NO_2 although positive identification cannot be made from this test.

3. Percent Recovery of NO from the Molecular Sieve 5A Column

Some difficulty arises in arriving at a meaningful derivation of the percent recovery of NO from the molecular sieve 5A column since the true desorption mechanism has not been unequivocally established based on the experimental findings. Assuming a desorption product of NO, the percent recovery can be expressed in a manner similar to Eq (6), i.e.,

$$PR = \frac{\mu\text{mole of NO desorbed}}{\mu\text{mole of NO sampled}} \times 100\%$$

$$= \frac{24{,}340 \text{ mV-sec}/\mu\text{mole NO sampled}}{48{,}905 \text{ mV-sec}/\mu\text{mole NO detected}} \times 100\%$$

$$= 48.8\% \qquad (13)$$

However, as discussed previously, the desorption product is more likely to be in the form of NO_2 rather than NO under present experimental conditions. Accordingly, the correct form of percent recovery should be

$$PR = \frac{\mu\text{mole of } NO_2 \text{ desorbed}}{\mu\text{mole of NO sampled}} \times 100\%$$

$$= \frac{24{,}340 \text{ mV-sec}/\mu\text{mole NO sampled}}{31{,}540 \text{ mV-sec}/\mu\text{mole } NO_2 \text{ detected}}$$

$$= 77.0\% \qquad (14)$$

where 31,540 mV-sec/μmole NO_2 detected is the calibrated value for NO_2 response previously described. Regardless of the actual desorption mechanism, the obtained percent recovery for either case is substantially higher than that of NO_2 adsorption. It is conceivable that the adsorption of NO_2 and NO-turned-NO_2 may follow different mechanisms. In the case of NO, the adsorption may be dictated by a process closely related to the catalytical effect of the sieve surface and more readily desorbed upon heating. The unexpected high PR value of NO also violates the stoichiometric relationship of the desorption mechansim of $3NO_2 + H_2O \rightarrow NO + 2HNO_3$ previously assumed, unless the formed HNO_3 can partially break through or further decompose under the present desorption conditions.

4. Effect of Interfering Gases

In principle any gases existing in ambient air that can be absorbed by the adsorption tube under the present sampling conditions and desorbed upon heating--with the desorption product accidentally also yielding a m/e = 30 in signal in the mass spectrometer--will interfere with the present method of analysis of NO and NO_2. However, to the author's knowledge, there is no commonly existing air pollutants that fit the above description and cause interference to any significant degree.

Among various nitrogen oxide compounds, nitrous oxide (N_2O) is known to exist in ambient air at considerably high concentrations (several hundred parts per million) and forms a significant amount of the NO^+ ion (m/e = 30) under electron impact. Fortunately, it was found in this laboratory that it cannot be adsorbed and subsequently desorbed with the molecular sieve 5A column used under the present experimental conditions. The interference is practically negligible for an N_2O/air mixture with N_2O concentration as high as 2000 ppm.

It has been reported [28] that nitrous acid anhydride, N_2O_3, and nitrogen tetroxice, N_2O_4, do not exist at concentrations of 100 ppm and below. Kinetic data show that their dissociation is practically instantaneous. Hence, these nitrogen oxides may be disregarded.

Nitrogen pentoxide is rarely found in ambient air because it is readily hydrated to nitric acid vapor and is also an unstable compound which is very sensitive to heat. The reported [28] half-life is 6 hr at 25°C, 86 min at 35°C, and only 5 sec at 100°C. The decomposition products are nitrogen dioxide and oxygen. It is also doubtful whether N_2O_5 can be physically retained by the 5A sorbent due to its relative larger molecular diameter.

Probably the most likely gas to interfere with the present method is nitric-acid vapor. It is known to be stable, to exist in the atmosphere at trace levels and to readily yield an NO^+ ion in the mass-spectrometric ion source. However, its adsorption and desorption characteristics on the 5A sieve are unclear at this time. Since it can also be absorbed in many metal and glass surfaces, it is doubtful whether it can be successfully introduced into the ion source and detected during desorption. Experimental testing is required for a better understanding of this potentially interfering gas.

20.1<

In addition to the NO^+ ion, several other ions such as $C_2H_6^+$, CH_2O^+, and CH_4N^+ also show the same nominal mass (i.e., m/e = 30). If the precursors of these ions come as the resulting products of the above adsorption-desorption procedure, they should also be considered as interfering compounds. Although there seems to be an endless list of compounds that are able to form one of these ions, probably, very few--if any--can cause severe interference which will affect the actual measurement. First of all, the majority of these compounds yield only the m/e = 30 ions with intensities much less than 5% of the most intense peak in each spectrum. Thus, the interfering effect is negligible unless their concentrations are very high in the ambient-air environment. On the other hand, most of these compounds that are capable of producing m/e = 30 ions are generally of a size which is too large to be adsorbed effectively by the sorbent currently employed which has an aperature of only 5 Å. Furthermore, even after adsorption these compounds may not be desorbed under the present desorption conditions.

In the actual case of interference, there are still ways of eliminating or minimizing this effect. The difference in mass between the NO^+ ion (m/e = 30.0061) and the above-mentioned ions ($C_2H_6^+$ ion with m/e = 30.0702, H_2O^+ ion with m/e = 30.0265, and CH_4N^+ ion with m/e = 30.0498) is large enough to be resolved by most mass spectrometer having moderate resolution. A proper choice of a GC column is sometimes very helpful in separating the interfering source and the true ion signal. Other methods such as trapping and absorption elimination may also prove to be effective for resolving the interference problem.

In conclusion, it appears that the present method of monitoring NO and NO_2 is free from the interference of other gases commonly existing in ambient air. However, more definite conclusions await further systematic laboratory experimentation.

E. Conclusion

The currently developed solid-sorbent mass-spectrometric method has been shown to be effective in monitoring both nitric oxide and nitrogen dioxide in ambient air at parts per-million levels. The sampling tube is compatible with the personnel-carryable sampling pump in every respect. Adsorption efficiency is quantitative for both NO and NO_2 over the entire experimental range. The desorption result is reproducible with accuracy better than $\pm$ 2%. However, the percent recovery for these two gases was found to be different, probably due to the different adsorption-desorption mechanisms involved, the details of which are only partially resolved in the present work.

It should be noted that although the present method has been tested only within the concentration range of interest to NIOSH, the present technique can be applied to other ranges provided the sampling conditions and amounts of solid sorbents are properly chosen. Thus, a longer sampling period is desired if the ambient air with NO or NO_2 concentration at sub-parts-per-million is to be sampled. On the other hand, in the case of a stationary source or vehicular-emission monitoring where the pollutants generally persist in the range of hundred parts-per-million, a greater amount of sieve sorbent with a shorter sampling time should suffice.

In the present work the mass spectrometer is chosen for identification and quantification of products released from the sorbent during desorption. Analysis using the mass spectrometer is rapid, sensitive, and unambiguous. However, it may not be popular due to the relatively high cost of the instrumentation. In a case where the sensitivity requirement is not extremely critical, the thermal desorption product can be simply collected and analyzed by the conventional titration method. One possible alternative to thermal desorption is solvent extraction. The central question will then be the development of a technique for the analysis of the extracted solution.

SECTION VI

INSTRUMENT-COMPUTER INTERFACING AND PROGRAMMING

MS-30

Preliminary work performed on the AEI MS-30/DS-50 mass spectrometer and data system has been described previously.[33] The data system is now fully operational and several modifications and improvements have been made. The Data General RDOS operating system has been modified to allow the entire system to be run from the CRT terminal rather than the teletype. The hard-copy photoprinter attachment to the CRT terminal may also be triggered automatically to provide a permanent record of the console dialog if desired. This increases the efficiency of operation substantially since the CRT terminal will print approximately 80 times faster than the Teletype.

Programs have been written to permit signal averaging of successive scans.[34] The current version of these programs relies on the reproducibility of the magnet scan (magnetic field strength versus time, measured from the start of the scan) to line up the mass scale for each successive run. The present operation of the DS-50 data collection is as follows: Each individual scan is centroided on-line using a preset hardware threshold. The time centroids are also converted to masses on-line using a predetermined time-to-mass scale as described previously.[35] The peak areas and corresponding masses are then stored on the disc. Subsequent programs perform the desired analyses off-line.

It is not possible to do all of the above processing on-line when signal averaging since the individual peaks might not be defined until several scans have been accumulated. It is also necessary to remove the

hardware threshold to avoid any loss of data in the individual scans. Thus, the signal-averaging program makes use of a DS-50 option which will allow raw "uncentroided" data to be collected. The signal-averaging program then averages the raw data off-line, calculates time centroids and peak areas using a software threshold, and stores the information on disc. An off-line time-to-mass conversion program (supplied with DS-50) is then used to convert the time centroids to masses, thus allowing the remaining DS-50 analysis programs to be run.

These programs have been tested and the reproducibility of the magnet scans found to be adequate for low-resolution spectra provided the magnet is allowed to cycle at least ten times before data collection is initiated. The reproducibility at high resolution has not been tested. Ultimately, we would want to consider installing a Hall probe to monitor the magnetic field strength directly. This would greatly increase the accuracy in which the mass values of successive scans can be lined up before the averaging is performed, as described previously.[36] No work has been done on rewriting the time-to-mass conversion portions of the DS-50 data system as yet, as AEI has been reluctant to make these programs available. It would probably be better (and easier) to write dedicated time-to-mass algorithms for the particular mass range desired (320-328) than to try to modify AEI's generalized routine.

SPARK-SOURCE MASS SPECTROMETER

No additional work has been done in this area since the previous report.[33] However, once the above system for the MS-30 is operational, it should be easy to connect the computer to the MS-7 rather than the MS-30.

The only difference would be the possible use of the Hall probe. However, based on past experience with the reproducibility of the magnet scan on the MS-30, an identical solution on the MS-7 would probably be attempted/ Some work would be required to interface the digital lines from the computer to the scan control circuits of the MS-7, but this should present no problems.

CROSSED BEAM AND CD-491 PROGRAMS

Data acquisition and analysis programs have been written for the crossed-ion molecular-beam apparatus and the DuPont CD-491 GC-MS system. These programs are capable of collecting data, controlling instrumental parameters such as scan speed, and performing subsequent analyses, all using the Hewlett-Packard 2116 computer with the manufacturer-supplied DOS-M system. The details of the operation of these programs have been described elsewhere.[37-40]

OTHER COMPUTER WORK

Some time has been spent adapting computer programs written and used by one of the authors (D. T. Terwilliger) at Purdue University for use on the presently available Hewlett-Packard computer systems. These programs included an operating system for an HP-2100 series computer in a non-disc environment as well as mass spectrometer data collection and analysis programs.[41] The operating system has been expanded to include the facilities of the disc and the Versatec printer/plotter which were not available previously. The system is now substantially easier to use and more efficient in its operation than the Hewlett-Packard-supplied DOS-M system which had been used exclusively in this laboratory previously. Most of the preliminary portions of the programming for the

spark-source mass spectrometer[36] were done on the Hewlett-Packard computer using the above system, and portions of some of the programs used at Purdue were directly applicable to the problem.

Analysis of the paper-tape output of a quadrupole GC-MS system used for routine herbicide analyses was performed using programs written under the above system. This GC-MS system consists of a Varian 2740 gas chromatograph equipped with a Model 8000 autosampler coupled to a Extranuclear quadrupole mass spectrometer.[42] Data is acquired by a Spectrophysics Autolab System 4 computing integrator interfaced to a teletype with a low-speed punch. The paper tape produced is read into the HP-2116 computer and the results of several runs can then be averaged and compared to a standard.[43] Concentrations and standard deviations were automatically computed and printed out for each series of runs.

LIST OF PROGRAMS

This list of programs can be divided into four sections. The first two contain the programs written for the Data General Nova computer system and the last two for the HP-2100 Series computers. Sections one and three contain general system programs which, while producing no data themselves, are necessary to write and debug all other programs. Sections two and four contain application programs written to perform specific tasks for specific systems.

Section 1

A. Modifications to HIPBOOT, SYS.SV, SYS.OL, and SYS.DR, all part of the Nova operating system RDOS to permit greater efficiency of operation.

1. Allow either the Teletype or the CRT terminal to serve as the system console device. Changeover from one to the other takes less than two minutes.
2. Simplify the startup and shutdown procedures considerably.

B. VDU, VDF, VDH, TTO. Allow for automatic paging and photoprinter triggering of the CRT display when used as the console.

C. CLONN, CLOFF. Allow the operator to start and stop the clock. Many analysis programs not needing the real-time clock will run faster with it off as system overload is substantially reduced.

D. TAPE. Allows the paper tape reader to be enabled for console input when the teletype is the console device. This allows repeated sequences of commands to be punched on tape rather than re-entered each time.

E. UPPER, LOWER. Allow the lower case facilities of the CRT terminal and the line printer to be used.

F. DLST, BLIST, OSRCH, SRCH. These programs will "de-assemble" binary instructions directly from core or from any selected portions of the disc or search for given strings in either the core of the disc as an aid to analyzing and modifying manufacturer-supplied system programs.

C. TCOPY. This program selectively copies a portion of one disc to another using only a single-disc drive. This is essential for performing any applications programming as there must be a means of transferring finished programs from one disc to another.

Section 2

A. CAT. Program to average several scans of uncentroided data and centroid the resulting average. This creates a data file suitable for processing by the DS-50 off-line time-to-mass conversion program.

B. PLOTT. Program to plot uncentroided data on the CRT.

C. NEWATOM. Modifications of the AEI program STHATOM which generates atomic composition reports. This program previously could take four to six hours to run depending on the data. The modified version runs in roughly one-fourth to one-third the time of the original.

D. DTTPLOT. Modifications of the AEI program PBMPLOT, eliminating several errors found to be present in the plotting of mass spectral data.

E. Double precision subroutines. Programs to perform 32-bit arithmetic operations which are necessary for the program CAT to function properly.

Section 3

A. Modifications to the T^2-MOS system used at Purdue to operate on the HP-2116 computer system presently available.

1. Sections were added to support the disc-drive, the Versatec printer/plotter, and the HP-CRT terminal.

2. The assembler was modified to produce output in a disc-compatible format.

3. The stand-alone version of the HP relocatable loader was modified to be compatible with and run under the above system.

B. Disc bootstrap loader and generalized system loader to permit the system to be started and binary programs to be loaded directly from the disc.

C. Disc-based SIO drivers to allow the HP fortran compiler and extended assembler to operate under the above system.

D. A de-assembler to aid in analyzing and modifying manufacturer supplied binary programs.

E. Programs to load HP-DOSM directly from the disc and to copy source programs from the disc to the DOSM users directory.

F. A variety of utility programs to copy programs, edit libraries, dump sections of the disc, etc.

Section 4

A. Test programs to collect, average, and analyze data from the spark-source mass spectrometer.

b. A program to generate a set of test data (using a random number generator) for the above program.

C. A program to plot and label data on the oscilloscope.

D. Modifications to HP-DOS Versaplot, a general purpose plotting system for the Versatec printer/plotter to run under the T^2-MOS system.

E. A program to analyze the output of the quadrupole mass spectrometer used for routine herbicide analyses.

F. A program to reformat the results of the DS-50 analysis of herbicide mixtures to be suitable for inclusion into Air Force technical reports.

G. A program to analyze the reproducibility of the magnet scans on the MS-30 mass spectrometer.

REFERENCES

1. Mass Spectrometric Studies, SRL Semiannual Status Report 6776-1 on USAF Contract No. F33615-73-C-4099 covering the period December 1972 - August 1973 (Systems Research Laboratories, Inc., Dayton, Ohio, August 1973).

2. Mass Spectrometric Studies, SRL Annual Status Report 6776-2 on USAF Contract No. F33615-73-C-4099 (Systems Research Laboratories, Inc., Dayton, Ohio, February 1974).

3. Mass Spectrometric Studies, SRL Semiannual Status Report 6776-3 on USAF Contract No. F33615-73-C-4099 covering the period February 1974 - August 1974 (Systems Research Laboratories, Inc., Dayton, Ohio, August 1974).

4. Mass Spectrometric Studies, SRL Annual Status Report 6776-4 on USAF Contract F33615-73-C-4099 (Systems Research Laboratories, Inc., Dayton, Ohio, February 1975).

5. R. L. C. Wu, E. G. Jones, B. M. Hughes, C. D. Miller, and T. O. Tiernan, "Crossed Beam Studies of High Temperature Molecules," Paper presented at the Gordon Research Conference on High Temperature Chemistry, Andover, New Hampshire, July 1974.

6. R. L. C. Wu, E. G. Jones, B. M. Hughes, C. D. Miller, and T. O. Tiernan, "A Crossed Beam Apparatus for Studying Ion-Molecule Reactions," Proceedings of the 22nd Annual Conference on Mass Spectrometry and Allied Topics, Philadelphia, Pa., 1974.

7. Ref. 1, pp. 35-38.

8. Ref. 2, pp. 106-120.

9. Ref. 3, pp. 85-99.

10. D. C. Fee, B. M. Hughes, T. O. Tiernan, C. E. Hill, Jr., and M. L. Taylor, "An Experimental Method for Identification of the Origin of USAF Herbicide-Orange Stocks," Progress Report submitted to Air Force Logistics Command in 1974.

11. B. M. Hughes, D. C. Fee, T. O. Tiernan, C. E. Hill, Jr., R. L. C. Wu, and M. L. Taylor, "Development and Application of Analytical Methodology for Detailed Characterization of Air Force Herbicide-Orange Stocks," Progress Report submitted to Air Force Logistics Command in 1974.

12. Ref. 4, pp. 21-46.

13. B. M. Hughes, D. C. Fee, M. L. Taylor, T. O. Tiernan, C. E. Hill, Jr., and R. L. C. Wu, "Analytical Methodology for Herbicide Orange. Volume I: Determination of Chemical Composition," ARL-TR-75-0110 (Vol. I) (Aerospace Research Laboratories, Wright-Patterson AFB, Ohio, 1975).

14. D. C. Fee, B. M. Hughes, M. L. Taylor, T. O. Tiernan, And C. E. Hill, Jr., " Analytical Methodology for Herbicide Orange. Volume II: Determination of Origin of USAF Stocks," ARL-TR-75-0110.(Vol. II) (Aerospace Research Laboratories, Wright-Patterson AFB, Ohio, 1975).

15. B. M. Hughes, C. D. Miller, M. L. Taylor, R. L. C. Wu, C. E. Hill, Jr., and T. O. Tiernan, "Rapid Technique for Quantifying Tetrachlorodibenzo-p-Dioxin Present in Chlorophenoxy Herbicide Formulations," Submitted to Analytical Chemistry in June 1975.

16. Ref. 2, pp. 77-103.

17. Ref. 3, pp. 56-84.

18. Ref. 4, pp. 47-64.

19. E. Stenhagen, S. Abrahamsson, and F. W. McLafferty (eds.), Atlas of Mass Spectral Data, Vol. 2 , pp. 1276-1277.

20. Index of Mass Spectral Data (ASTM Committee E-14, Philadelphia, Pa., September 1963), p. 84.

21. M. Hudlicky, Organic Fluorine Chemistry (Plenum Press, New York, 1971), pp. 142-144.

22. DuPont Bulletin No. FST-1, "Freon" TF Solvent (E. I. DuPont de Nemours and Co., Inc., Freon Products Division, Wilmington, Delaware), p. 4.

23. T. O. Tiernan, B. M. Hughes, C. Chang, R. P. Clow, and M. L. Taylor, "Development and Evaluation of Solid Sorbents for Monitoring Work-Place Air Pollutants," Annual Summary Report (Aerospace Research Laboratories, Wright-Patterson AFB, Ohio, 31 December 1973).

24. T. O. Tiernan, C. Chang, B. M. Hughes, R. P. Clow, and M. L. Taylor, "Development and Evaluation of Solid Sorbents for Monitoring Work-Place Air Pollutants," Quarterly Progress Report (Aerospace Research Laboratories, Wright-Patterson AFB, Ohio, 31 March 1974).

25. T. O. Tiernan, C. Chang, B. M. Hughes, R. P. Clow, and M. L. Taylor, "Development and Evaluation of Solid Sorbents for Monitoring Work-Place Air Pollutants," Quarterly Progress Report (Aerospace Research Laboratories, Wright-Patterson AFB, Ohio, 30 June 1974).

26. B. B. Sundaresan, C. I. Harding, F. P. May, and E. R. Hendrickson, Env. Sci. and Tech. 1, 151 (1967).

27. W. Joith, A. T. Bell, and S. Lynn, Ind. Eng. Chem. Process Res. Develop. 11, 434 (1972).

28. B. E. Saltzmann, Anal. Chem. 26, 1949 (1954).

29. J. W. Mellor, "A Comprehensive Treatise of Inorganic and Theoretical Chemistry, Vol. VII (John Wiley and Sons, Inc., New York, 1962), p. 532.

30. M. B. Jacobs and S. Hockheiser, Anal. Chem. 30, 426 (1958); E. L. Merryman, C. W. Spicer, and A. Levy, Environ. Sci. and Tech. 7, 1056 (1973) and references quoted therein.

31. D. A. Levaggi, et al., Environ. Sci. Tech. 8, 348 (1974) and references quoted therein.

32. D. A. Levaggi, W. Sin, and M. Feldstein, J. Air Poll. Cont. Assoc. 23, 30 (1973).

33. Ref. 4, pp. 101-103.

34. A list of all programs with a description of each is given at the end.

35. Ref. 4, p. 102.

36. Ref. 4, p. 103 (Section B).

37. Users Manual for Crossed Ion Molecular Beam Apparatus, Contract No. F33615-72-C-1465 (Systems Research Laboratories, Inc., January 1973).

38. B. M. Hughes, D. C. Fee, T. O. Tiernan, C. A. Davis, and M. L. Taylor, paper published in Proceedings of the Twenty-Second Annual Conference on Mass Spectrometry and Allied Topics, Philadelphia, Pa., May 1974.

39. Ref. 3, Appendix A.

40. Ref. 2, pp. 106-111.

41. D. T. Terwilliger, J. H. Beynon, and R. G. Cooks, Int. J. Mass Spec. Ion Phys. 14, 15 (1974).

42. Ref. 4, pp. 22-25.

43. Ref. 4, Appendix B for examples of output from this program.

PUBLICATIONS RESULTING FROM THIS CONTRACT

E. G. Jones, A. K. Bhattacharya, and T. O. Tiernan, "Formation of the Dimer Cation $(C_6H_6)_2^+$ in Gaseous Benzene," Int. J. Mass Spectrom. Ion Phys. 17, 141 (1975).

E. G. Jones, B. M. Hughes, D. G. Hopper, and T. O. Tiernan, "Low Energy He^+/H_2 Interactions," Published in Proceedings of 23rd Annual Conference on Mass Spectrometry and Allied Topics, Houston, Texas, 1975.

C. Chang, T. O. Tiernan, B. M. Hughes, and M. L. Taylor, "Development of Solid Sorbent-Mass Spectrometric Techniques for Low-Level Monitoring of NO and NO_2 in Air," Published in Proceedings of 23rd Annual Conference on Mass Spectrometry and Allied Topics, Houston, Texas, 1975.

M. L. Taylor, B. M. Hughes, T. O. Tiernan, R. L. C. Wu, and D. T. Terwilliter, "Determination of Tetrachlorodibenzo-p-Dioxin in Chemical and Environmental Matrices," Published in Proceedings of 23rd Annual Conference on Mass Spectrometry and Allied Toipcs, Houston, Texas, 1975.

M. B. Hughes, D. C. Fee, M. L. Taylor, T. O. Tiernan, C. E. Hill, Jr., and, R. L. C. Wu, "Analytical Methodology for Herbicide Orange. Volume I. Determination of Chemical Composition," ARL-TP-75-0110 (Vol. 1) (Aerospace Research Laboratories, Wright-Patterson AFB, Ohio, 1975).

D. C. Fee, B. M. Hughes, M. L. Taylor, T. O. Tiernan, and C. E. Hill, Jr., "Analytical Methodology for Herbicide Orange. Volume II. Determination of Origin of USAF Stocks," ARL-TR-75-0110 (Vol. II) (Aerospace Research Laboratories, Wright-Patterson AFB, Ohio, 1975).

R. L. C. Wu and T. O. Tiernan, "Collision Induced Dissociation Reaction of Molecular Negative Ions, CO_3^-, N_2O^-, and NO_2^-," Published in Proceedings of 23rd Annual Conference on Mass Spectrometry and Allied Topics, Houston, Texas, 1975.

E. G. Jones, B. M. Hughes, D. C. Fee, and T. O. Tiernan, "Luminescence from Low Energy He^+/Xe Charge Transfer Reactions," Submitted to Chemical Physics Letters.

R. L. C. Wu, T. O. Tiernan, D. G. Hopper, and A. C. Wahl, "Characterization of the Potential Energy Surface of the $X^2A^1(^2\Pi)$ State of N_2O^-," Submitted to Journal of Chemical Physics.

R. L. C. Wu and T. O. Tiernan, "Collision-Induced Dissociation of CO_3^-," Submitted to Journal of Chemical Physics.

B. M. Hughes, C. D. Miller, M. L. Taylor, R. L. C. Wu, C. E. Hill, Jr., and T. O. Tiernan, "Rapid Technique for Quantifying Tetrachlorodibenzo-p-Dioxin Present in Chlorophenoxy Herbicide Formulations," Analytical Chemistry - In Press.

T. O. Tiernan, C. Chang, B. M. Hughes, R. P. Clow, R. L. C. Wu, and M. L. Taylor, "Development and Evaluation of Solid Sorbents for Monitoring Work-Place Air Pollutants," Quarterly Progress Reports submitted to NIOSH, Cincinnati, Ohio, in September 1973, December 1973, March 1974, and June 1974.

M. L. Taylor and B. M. Hughes, "Determination of Parts-per-Million Levels of TCDD in Herbicide-Orange Using Gas Chromatograph and Gas Chromatography-Mass Spectrometry Techniques," Presented at the EPA-Sponsored Planning Session on Dioxin held 25 and 26 July 1974 in Wash., D. C.

R. L. C. Wu, E. G. Jones, B. M. Hughes, C. D. Miller, and T. O. Tiernan, "Crossed-Beam Studies of High Temperature Molecules," Presented at the Gordon Research Conference on High Temperature Chemistry, Andover, New Hampshire, in July 1974.

D. C. Fee, B. M. Hughes, T. O. Tiernan, C. E. Hill, and M. L. Taylor, "An Experimental Method for Identification of the Origin of USAF Herbicide-Orange Stocks," Report submitted to the Air Force Logistics Command in 1974.

B. M. Hughes, D. C. Fee, T. O. Tiernan, C. E. Hill, Jr., R. L. C. Wu, and M. L. Taylor, "Development and Application of Analytical Methodology for Detailed Characterization of Air Force Herbicide-Orange Stocks," Report submitted to the Air Force Logistics Command in 1974.

B. M. Hughes, D. C. Fee, T. O. Tier an, C. A. Davis, and M. L. Taylor, "A Disc-Oriented GC-MS Computer DAta Acquisition/Display System," Published in the Proceedings of the 22nd Annual Conference on Mass Spectrometry and Allied Topics, Philadelphia, Pa., in 1974.

E. G. Jones, D. C. Fee, B. M. Hughes, and T. O. Tiernan. "Visible Emissions Produced from He^+/Atom and He^+/Molecule Collisions," Published in the Proceedings of the 22nd Annual Conference on Mass Spectrometry and Allied Topics, Philadelphia, Pa., in 1974.

R. L. C. Wu, E. G. Jones, B. M. Hughes, C. D. Miller, and T. O. Tiernan, "A Crossed Beam Apparatus for Studying Ion-Molecule Reactions," Published in Proceedings of the 22nd Annual Conference on Mass Spectrometry and Allied Topics, Philadelphia, Pa., in 1974.

R. P. Clow, T. O. Tiernan, and B. M. Hughes, "Reactions of H_3^+, H_3P^+, and NH_4^+ with Hydrogen, Water, and Ammonia," Published in the Proceedings of the 22nd Annual Conference on Mass Spectrometry and Allied Topics, Philadelphia, Pa., in 1974.

B. M. Hughes, E. G. Jones, and T. O. Tiernan, "Vacuum Ultraviolet Emissions from He^+/Rare Gas Collisions," Presented at the 26th Annual Gaseous Electronics Conference in Madison, Wisconsin, in 1973.

R. L. C. Wu, E. G. Jones, and T. O. Tiernan, "Application of Crossed Ion-Molecular Beam Apparatus in the Study of High-Temperature Molecules," Presented at the Midwest High-Temperature Chemistry Conference, Evanston, Illinois, in June 1973.

B. M. Hughes, E. C. Jones, and T. O. Tiernan, "Vacuum Ultraviolet Emissions from He^+/Rare Gas Collisions," Presented at the 8th International Conference on the Physics of Electronic and Atomic Collisions, Belgrade, 1973.

T. O. Tiernan, B. M. Hughes, J. C. Haartz, M. L. Taylor, and R. L. C. Wu, "Progress Report: Mass Spectrometric Studies of Interactions of Selected Adsorbents with Gaseous Pollutants," Report assembled for the National Institute of Occupational Safety and Health (NIOSH), Cincinnati, Ohio.

J. C. Haartz and T. O. Tiernan, "Progress Report: Spark-Source Mass-Spectrometric Studies of Experimental Geiger-Müller Tubes for Application to Aircraft Oil-Flow Detection Systems," Report submitted to Air Force Flight Dynamics Laboratory.

D. . Fee, B. M. Hughes, M. L. Taylor, and T. O. Tiernan, "Progress Report c Herbicide Characterization," Report submitted to Air Force Logistics Command.

B. M. Hughes, D. C. Fee, T. O. Tiernan, M. L. Taylor, C. E. Hill, Jr., and C. A. Davis, "Progress Report No. 2 on the Characterization of Gulfport Herbicide Orange," Report submitted at the USAF Environmental Health Laboratory, Kelly AFB, Texas.

J. C. Haartz, "Spark-Source Mass-Spectrometric Analysis Report of Jet-Engine Blades," Report submitted to Metallurgy and Ceramics Research Laboratory, Aerospace Research Laboratories, Wright-Patterson AFB, Ohio.

B. M. Hughes, E. C. Jones, C. D. Miller, and T. O. Tiernan, "Light Emission from Low-Energy Ion-Neutral Collisions," Published in Proceedings of the 21st Annual Conference on Mass Spectrometry and Allied Topics, San Francisco, Calif., 1973.

R. L. C. Wu and T. O. Tiernan, "Collision-Induced Dissociation Reactions of Molecular Negative Ions: O_2^-, NO^-, and NO_2^-," Published in Proceedings of the 21st Annual Conference on Mass Spectrometry and Allied Topics, San Francisco, Calif., 1973.

M. L. Taylor, R. L. C. Wu, C. E. Hill, Jr., E. L. Arnold, B. M. Hughes, and T. O. Tiernan, "Determination of Trace Quantities of Chlorophenoxy-Type Herbicides and Related Chlorinated Residues in Soil," Published in Proceedings of the 21st Annual Conference on Mass Spectrometry and Allied Topics, San Francisco, Calif., 1973.

END
DATE
FILMED
2-11-76
NTIS